

# Radiolaria from the Late Eocene Oamaru Diatomite, South Island, New Zealand

Barry O'Connor

Department of Geology, University of Auckland, Private Bag 92019, Auckland, New Zealand

**ABSTRACT:** Radiolarian faunas from seven localities of the well known Late Eocene Oamaru Diatomite were studied. All samples contained well preserved Radiolaria, generally of common or greater abundance, along with numerous sponge spicules and diatoms. Radiolarian faunal composition confirms a Late Eocene age for the Oamaru Diatomite. The Radiolaria are documented, with 24 new species described and three new genera erected. The new species are *Tricorporisphaera bibula*, *Zealithapium oamaru* (Actinommidae), *Plectodiscus runanganus* (Porodiscidae), *Plannapus hornibrooki*, *P. mauricei*, *Spirocyrtes greeni* (Artostrobiidae), *Botryocella pauciperforata* (Cannobotryidae), *Carpocanopsis ballisticum* (Carpocaniidae), *Verutotholus doigi*, *V. edwardsi*, *V. mackayi* (Neosciadiocapsidae), *Lithomelissa lautouri*, *Velicucullus fragilis* (Plagoniidae), *Lamprocyclas particollis* (Pterocorythidae), *Artophormis fluminafauces*, *Eucyrtidium ventriosum*, *Eurystomoskevos cauleti*, *Lophocyrtes* (L.) *haywardi*, *Lychnocanium alma*, *L. waiareka*, *L. waitaki*, *Pterosyringium hamata*, *Sethochytris cavipodis* and *Thyrsoyrtis* (T?) *pinguisicoides* (Theoperidae). The new genera are *Tricorporisphaera*, *Zealithapium* (Actinommidae), and *Verutotholus* (Neosciadiocapsidae). Emendations are proposed to the family Neosciadiocapsidae and the genus *Eurystomoskevos*, and *Pterosyringium* is raised from subgeneric to generic level.

## INTRODUCTION

Since its first recognition as a rock unit by McKay (1877), and the subsequent discovery of its siliceous microfossil content by Lautour in 1882 (although first described in Grove and Sturt 1886), the Oamaru Diatomite has been extensively studied, mainly by amateur microscopists. The first published account of microfossils from the unit (*ibid*) featured diatoms, and it is this group that has received the most attention, with numerous subsequent publications pertaining to them. Other microfossil groups are present in the diatomite including foraminifera, sponge spicules, calcareous nannoplankton, ostracods, silicoflagellates, and radiolarians, with all except the radiolarians having been studied taxonomically to some extent. Radiolaria are well preserved and common throughout the diatomite but until now no systematic description has been available. Passing mention of their presence has been made by Grove and Sturt (1886), Lautour (1889), Hinde and Holmes (1892) and Park (1918). Doig, in Edwards (1991), listed their abundance (as a ratio to diatoms) and distribution, and Sanfilippo (1990) recorded specimens from the Oamaru Diatomite in her study of the genus *Lophocyrtes*.

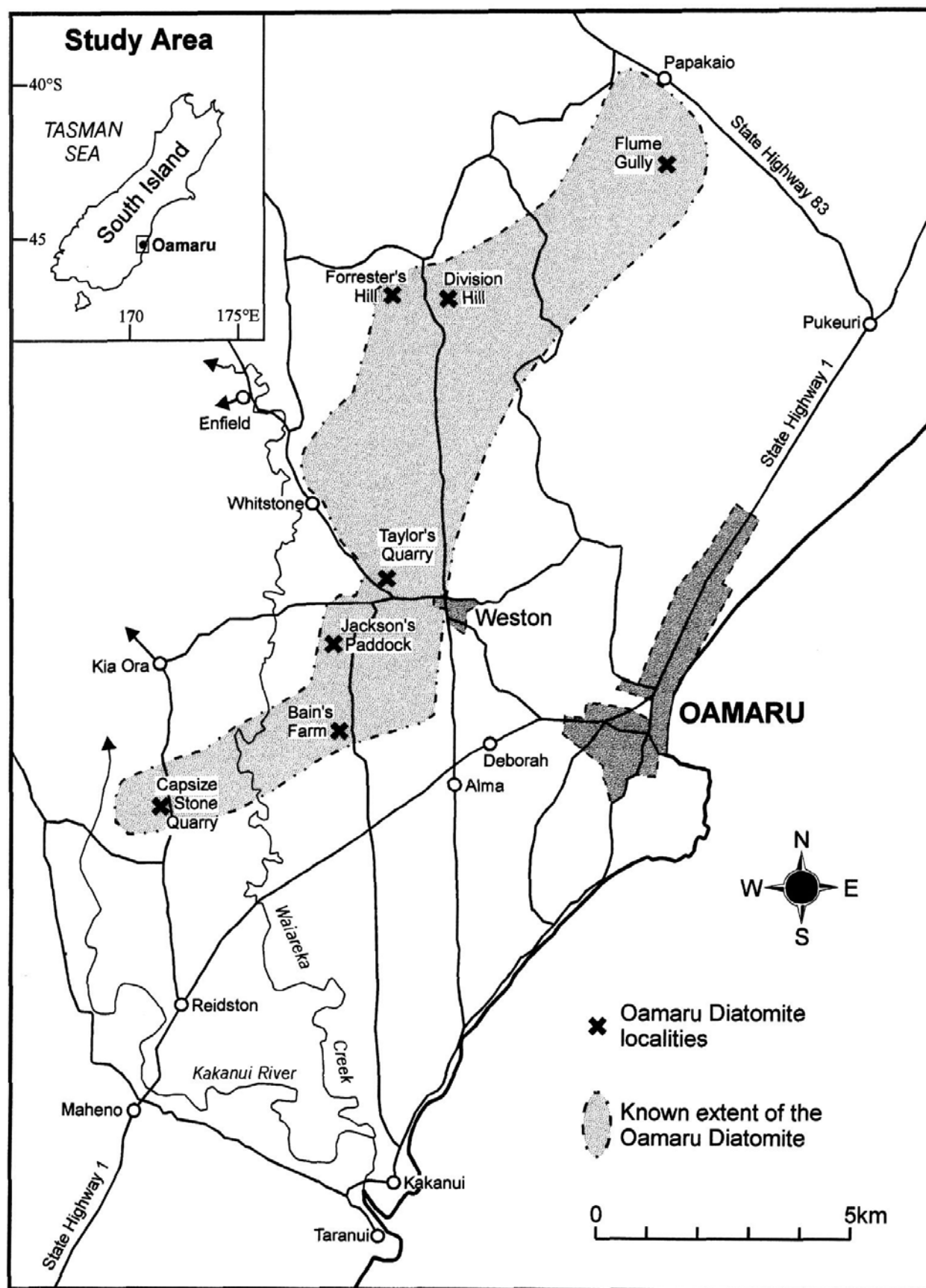
The Oamaru Diatomite is a member of the Waiareka Volcanics, a formation within the Late Eocene to Early Oligocene Alma Group of the Oamaru area, characteristic strata which consist of a complex interfingering of biogenic and pyroclastic sediments with pillow lavas and intrusives. The diatomite overlies tuff of the Lorne Pyroclastics and usually underlies, and is considered a lateral equivalent to the lower part of, the bryozoan-rich Ototara Limestone (Edwards 1991). Its known extent is a 17km long by up to 3km wide NE/SW-trending strip situated in the western part of

the Oamaru district (text-fig. 1), it covers an area of approximately 25km<sup>2</sup> and, where well exposed, ranges from 21m to 41m in thickness. Lithologically the Oamaru Diatomite is not a true diatomite, the diatom content varying considerably and the total siliceous content never greater than about 60%. In addition to the microfossils mentioned above there are also rare macrofossils and a varying clay and silt content. It is thought that the diatomite was deposited in a basin about 50km offshore, under quiet conditions in marginally tropical to warm subtropical waters of 75m to 150m depth. The basin, created by volcanism, was starved of terrigenous sediment, allowing it to be gradually filled with biogenic remains derived largely from plankton blooms maintained by nutrient-rich upwelling waters near the basin margin. For a detailed account of the history, fossil content, lithostratigraphic associations, paleoenvironment and mineralogy, and a comprehensive bibliography on the Oamaru Diatomite see Edwards (1991).

## MATERIALS AND METHODS

Twenty-three samples from seven localities (text-fig. 1) were studied. Approximate stratigraphic distances between samples (lowest number = oldest sample; see Table 1 for explanations of abbreviations) at each locality are as follows (from Edwards 1991):

BN1→BN2 - 2.1m; BN2→BN3 - 2.3m; BN3→BN4 - 1.7m; BN4→BN5 - 6.9m; BN5→BN6 - 1.7m; BN6→BN7 - 2.5m; BN7→BN8 - 4.4m; total stratigraphic distance - 21.6m, JP1→JP2 - 35.6m = total stratigraphic distance, FH1→FH2 - 3.8m; FH2→FH3 - 1.3m; total stratigraphic distance - 5.1m,



TEXT-FIGURE 1

Map of the Oamaru area showing the known extent of the Oamaru Diatomite and the localities of the studied samples.



TABLE 1

Sample information and abundances of new taxa. CQ - Capsize Stone Quarry, BN - Bain's Farm, JP - Jackson's Paddock, FH - Forrester's Hill, Division Hill, FG - Flume Gully, CS - Cormack's Siding (Taylor's Quarry). Abundances in italics are from picking tray counts, those in plain type are from strewn slides. See text for explanation of symbols.

Sample #	NZ Fossil Record # (J41/f)	Grid Reference (J41/f)	Density	Abundance	Age	<i>Tricorptisphaera bibula</i>	<i>Zedlithapium oamaru</i>	<i>Plectodiscus runanganus</i>	<i>Planapap hornibrooki</i>	<i>Planapap mauricei</i>	<i>Spirocystis greeni</i>	<i>Botryocella pauciperforata</i>	<i>Carpocarpopsis ballisticum</i>	<i>Verutolithus doigi</i>	<i>Verutolithus edwardsi</i>	<i>Verutolithus mackayi</i>	<i>Lithomelissa lautouri</i>	<i>Velicacanthus fragilis</i>	<i>Lumprocycas parvicollis</i>	<i>Artophormis fluminae</i>	<i>Eucyrtidium ventriosum</i>	<i>Eucystomoskevos cauleti</i>	<i>Lophocyrts (L.) haywardi</i>	<i>Lychnocanium alma</i>	<i>Lychnocanium waitareka</i>	<i>Lychnocanium waitaki</i>	<i>Pterocyringium hamata</i>	<i>Selchochyris caripodis</i>	<i>Thyrocyrtis (T. ?) pinguisoides</i>		
CQ1	8961	404637	C	A	eAr	-	-	R*	-	R	-	R	-	-	-	-	-	-	R*	-	R	R	-	-	-	-	-	F*	-	-	
BN1	8964	436652	A	A	"	-	R	R*	F	F	-	-	R	F	-	-	R	-	R	R*	R	-	R	R	-	R	R	R	-	R	
BN2	8965	"	E	A	"	-	R	F	F	R	-	-	R	R	-	-	R	-	F	F	R	-	R	-	R	R	R	F	-	R	
BN3	8966	"	C	C	"	-	-	R*	R	F	-	-	-	R	-	-	-	-	R	R	-	-	R	-	R	R	R	R*	-	R	
BN4	8967	"	A	E	"	-	-	-	R	C	-	-	-	F	-	-	-	R	R*	R	R	-	R	R	R	R	-	R*	-	R	
BN5	8968	438655	R	C	"	-	-	R*	R	R	-	-	R	-	-	-	-	-	R*	-	R	-	-	-	-	R	R	R	R	R	
BN6	8969	439651	C	A	"	-	-	R	R	R	-	-	R	R	-	-	-	R	R*	R	R	R	R	R	-	R	R	R	R	-	
BN7	8970	438655	C	A	"	-	-	-	R	R	-	-	F	R	-	-	R	-	R	-	R	-	-	R	R	R	R	R	-	-	
BN8	8971	439655	R	F	"	-	R	-	-	-	-	-	-	R	-	-	-	-	-	-	-	-	-	-	-	R	-	-	-	-	
JP1	8914	436668	F	A	"	R	R	R	R	-	-	-	-	F	-	R	-	R	R	R	R	-	-	R	R	-	R	-	-	-	
JP2	8882	438669	F	A	lAr	R	-	R	-	R	-	-	-	-	-	-	-	-	R	-	R	R	-	-	-	-	-	R	-	-	
FH1	8096	449734	C	E	lstAr	R	-	-	R	R	R	-	R	-	R	-	-	-	C*	-	-	R	R	-	-	-	-	R	-	-	
FH2	8195	"	F	E	eLwh	-	R	-	-	R	R	-	-	-	-	-	-	-	R	-	R	-	-	-	-	-	-	R	-	-	
FH3	8994	"	F	A	"	R	-	-	R	-	-	-	-	-	-	-	-	-	R	-	-	-	-	-	-	-	-	R*	R	-	
DH1	8196	459736	R	A	eAr	-	-	R	R	R	R	R	-	-	-	-	-	-	R	-	R	R	-	-	R	-	-	F	-	-	
DH2	8996	"	F	E	"	R	R	R	-	R	R	-	-	-	R	-	-	-	R	-	R	R	-	-	-	-	-	R	R	-	
DH3	8997	"	F	C	lAr	R	-	R	-	-	-	-	-	-	-	-	-	-	R	-	R	-	-	-	-	-	-	R	-	-	
FG1	8002	503760	E	E	eAr	R	R*	R	R	R	-	-	F*	A	R	R	R	R	F	R	R	-	-	R	C*	R	A*	R	-	-	
FG2	8197	"	A	E	"	R	-	R*	F	C	R	-	F*	F*	-	R	R	R	R*	-	R	-	R	R	C*	R	F*	R	R	R	
FG3	8003	"	C	A	"	-	-	R	R	R	-	-	C	R	-	R	-	-	R	-	R	-	-	R	R*	R	C	-	-	-	
FG4	8004	504761	A	E	"	-	R*	C*	-	R	-	-	R	R	-	-	-	-	R	-	R	-	-	-	-	R	-	A*	R	-	
FG5	8005	"	F	A	"	R	-	R	-	R	R	-	-	-	-	-	-	-	R	-	R	R	-	-	-	-	-	F	-	R	
CS1	8888	449679	A	A	"	-	-	R*	R	R	-	-	-	R	-	-	-	-	R	R	-	R	R	-	R	-	-	R	-	-	-

DH1→DH2 - 8m; DH2→DH3 - 4.6m; total stratigraphic distance - 12.6m,

FG1→FG2 - 1.3m; FG2→FG3 - 10.4m; FG3→FG4 - 1.3m; FG4→FG5 - 6.9m; total stratigraphic distance - 19.9m.

All samples were porous, low density, soft, cream siltstone, ie. typical Oamaru Diatomite. Virtually all yielded well preserved Radiolaria of common or greater abundance, as well as numerous diatoms and sponge spicules, and rare dinoflagellates and silicoflagellates (calcareous fossils were destroyed during processing).

Samples were processed and strewn slides and SEM stubs prepared as outlined in O'Connor (1994, 1997a). Categories of sample density and sample abundance are as follows:

	DENSITY		ABUNDANCE
	# rads/slide	# rads/tray	# rads/gram
Rare (R)	<50	<200	<20
Few (F)	50-200	200-800	20-100
Common (C)	201-500	>800	101-300
Abundant (A)	501-1000	-	301-800
Extremely Abundant (E)	>1000	-	>800

Abundances of new taxa on a strewn slide (22mm x 40mm) or picking tray (54mm x 76mm) are from a total count of each slide or tray and are as follows - **Rare** (1-4 per slide/1-15 per tray); **Few** (5-10 per slide); **Common** (11-20 per slide); **Abundant** (21-40 per slide). Table 1 lists locality information, density, abundance, and age for each sample, along with abundances of new taxa. Ages are **eAr** (early Runangan), **lAr** (late Runangan), **lstAr** (latest Runangan), and **eLwh** (early Whaingaroan) and are based on data from Edwards (1991). New taxa abundances in italics are from picking tray counts and those in plain type from strewn slides. An "\*" denotes that the count may be low due to breakage, making certain identification difficult. Table 2, following the species list, shows the distribution of the rest of the taxa identified in the studied samples.

Terminology for internal skeletal elements and external parts of the nassellarian skeleton is that used in O'Connor (1997a & b) with the following additional terms being applied:

for *Botryocella* (see text-fig. 4; pl. 1, fig. 21b) -  
**A-II**, **A-lr**: arches joining bar **A** to bars **II** and **lr**,  
**A-(A-II)**, **A-(A-lr)**: arches joining bar **A** to arches **A-II** and **A-lr**,  
**(A-II)-LI**, **(A-lr)-Lr**: arches joining arches **A-II** and **A-lr** to bars **LI** and **Lr**,  
**Vau**, **Val**: upper and lower vertical arches,

for *Carpocanopsis* (see text-fig. 5; pl. 2, fig. 5) -  
**cl, cr**: bars extending from central parts of arches **V-Ll** and **V-Lr** to cephalic wall,  
**A-cl, A-cr**: arches joining bar **A** to bars **cl** and **cr**,  
**(A-cl)-Cl, (A-cr)-Cr**: arches joining arches **A-cl** and **A-cr** to bars **Cl** and **Cr**,

for *Velicucullus* (see text-fig. 8; pl. 3, fig. 4b) -  
**A-D**: arch extending from bar **A** to bar **D**,  
**A-V**: arch extending from bar **A** to bar **V**,

for *Pterosyringium* (see text-fig. 14; pl. 4, figs. 21a, b) -  
**A-(V-Ll), A-(V-Lr)**: arches joining bar **A** to arches **V-Ll** and **V-Lr**.

Plates were prepared as follows: individual images were scanned directly from negatives (transmitted light negatives at a resolution of 800dpi, scanning electron micrograph negatives at a resolution of 600dpi) into Adobe Photoshop, where they were enhanced to uniform brightness and contrast, and unnecessary backgrounds erased. Completed images were imported into Corel Draw where they were resized, positioned, and plate and figure numbers, labels, scale bars, and arrows added. The resultant plates were printed on an ALPS Photocolour Printer.

## BIOSTRATIGRAPHY

From the samples investigated in this study a reasonably diverse radiolarian fauna consisting of approximately 127 species (24 new), from more than 50 genera (three new) has been documented (approx. 46 species of spumellarians, 65 species of cyrtids, and 16 species of spyrids). Of course this is not a full accounting of taxa as some species will have been inadvertently missed because of extreme rarity, while others have been grouped due to uncertain taxonomy (as in the case of some actinommids). Based on foraminifera and calcareous nannoplankton, the age of the Oamaru Diatomite has previously been determined as ranging from latest Eocene to earliest Oligocene (Runangan to early Whaingaroan) (Edwards 1991). The overall composition of the fauna in this study supports a Late Eocene (Runangan to earliest Whaingaroan) age for the Diatomite, using age ranges determined from DSDP Site 277 (Hollis et al. 1997). The presence of *Zealithapium mitra* and *Lychnocanium amphitrite* give an upper age limit of Late Eocene. Although *L. amphitrite* has been documented from the Early Oligocene of Northland (O'Connor 1993), those occurrences may have been due to reworking as it was not encountered that late at Site 277. Other taxa, eg. *Amphisphaera* aff. *spinulosa*, *Heliodiscus inca*, *Prunopyle fragilis*, *P. polyacantha*, *Spongopyle osculosa*, *Pseudodictyophimus gracilipes*, *Eucyrtidium spinosum*, have an earliest occurrence at Site 277 of Late Eocene and provide a lower age limit. No radiolarian taxa present indicate an Early Oligocene age for any of the studied samples, but it must be noted that not all stratigraphic levels from all localities were investigated, so Early Oligocene indicators may occur elsewhere in the Diatomite. Two species, *Spongodiscus cruciferus* and *Amphicraspedum prolixum*, are probably reworked as they normally only range up to the Middle Eocene.

## SYSTEMATIC PALEONTOLOGY

All type material is lodged with the Department of Geology, University of Auckland. Holotypes are on strewn slides and paratypes on strewn slides or scanning electron microscope

stubs. Individual specimens are identified by **R** (= Radiolaria), followed by a running number as allocated in the University of Auckland Department of Geology Catalogue of Type and Figured Specimens. Rock samples from which Radiolaria were obtained are stored at the Institute of Geological and Nuclear Sciences, Lower Hutt, and are quoted as follows: **J41** - NZMS260 map sheet reference, /**xxxx** - locality number in the archival New Zealand Fossil Record Files maintained by the Geological Society of New Zealand. Locality grid references refer to NZMS260 series topographic maps, scale 1:50 000, and read as follows: **J41** - map sheet reference, /**xxxxxx** - easting and northing from map sheet. The terms **cf.** and **aff.** are applied in the sense of Bengtson (1988).

Order SPUMELLARIA Ehrenberg 1875

Family ACTINOMMIDAE Haeckel 1862, emend. Sanfilippo and Riedel 1980

Subfamily ACTINOMMINAE Haeckel 1862, emend. Petrushevskaya and Kozlova 1972

Genus *Tricorporisphaera* O'Connor n. gen.

Plate 1, figures 1a-2; plate 5, figures 1a-3

*Description*: Test of three concentric spheroidal shells; inner medullary shell of generally regular porous structure, joined to outer medullary shell by six orthogonal primary bars; outer medullary shell and cortical shell of very irregular meshwork, joined by the six primary bars plus numerous other bars originating from and joining to pore bar junctions; primary bars extend outside as spines.

*Type Species*: *Tricorporisphaera bibula* O'Connor n. sp.

*Species included*: *Tricorporisphaera bibula* O'Connor n. sp. (described below).

*Etymology*: Combination of the Latin *tricorporis* (three-bodied), and *sphaera* (sphere) - refers to the three spheroidal shells.

*Discussion*: This genus is erected because no other genus possesses the same combination of morphological characteristics, and is included in the Actinommidae because of its concentric spheroidal nature. *Tricorporisphaera* differs from such structurally similar actinomid genera as *Hexastylus* Haeckel 1881, *Hexalonche* Haeckel 1881 and *Hexacontium* Haeckel 1881 by the irregular nature of the outer medullary and cortical shells and by their being joined by numerous bars, rather than just the six primary bars. The genera *Styptosphaera* Haeckel 1881, *Plegmosphaera* Haeckel 1881, *Spongoplegma* Haeckel 1881, and *Spongodictyum* Haeckel 1862 all appear similar to *Tricorporisphaera* but they lack the primary bars, and further differ in the following ways: *Styptosphaera* differs by consisting entirely of an irregular spongy framework with no regular inner structures, or cavities where they may have existed before dissolution; *Plegmosphaera* differs by consisting of a hollow spongy sphere, with no medullary shells; *Spongoplegma* differs by being a thick spongy framework with only one medullary shell; *Spongodictyum* differs as for *Spongoplegma* but has two medullary shells (it seems probable that *Plegmosphaera*, *Spongoplegma*, and *Spongodictyum* are synonymous [*Spongodictyum* would have priority], with one or both medullary shells having been subject to dissolution, [the same may also be true for *Hexastylus*, *Hexalonche*, and

*Hexacantium*, where *Hexastylus* would have priority)). *Peritivator* Pessagno 1976 is also similar to *Tricorporisphaera*, having irregular outer medullary and cortical shells, but it is ellipsoidal and has no radial bars or spines.

***Tricorporisphaera bibula* O'Connor n. sp.**

Plate 1, figures 1a-2; plate 5, figures 1a-3

**Description:** Inner medullary shell spheroidal, thin walled (often dissolved or extensively etched), smooth surfaced; pores circular to ovate, large with respect to pore bars, four to five on half equator, roughly hexagonally arranged; pore bars circular to elliptical in cross section.

Outer medullary shell spheroidal, of irregular meshwork; pores circular to subangular, irregular in size and distribution, generally large with respect to pore bars (up to approx. 55µm across); pore bars circular to elliptical in cross section.

Cortical shell as for outer medullary shell but pores tend to be slightly smaller (up to approx. 45µm across); surface rough due to irregular nature and small conical spines projecting from pore bars and pore bar junctions.

Six orthogonal, three-bladed, primary bars extend from surface of inner medullary shell to cortical shell, more stout between outer medullary shell and cortical shell than between inner and outer medullary shells; extend outside as six orthogonal, distally pointed, three-bladed spines (50-80µm long on observed specimens); outer medullary shell and cortical shells also joined by numerous other bars generally less stout than primary bars, circular to elliptical in cross section, extending from pore bar junctions of outer medullary shell to those of cortical shell.

**Dimensions:** Range of 20 specimens (Holotype measurement given in parentheses): diameter of inner medullary shell: 37-50µm (50µm); diameter of outer medullary shell: 108-165µm (165µm); diameter of cortical shell: 182-290µm (290µm).

**Etymology:** From the Latin *bibulus* (spongy) - refers to the irregular nature of the outer medullary and cortical shells.

**Holotype and Type Locality:** R386, Flume Gully (J41/f8002), Oamaru.

**Discussion:** *Tricorporisphaera bibula* differs from *Peritivator labyrinthi* Pessagno 1976 by being spheroidal, rather than ellipsoidal, and by having primary radial bars, and a cortical shell with generally smaller pores than the outer medullary shell; from *Peritivator ? dimitricai* Nishimura 1992 by having a much more irregular meshwork to the outer shells, a larger outer medullary shell with respect to the cortical shell, and primary radial bars; from *Styptosphaera ? spumacea* Haeckel 1887 (Nigrini 1970; Nigrini and Lombardi 1984) by having concentric shells, primary radial bars, and spines on the surface of the cortical shell; from *Actinomma kerguelensis* Caulet 1991 by having three, rather than four shells, outer shells with more irregularly sized and arranged pores, greater spacing between the outer two shells, and fewer bars connecting them.

**Genus *Zealithapium* O'Connor n. gen.**

Plate 2, figures 6-11; plate 5, figures 29a-32; plate 9, figure 47

**Description:** Shell conical, ovate or spheroidal, with narrow, latticed, conical upper part; bearing spine at narrow end; ap-

erture generally present opposite narrow end; pores generally large with respect to pore bars; surface smooth to rough.

**Type Species:** *Zealithapium oamaru* O'Connor n. sp.

**Species Included:** *Lithapium plegmacantha* Riedel and Sanfilippo; *L. anoectum* Riedel and Sanfilippo; *L. mitra* (Ehrenberg); *Zealithapium oamaru* O'Connor n. sp. (described below).

**Etymology:** *Zea* denotes the New Zealand occurrence of the type species; *Lithapium* is retained due to its common usage to the present time.

**Discussion:** Riedel and Sanfilippo (1970) tentatively assigned three species to the genus *Lithapium* Haeckel - *L. ? mitra* (Ehrenberg 1873), *L. ? anoectum* Riedel and Sanfilippo 1970 and *L. ? plegmacantha* Riedel and Sanfilippo 1970; (Nishimura 1990 as *L. ? sp.*) - saying that the assignment did not imply any relationship to the type species of the genus, ie. *L. pyriforme* Haeckel 1887 (p. 303, pl. 14, fig. 9). In addition they noted that *L. ? plegmacantha* and *L. ? anoectum* could also have been placed in either *Dorysphaera* Hinde 1890 or *Monostylus* Cayeux 1897 (subsequently synonymized with *Dorysphaera* by Squinabol 1903). Sanfilippo and Riedel 1973 (also see Riedel and Sanfilippo 1981) established an evolutionary relationship between the three species, positively assigned them to *Lithapium*, and postulated that *Entapium chaenapium* Sanfilippo and Riedel 1973 was the ancestor of the lineage. None of the three species included in *Lithapium* by Sanfilippo and Riedel resemble the type species, an ellipsoidal spumellarian with one polar spine, or other species subsequently assigned to the genus, eg. *L. halicapsa* Haeckel 1887, *L. monocyrtis* Haeckel 1887, *L. monoceros* (Rüst) 1885, *L. spinosum* Rüst 1898, *L. pruniforme* Rüst 1898, *L. aculeatum* Rüst 1898. Neither do they resemble the type species of *Dorysphaera*, *D. reticulata* Hinde 1890, nor other taxa assigned to that genus. The oldest member of the *Lithapium* lineage, *L. plegmacantha*, although spheroidal, has the narrow, latticed, conical upper part characteristic of members of the lineage (also see illustrations in Riedel and Sanfilippo 1981, 1986).

Because the three members of *Lithapium* constituting the lineage documented by Sanfilippo and Riedel (1973) are dissimilar to the type species of the genus, and to that of the other genus proposed for their placement, ie. *Dorysphaera*, it is herein proposed that the taxa comprising the lineage *L. plegmacantha*, *L. anoectum* and *L. mitra* be removed from *Lithapium* and placed in the newly erected genus *Zealithapium*, along with the obviously related new species, *Z. oamaru*, described below.

***Zealithapium oamaru* O'Connor n. sp.**

Plate 2, figures 6-11; plate 5, figures 29a-32

**Description:** Shell consists of upper narrow conical part and lower ovoid to spheroidal part (the terms upper and lower do not refer to orientation during life; they are convenient references to the two distinct parts of the shell); generally bearing conical spine at apex of narrow part; whole surface covered with conical spines originating from pore bar junctions, may be long (80-90µm); pores on upper part smaller than those on lower part, circular to subangular, roughly longitudinally aligned; contour change generally evident between upper and lower parts; pores on lower part large (approx. 2.3-3.8



times larger than those on upper part), circular to subangular, rough longitudinal alignment continuing from upper part; aperture constricted; termination generally ragged, often surrounded by downwardly directed spines, occasionally seen as a rim of pore bars.

**Dimensions:** Range of 24 specimens (Holotype measurement given in parentheses): length of spine at apex of upper part: 10-43µm (35µm); length of upper part: 36-62µm (45µm); length of lower part: 150-236µm (200µm); maximum width of shell: 167-214µm (180µm); maximum diameter of pores on upper part: 10-18µm (16µm); maximum diameter of pores on lower part: 33-55µm (38µm); maximum number of pores on half equator of lower part: 7-9 (8); maximum number of pores in longitudinal pore row of whole shell: 10-12 (10).

**Etymology:** The Maori name for the town which lends its name to the Oamaru Diatomite; used as a noun in apposition.

**Holotype and Type Locality:** R447, Flume Gully (J41/8002), Oamaru.

**Discussion:** *Zealithapium oamaru* differs from *Z. mitra* (pl. 9, fig. 47) by having two distinct parts separated by a contour change; from *Z. anoectum* by being larger, and by having less regularly arranged pores, a more spiny surface, and often long spines projecting from the surface; from *Z. plegmacantha* by possessing an aperture, and much larger, more irregular and irregularly arranged pores.

Family PORODISCIDAE Haeckel 1862, emend. Kozlova 1967

Genus PLECTODISCUS Kozlova

*Plectodiscus* Kozlova in Petrushevskaya and Kozlova 1972, p. 526. Type species: *Porodiscus circularis* Clark and Campbell 1942, p. 42, pl. 2, figs. 2, 6, 10, (O.D.).

***Plectodiscus runanganus* O'Connor n. sp.**

Plate 1, figures 3a-6; plate 5, figures 4a-7

**Description:** Test generally circular in equatorial plane, biconvex in cross section, margin rounded; consisting of inner spheroidal shell and 5-7 systems (terminology of Kozlova 1967) which, when viewed perpendicular to equatorial plane, may appear as concentric rings or as single or double spiral; inner 3 systems spheroidal to ellipsoidal, outer systems reduced to annular rings encircling test in equatorial plane, ie. only equatorial girdle (*ibid*) fully developed in these systems; in equatorial plane distance between systems increases slightly toward shell margin; systems connected by numerous bars radiating from and perpendicular to inner spheroidal shell, bars circular to elliptical in cross section; pores circular to elliptical, irregular in size and distribution on all systems, smallest on inner spheroidal shell; surface of test rough due to numerous proximally bladed (because of their origin from pore bars), distally conical radial spines projecting from pore bar junctions, spines perpendicular to inner spheroidal shell; low, discontinuous ridges following concentric or spiral pattern may be present on shell surface between spines; on some specimens large irregularly spaced conical spines project from shell margin (approx. 40-150µm long), coincident with radial bars.

**Dimensions:** Range of 35 specimens (Holotype measurement given in parentheses): diameter of shell excluding mar-

ginal spines: 160-240µm (210µm); total number of concentric rings, ie. number of systems plus inner shell: 6-8 (8); distance between outer 3 systems in the equatorial plane: 15-20µm (15-18µm).

**Etymology:** Refers to the Runangan occurrence in this study.

**Holotype and Type Locality:** R393, Cormack's Siding (Taylor's Quarry) (J41/f8888), Oamaru.

**Discussion:** *Plectodiscus runanganus* is included in *Plectodiscus* because it is biconvex in cross section with the first system having fully developed girdles (definition of Kozlova in Petrushevskaya and Kozlova 1972). It differs from similar members of the genus in the following ways: from *P. circularis* Clark and Campbell 1942 (Petrushevskaya and Kozlova 1972; Sanfilippo and Riedel 1973; Nishimura 1992) by being circular, rather than oval (although many specimens of *P. circularis* illustrated in those papers are circular), and by having more systems (6-8 cf. 4-6 for *P. circularis*), less distance between systems (15-20µm cf. 20-35µm for *P. circularis*), and pores irregular in size and distribution; from *P. bergontianus* Carnevale 1908 (Petrushevskaya and Kozlova 1972) by its generally smaller size (average diameter 190µm cf. 230-240µm for *P. bergontianus*) and by having a spiny surface and pores irregular in size and distribution. *Plectodiscus runanganus* appears similar to *Plectodiscus* sp. illustrated in Petrushevskaya and Kozlova (1972, pl. 19, fig. 14).

A specimen illustrated in Sanfilippo and Riedel (1973, pl. 31, fig. 7) as *Xiphospira circularis*, although similar to *P. runanganus*, differs by being less biconvex, and by having numerous and more regularly arranged marginal spines, and generally regularly arranged pores. However, the figured specimen differs from *X. circularis* (as defined in *ibid*, p. 526) by having more systems and less distance between them.

Order NASSELLARIA Ehrenberg 1875

Suborder CYRTIDA Haeckel 1862, emend. Petrushevskaya 1971a

Family ARTOSTROBIIDAE Riedel 1967a, emend. O'Connor 1997a

Genus *Plannapus* O'Connor

*Plannapus* O'CONNOR 1997a, p. 69.

**Type species:** *Dicolocapsa microcephala* Haeckel 1887, p. 1312, pl. 57, fig. 1, *sensu* O'Connor 1997a, (O.D.).

**Discussion:** The following taxa are considered to belong in *Plannapus* (some were transferred in O'Connor 1997a, the rest herein). Synonymies are not necessarily complete but are meant to convey the author's concept of the species:

*Dicolocapsa microcephala* Haeckel 1887, p. 1312, pl. 57, fig. 1, *sensu* O'Connor 1997a, p. 70, pl. 1, figs. 10-14, pl. 5, figs. 10-12, pl. 6, figs. 1-5 (as *Plannapus microcephalus*).

*Dictyocephalus australis* Haeckel 1887, p. 1306, pl. 62, fig. 1; Nishimura 1990, p. 163, figs. 35.7a-9b.

*Dictyocephalus mediterraneus* Haeckel 1887, p. 1307, pl. 62, fig. 2; Petrushevskaya 1969, figs. 8.7, 8; *Tricolocapsa papillosa mediterranea* (Haeckel), Petrushevskaya 1971b, figs. 91.7, 8.

*Dictyocephalus* sp. Petrushevskaya 1969, fig. 8.10;  
*Tricolocapsa* sp. B (Petrushevskaya), Petrushevskaya  
 1971b, fig. 91.10.

*Dictyocephalus* sp. Nishimura 1990, p. 165, figs. 35.6a, b.

*Eucyrtidium papillosum* Ehrenberg 1872a, p. 310, 1872b, p. 293, pl. 7, fig. 10; *Dictyocephalus papillosum* (Ehrenberg), Riedel 1958, p. 236, text-fig. 8, pl. 3, fig. 10; *Dictyocryphalus papillosum* (Ehrenberg), Nigrini 1967, p. 63, pl. 6, fig. 6; *Tricolocapsa papillosa* (Ehrenberg), Petrushevskaya 1971b, fig. 91.10.

*Plannapus hornibrooki* O'Connor n. sp. (below).

*Plannapus mauriceae* O'Connor n. sp. (below).

*Theocampe ? stathmepora* Foreman 1968, p. 54, pl. 6, fig. 16.

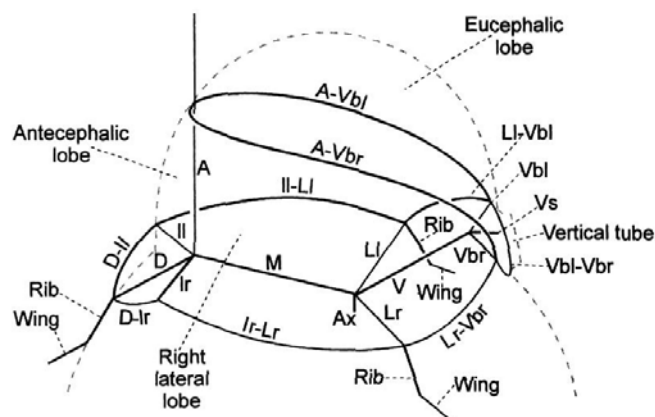
***Plannapus hornibrooki* O'Connor n. sp.**

Plate 1, figures 7a-10; plate 5, figures 8a-11

**Description:** Cephalis internally spheroidal, externally hemispheroidal to inflated truncate-conical because lower part enveloped by upper thorax; surface dimpled or with low, irregular, discontinuous ridges; bearing anteriorly offset, tiny, three-bladed apical horn; pores sparse, circular to subcircular, irregular in size and distribution; vertical tube at posterior base of cephalis, generally circular in transverse section, often externally expressed as very low truncate-conical protrusion (pl. 1, fig. 7a, b, 8a, b); collar stricture generally externally visible as slight change in shell contour.

Thorax truncate-ovoid; approximately same width distally as proximally, greatest width generally at mid-thorax; generally circular in transverse section but some specimens may be slightly laterally compressed; uppermost part envelopes lower cephalis; surface slightly rough due to dimples or low, discontinuous, irregular ridges; pores circular to subcircular, small, widely spaced, generally roughly quincuncially arranged, flush with thoracic surface; three internally distinct, externally indistinct ribs corresponding to **D**, **LI** and **Lr** may extend outside as tiny wings on mid to upper part of thorax; generally no marked external contour change between thorax and peristome; peristome short, often smooth (or less rough than thorax), internally cylindrical, externally inverted truncate-conical; aperture constricted; termination smooth.

Internal skeletal elements consist of bars **A**, **D**, **V**, **M**, **LI**, **Lr**, **II**, **Ir**, **Vbl**, **Vbr**, arches **A-Vbl**, **A-Vbr**, **LI-Vbl**, **Lr-Vbr**, **Vbl-Vbr**, **II-LI**, **Ir-Lr**, **D-II**, **D-Ir** and spines **Ax**, **Vs** (text-fig. 2; pl. 1, fig. 10); **A** extends freely upwards from **M** to wall of cephalis and extends outside as apical horn; **V** extends obliquely upwards from **M** to bars **Vbl** and **Vbr**; short **Vs** extends into vertical tube from intersection of **V**, **Vbl** and **Vbr**; **Ax** reduced to a node; **D** extends obliquely downwards from **M** to join thoracic wall, becomes rib, may extend outside as small wing; **LI** and **Lr** extend laterally to arches then continue obliquely downwards to join thoracic wall, become ribs, may extend outside as small wings; **II** and **Ir** extend laterally to join cephalic wall; arches **A-Vbl** and **A-Vbr** fused to cephalic wall, curve downwards from intersection of **A** with cephalis to join bars **Vbl** and **Vbr** at cephalic wall; bars **Vbl** and **Vbr** and arches **LI-Vbl**, **Lr-Vbr**, **II-LI**, **Ir-Lr**, **D-II**, **D-Ir** form ring at base of cephalis; arch **Vbl-Vbr** forms lower base of vertical tube.



TEXT-FIGURE 2

Schematic illustration of the internal skeleton of *Plannapus hornibrooki* (oblique lateral view, not to scale).

**Dimensions:** Range of 43 specimens (Holotype measurement given in parentheses): length of apical horn: 4-12µm (8µm); length of cephalis: 15-20µm (18µm); maximum width of cephalis: 26-37µm (35µm); length of thorax: 70-87µm (82µm); maximum width of thorax: 65-85µm (76µm); maximum number of pores on half equator of thorax: 8-11 (10); maximum number of pores in longitudinal pore row on thorax: 5-7 (7).

**Etymology:** In honour of Dr N. de B. Hornibrook for his vast contribution to micropaleontology and biostratigraphy, both in New Zealand and abroad, and in particular for his work on the Oamaru Diatomite.

**Holotype and Type Locality:** R401, Flume Gully (J41/f8003), Oamaru.

**Discussion:** *Plannapus hornibrooki* is placed in *Plannapus* because it is a two-segmented artostrobiid (see O'Connor 1997a). It differs from other members of the genus in the following ways (see Genus *Plannapus* for synonyms): from *P. australis* (Haeckel) by having a vertical tube that is larger in transverse section and not as prominent, pores that are flush with the surface of the thorax, smaller and more thoracic pores, and a shorter and less constricted peristome; from *P. mediterraneus* (Haeckel) by being more inflated and by having smaller, more and wider-spaced pores, no marked contour change between thorax and peristome, and dimples or ridges on the surface; from *P. microcephalus* (Haeckel) by having a smaller apical horn, larger thoracic pores, a less prominent vertical tube that is larger in transverse section, a dimpled or ridged thoracic surface, and by not being markedly laterally compressed in the sagittal plane; from *P. papillosum* (Ehrenberg) by having thoracic pores which are flush with the surface and more numerous and smaller, dimples or ridges on the thorax, markedly smaller wings, a shorter peristome with a smooth termination, and by not having a marked contour change between thorax and peristome; from *Plannapus* sp. (Nishimura) by being more inflated and by having dimples or discontinuous irregular ridges on the thorax, thoracic pores which are flush with the thoracic surface and more numerous, a less prominent vertical tube that is larger in transverse section, and a shorter peristome; from *Plannapus*



sp. (*Petrushevskaya*) by being more inflated, and by having more and smaller pores, pores which are flush with the thoracic surface, dimples or ridges on the thorax, and a shorter peristome with a smooth termination. *Petrushevskaya* (1969, fig. 8.9) illustrated as *Dictyocephalus mediterraneus*? a specimen that appears very similar to *P. hornibrooki* but has a longer peristome and is less inflated. It is also much younger, being dated in the figure caption as Recent.

***Plannapus mauricei* O'Connor n. sp.**

Plate 1, figures 11-14; plate 5, figures 12a-15

**Description:** Cephalis internally spheroidal, externally hemispheroidal to inflated truncate-conical because lower part enveloped by upper thorax; surface smooth to dimpled; bearing anteriorly offset, very short, three-bladed apical horn; pores sparse, circular to subcircular, irregular in size and distribution; generally unobtrusive vertical tube posteriorly located at base of cephalis, relatively large and generally circular in transverse section, may be expressed externally as very short, truncate cone (pl. 1, figs. 11, 12); collar stricture generally externally expressed as slight change in shell contour.

Thorax truncate-ovoid; approximately same width distally as proximally; widest part at or slightly below mid thorax; pores large, circular to subcircular, countersunk, hexagonally framed, generally quincuncially arranged, with generally slight size increase to widest part of thorax then slight decrease to peristome; low longitudinal ridges separating longitudinal pore rows begin just below collar stricture and terminate at peristome, zigzag slightly due to their origin as pore bars; distal-most pore row downward directed and pore bars join to peristome; three internally distinct, externally indistinct ribs corresponding to **D**, **Ll** and **Lr** may extend outside as tiny wings on upper thorax (pl. 5, fig. 15); no external contour change between thorax and peristome; peristome short, smooth, poreless, externally inverted truncate-conical, internally cylindrical; aperture constricted; termination smooth.

Internal skeletal structure as for *P. hornibrooki* except that arches **Ll-Vbl**, **Lr-Vbr**, **ll-Ll**, **lr-Lr**, **D-ll** and **D-lr** are not fused to cephalic wall, but are joined to it by short accessory bars and the extensions of bars **Ll** and **Lr**; bars **ll** and **lr** extend to arches, rather than to cephalic wall.

**Dimensions:** Range of 40 specimens (Holotype measurement given in parentheses): length of apical horn: 5-12µm (8µm); length of cephalis: 14-18µm (17µm); maximum width of cephalis: 28-35µm (30µm); length of thorax: 60-85µm (70µm); maximum width of thorax: 63-80µm (72µm); maximum number of pores on half equator of thorax: 11-15 (12); maximum number of pores in longitudinal pore row on thorax: 7-10 (8).

**Etymology:** In honour of my father, Maurice O'Connor.

**Holotype and Type Locality:** R409, Flume Gully (J41/f8005), Oamaru.

**Discussion:** *Plannapus mauricei* is placed in *Plannapus* because it is a two-segmented artostrobiid (see O'Connor 1997a). It differs from other members of the genus in the following ways (see *Plannapus* for synonymies): from *P. hornibrooki* O'Connor by having more and hexagonally framed thoracic pores that are not flush with the surface of the thorax (ie. countersunk), longitudinal ridges separating pore rows, and a downwardly directed pore row just before the peristome; from *P. australis* (Haeckel) by being more inflated, and by having

more thoracic pores, longitudinal ridges separating pore rows, a less prominent vertical tube that is larger in transverse section, no contour change between thorax and peristome, and a shorter peristome; from *P. mediterraneus* (Haeckel) by having more and hexagonally framed and countersunk thoracic pores, longitudinal ridges separating pore rows, no contour change between thorax and peristome, and a shorter peristome; from *P. microcephalus* (Haeckel) by not being laterally compressed in the sagittal plane and by having a shorter apical horn, more and larger and hexagonally framed and countersunk thoracic pores, longitudinal ridges separating pore rows, and a row of downwardly directed pores whose pore bars join to the peristome; from *P. papillosus* (Ehrenberg) by having more and regularly arranged thoracic pores, longitudinal ridges separating pore rows, and a shorter peristome that is not distinguished from the thorax by a contour change; from *Plannapus* sp. (Nishimura) by having a less prominent vertical tube that is larger in transverse section, more thoracic pores in a longitudinal pore row, more longitudinal pore rows, and a shorter peristome that is not distinguished from the thorax by a contour change; from *Plannapus* sp. (*Petrushevskaya*) by having a less prominent vertical tube, more thoracic pores, longitudinal ridges separating pore rows, a shorter peristome, and a smooth termination.

Genus *Spirocyrtis* Haeckel, emend. Nigrini 1977  
*Spirocyrtis* HAECKEL 1881, p. 438.

**Type species:** *S. scalaris* Haeckel 1887, p. 1509, pl. 76, fig. 14, (fide Campbell 1954, p. D142).

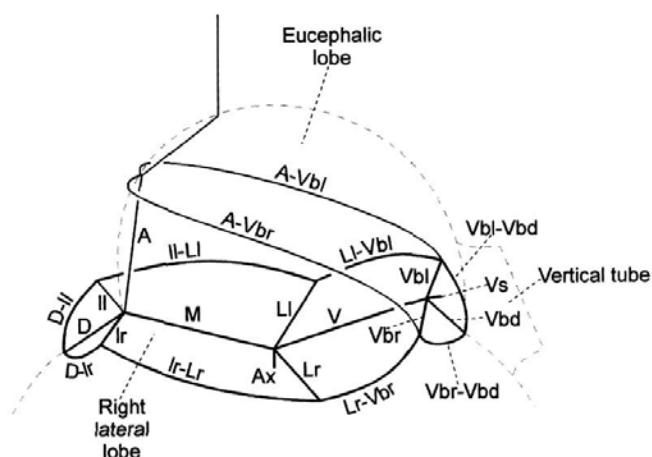
**Discussion:** Nigrini (1977) emended *Spirocyrtis* to include distally expanding artostrobiids with more than four segments, sharply rounded to angular intersegmental constrictions, a flared vertical tube, and an apical horn or tube. These features are present in *S. greeni*, although the vertical tube is not seen to flare and, rather than being an integral part of the cephalis, grows from the shell surface, generally being under-developed or lost due to breakage. In addition, the internal skeletal structure of *S. greeni* differs from that of other *Spirocyrtis* species investigated by the author and *S. scalaris* illustrated in Nishimura and Yamauchi (1984, pl. 40, fig. 11b as *S. cornutella*) by having bars **A**, **D**, **ll**, **lr**, **Vbl** and **Vbr** incorporated in the shell wall as distinct pore bars, rather than being free inside the cephalis as in *S. proboscis* O'Connor 1994 (1997a, pl. 11, fig. 2), *Spirocyrtis* sp. O'Connor (1997a, pl. 11, fig. 3) and *S. scalaris*. Bars **Vbl** and **Vbr** are also shorter and stouter than those of these three species. Because *S. greeni* precedes (and later occurs with) *S. proboscis* and *Spirocyrtis* sp. in the stratigraphic column, these differences may be ancestral, with "normal" elemental layouts and an integrated vertical tube forming in the later taxa.

***Spirocyrtis greeni* O'Connor n. sp.**

Plate 1, figures 15-20b; plate 5, figures 16a-19

? *Eucyrtidium acuminatum* (Ehrenberg). - BURY 1862, pl. 1, fig. 1.  
*Spirocyrtis*? sp. O'CONNOR 1993, p. 56, pl. 5, fig. 7, pl. 10, fig. 13

**Description:** Cephalis internally subspheroidal, externally hemispheroidal because lower part enveloped by upper thorax; surface rough due to presence of tiny thorns; bearing long, stout, conical, slightly anteriorly offset apical horn with small thorns beginning between 1/4 to 2/3 up its length, may curve distally; pores circular to subcircular, irregular in size and arrangement; two large pores on anterior cephalis, one at base of apical horn, the other just above collar stricture, both bisected by **A** (pl. 1,



**TEXT-FIGURE 3**  
Schematic illustration of the internal skeleton of *Spirocyrtis greeni*  
(oblique lateral view, not to scale).

fig. 19); eucephalic lobe apically opens into apical horn via pore which exits on lower posterior part of horn (pl. 1, fig. 20a); large pore on posterior base of cephalis (pl. 1, fig. 20a); large vertical tube grows from shell surface to surround large posterior pore and extends onto upper thorax (pl. 1, fig. 15, pl. 5, figs. 18, 19); collar stricture externally visible as contour change.

Thorax inflated truncate-conical to campanulate; greatest width reached above lumbar stricture; surface slightly rough due to irregularly distributed tiny thorns or, on rare specimens, low, discontinuous ridges on pore bars; pores circular to subcircular, transversely aligned; large anteriorly located pore just below collar stricture, bisected by **D** (pl. 1, fig. 19); lumbar stricture externally rounded, defined internally as smooth, poreless transverse ring.

Post-thoracic segments inflated truncate-conical to truncate-ovate to truncate-spheroidal; wider proximally than distally; each subsequent segment wider than previous one; surface smooth to slightly roughened by tiny thorns on pore bars; pores as for thorax, increasing in size on each subsequent segment; strictures same as lumbar stricture, may not be parallel to each other; termination ragged as though broken along pore row, probably because observed specimens are incomplete.

Internal skeletal elements consist of bars **A**, **M**, **D**, **V**, **Ll**, **Lr**, **Il**, **Ir**, **Vbl**, **Vbr**, **Vbd**, spines **Ax**, **Vs**, and arches **A-Vbl**, **A-Vbr**, **Ll-Vbl**, **Lr-Vbr**, **Vbl-Vbd**, **Vbr-Vbd**, **Il-Ll**, **Ir-Lr**, **D-Il**, **D-Ir** (text-fig. 3; pl. 1, figs. 19, 20a, b); bar **A** extends upwards from **M** to arches then continues obliquely upwards to top of cephalis, incorporated in anterior cephalic wall as pore bars which bisect two large anterior pores, projects outside as apical horn; bar **D** extends obliquely downwards from **M**, incorporated in thoracic wall as pore bar which bisects large anterior pore on upper thorax (pl. 1, fig. 19); **Il** and **Ir** incorporated in cephalic wall as pore bars at collar stricture (pl. 1, fig. 19); **Ll** and **Lr** extend laterally to join cephalic wall at collar stricture; **V** extends obliquely upwards from **M** to top of large posterior pore; **Vbl** and **Vbr** short, extend laterally from end of **V**, incorporated in cephalic wall as pore bars that delineate top of large posterior pore (pl. 1, fig. 20a); **Vbd** thin, extends obliquely downwards

from **V** just before intersection of **V** with **Vbl** and **Vbr** to join cephalic wall at base of large posterior pore (pl. 1, fig. 20a); spine **Vs** short, extends freely into vertical tube from intersection of **V**, **Vbl** and **Vbr**; spine **Ax** short; arches **Vbl-Vbd** and **Vbr-Vbd** form sides and base of large posterior pore (pl. 1, fig. 20a); from point about half way up **A**, ie. where **A** becomes obliquely upwardly directed, arches **A-Vbl** and **A-Vbr** curve downwards (pl. 1, fig. 19), incorporated in cephalic wall and join bars at collar stricture, often indistinct; arches **Ll-Vbl** and **Lr-Vbr** short, along with arches **ll-Ll** and **lr-Lr** form partial ring fused to cephalic wall at base of cephalis; arches **D-ll** and **D-lr** incorporated in upper thoracic wall.

*Dimensions:* Range of 31 specimens (Holotype measurement given in parentheses): length of apical horn: 24-54µm (35µm); length of cephalis: 16-22µm (17µm); maximum width of cephalis: 19-28µm (22µm); length of thorax: 19-40µm (26µm); maximum width of thorax: 36-52µm (40µm); maximum number of pores on half equator of thorax: 12-18 (14); number of transverse pore rows on thorax: 5-10 (8); length of abdomen: 21-35µm (27µm); maximum width of abdomen: 50-65µm (50µm); maximum number of pores on half equator of abdomen: 16-19 (16); number of transverse pore rows on abdomen: 5-12 (7); length of first post-abdominal segment: 23-41µm (36µm); maximum width of first post-abdominal segment: 61-98µm (78µm); maximum number of pores on half equator of first post-abdominal segment: 17-23 (23); number of transverse pore rows on first post-abdominal segment: 6-11 (8).

**Etymology:** In honour of Dr Colin Green of the Anatomy Department, School of Medicine, University of Auckland, for his endless patience and many hours of help in the use of the confocal laser scanning microscope (see O'Connor 1996).

*Holotype and Type Locality:* R419, Flume Gully (J41/f8005), Oamaru.

**Discussion:** The vertical tube of *Spirocyrtis greeni* is often missing or only partially present, probably because of breakage or dissolution. It differs from all other members of the genus in its internal structure (see discussion for *Spirocyrtis*), and by having a vertical tube that is not an integral part of the cephalis, and a distally thorned, conical apical horn. In addition it further differs from *S. gyrosularis* Nigrini 1977 by having fewer segments and generally more pores on them; from *S. scalaris* Haeckel 1887 by having rounded and fewer post thoracic segments; from *S. subscalaris* Nigrini 1977 by having a generally more distinct collar stricture and more pores on post cephalic segments; from *S. subtilis* Petrushevskaya (in Petrushevskaya and Kozlova 1972) by being generally wider and by having only one cephalic tube (if present), fewer segments, and generally more pores per post cephalic segment; from *S. proboscis* O'Connor 1994 by having only one cephalic tube (if present), and rounded post thoracic segments with more pores.

Later specimens of *S. greeni*, such as that illustrated in O'Connor (1993, pl. 5, fig. 7, pl. 10, fig. 13) from the early Oligocene of Northland, New Zealand, tend to have a rougher surface to the thorax and sometimes the abdomen. The pores are also generally larger than on specimens investigated herein and the thorax is often wider than the abdomen.

Bury (1862, pl. 1, fig. 1) illustrated, as *Eucyrtidium acuminatum*, a specimen that appears similar to *S. greeni* in general form but differs by having fewer pore rows per segment, and an apparently smooth termination, and the lower part of the

cephalis is not enveloped by the upper thorax. Another species, described and illustrated by Rüst (1898, p. 57, pl. XVI, fig. 16) as *Phormocampe helena*, although similar to *S. greeni*, is much older (described from Lower Jurassic coprolites), larger, and has a shorter, more stout apical horn, post-cephalic segments that are less inflated, and four transverse pore rows on each of the last few segments arranged so that two rows of large pores are located in the centre with a row of smaller pores adjacent to each stricture.

*Spirocyrtis greeni* is the oldest *Spirocyrtis* yet described, extending the range of the genus down to the latest Eocene. Nigrini (1985) extended the first occurrence of *Spirocyrtis subtilis*, then the oldest known member of the genus, from the lower *Stichocorys wolffii* Zone (as stated in Nigrini 1977) down to the mid-*Theocyrtis tuberosa* Zone, predating the original first occurrence by some 13+ Myrs. In Northland, New Zealand, rare occurrences of *S. subtilis* have been noted down to the lowermost Oligocene (upper *Cryptocarpium ornatum* Zone), predating Nigrini's new first occurrence by another 1-2 Myrs (O'Connor, unpublished data). *S. proboscis* also has a first observed occurrence in the upper *Cryptocarpium ornatum* Zone and neither of these taxa was seen in this study to occur with *S. greeni*.

Family CANNOBOTRYIDAE Haeckel 1881, emend. Riedel 1967b

Genus *Botryocella* Haeckel, *sensu* Petrushevskaya 1971b  
*Botryocella* HAECKEL 1887, p. 1116.

Type species: *Lithobotrys nucula* Ehrenberg 1873, p. 238, 1875, pl. 3, fig. 16, (*vide* Campbell 1954, p. D144).

**Discussion:** *Botryocella* is applied mostly in the sense of Petrushevskaya (1971b) to forms in which the eucephalic lobe is almost entirely sunken into the shell, so there is little or no contour change along the posterior margin of the cephalis, i.e. the eucephalic lobe does not bulge out of the cephalis to any great extent in lateral view, although it is not entirely enveloped by other cephalic lobes as occurs in *Centrobotrys* Petrushevskaya (1965). Parts of the eucephalic lobe are also exposed laterally. In addition the collar stricture is not externally well defined (see Petrushevskaya 1971b, fig. 78.XI, fig. 82.III, V). It differs from *Botryopyle* Haeckel 1881, (*sensu* Petrushevskaya 1971b) which has a protruding eucephalic lobe, i.e. a large bulge in the posterior contour of the cephalis, and generally an externally well defined collar stricture, and from *Acrobotrys* Haeckel 1881, (*sensu* Petrushevskaya 1971b) where the ante and postcephalic lobes terminate in long, well developed tubes. The use of this definition excludes many species previously assigned to *Botryocella*, e.g. *B. multicellularis* Haeckel 1887, *B. quadricellularis* Haeckel 1887, *B. appenninica* Vinassa de Regny 1900, some of which would be better placed in *Botryopyle*.

Riedel and Sanfilippo (1971) included a number of forms under the name *Botryopyle dictyocephalus* Haeckel group, many of which should probably be transferred to *Botryocella* as their eucephalic lobes are almost entirely sunken into the shell and they have little or no collar stricture. *Botryopyle dictyocephalus* has a protruding eucephalic lobe and a generally well defined collar stricture (see Haeckel 1887, pl. 96, fig. 6; Petrushevskaya 1965, fig. 6, 1971b, fig. 83).

*Botryocella pauciperforata* O'Connor n. sp.

Plate 1, figures 21a-24; plate 5, figures 20a-24

*Botryocella* sp. O PETRUSHEVSKAYA 1971b, figs. 82.V, VI.

*Botryopyle dictyocephalus* Haeckel group, RIEDEL and SANFILIPPO 1971, p. 1602, pl. 3F, figs. 9, 12 (*partim*); O'Connor 1993, p. 56, pl. 10, fig. 15.

*Botryocella* aff. *cribrosa* group, PETRUSHEVSKAYA and KOZLOVA 1972, pl. 39, fig. 4 (*partim*).

*Botryocella* sp. RIEDEL and SANFILIPPO 1977, pl. 15, fig. 9.

**Description:** Cephalis largest part of shell, distinctly lobed; surface mostly smooth; pores circular to subcircular, irregular in size and distribution; antecephalic lobe reniform, envelopes anterior of eucephalic lobe, apex often slightly elongate with large pores, i.e. vaguely tube-like but not apically open (pl. 1, figs. 21a, 23, pl. 5, figs. 20a, b, 23), central area of lobe generally poreless and dimpled; postcephalic lobe funnel-shaped, i.e. wide proximally and narrowing to a tube distally, tube short, circular to ovate in transverse section, downwardly-directed; upper part of postcephalic lobe envelopes lower posterior part of eucephalic lobe; eucephalic lobe externally hemispherical with internal posterior "neck", generally poreless or with very few pores, dimpled, externally delineated by furrow; lateral lobes small; collar stricture generally externally vague.

Thorax cylindroid, may be medially inflated, generally tapering distally; generally widest at or just after collar stricture; surface smooth; pores circular to subcircular, irregular in size and distribution; three small wings often present on upper thorax, corresponding to D, LI and Lr (pl. 1, fig. 21b); termination variable - sometimes smooth, poreless, inverted truncate-conical peristome with smooth, undulating or ragged termination, and slightly constricted aperture (pl. 1, figs. 23, 24, pl. 5, figs. 20a, b); sometimes aperture closed with flat porous base (pl. 1, figs. 22a, b).

Internal skeleton consists of at least bars D, A, M, V, LI, Lr, II, Ir, spines Ax, Vs, and arches A-II, A-Ir, A-(A-II), A-(A-Ir), (A-II)-LI, (A-Ir)-Lr, V-LI, V-Lr, II-LI, Ir-Lr, D-II, D-Ir, VAu, VAI (text-fig. 4; pl. 1, fig. 21b, pl. 5, fig. 24); D long, extends obliquely downwards from M to join cephalic wall at collar stricture, generally trifurcated with central branch extending obliquely downwards, may extend outside as small wing on upper thorax, other two branches extend obliquely upwards to join cephalic wall; A extends freely upwards from M but stops before top of cephalis (so technically a spine); V extends obliquely upwards from M to arches; Vs long, extends obliquely downwards from intersection of V, V-LI and V-Lr; II and Ir long, extending laterally to join cephalic wall; LI and Lr extend to arches then continue obliquely downwards to join cephalic wall, may extend outside as small wings on upper thorax; spine Ax moderately long, pointed; arches D-II, D-Ir, II-LI, Ir-Lr, V-LI and V-Lr form ring at base of cephalis; D-II and D-Ir fused to cephalic wall; II-LI and Ir-Lr fused to cephalic wall from II and Ir to about half way along their length, then free to LI and Lr; V-LI and V-Lr free of cephalic wall; arches VAu and VAI fused to cephalic wall at their apices, define upper and lower limits respectively of postcephalic lobe; from point about half way up A arches A-II and A-Ir curve downwards laterally, free at first then fused to cephalic wall, to join II and Ir at cephalic wall (pl. 5, fig. 24); from intersection of A-II and A-Ir with cephalic wall arches (A-II)-LI and (A-Ir)-Lr curve downwards posteriorly, fused to cephalic wall at first, becoming free to join LI and Lr at intersection of bars with V-LI and V-Lr; arches A-II, A-Ir, (A-II)-LI and (A-Ir)-Lr define lateral lobes; from point just before top of



A arches **A-(A-II)** and **A-(A-Ir)** curve laterally downwards (pl. 5, fig. 24), free of cephalic wall although may be joined to it by short lateral bars, intersect **A-II** and **A-Ir** approximately where they become fused to cephalic wall, define anterior limit of eucephalic lobe.

**Dimensions:** Range of 24 specimens (Holotype measurement given in parentheses): horizontal length of postcephalic lobe: 26-40µm (30µm); vertical length of antecephalic lobe: 60-77µm (70µm); vertical length of eucephalic lobe: 30-42µm (33µm); length of thorax: 55-70µm (65µm); maximum width of thorax: 57-73µm (60µm).

**Etymology:** From the Latin *pauci* (few), and *perforatum* (pierce) - refers to the generally poreless nature of the eucephalic lobe and central part of the antecephalic lobe.

*Holotype and Type Locality:* R427, Capsize Stone Quarry (J41/f8961), Oamaru.

*Discussion:* *Botryocella pauciperforata* differs from *B. nasuta* Ehrenberg 1873 (1875, as *Lithobotrys nasuta*) by having a flat, rather than curved, closure to the thorax (when closed), a larger eucephalic lobe with respect to the antecephalic lobe and a eucephalic lobe not completely sunken into the other lobes; from *Botryocella* ? sp. B Petrushevskaya 1965 by having a larger eucephalic lobe, a short tube off the postcephalic lobe, and a generally poreless eucephalic lobe and central area of the antecephalic lobe; from many of the specimens of *Botryocella* illustrated by Riedel and Sanfilippo (1971) as *Botryopyle dictyocephalus* by having a larger eucephalic lobe and a vague tube-like form to the upper antecephalic lobe; from *B. multicellaris* (in Petrushevskaya and Kozlova 1972) by lacking a tube at the base of the antecephalic lobe (as in *ibid.*, pl. 39, fig. 8) and by having a larger eucephalic lobe (cf. *ibid.*, pl. 39, fig. 10); from *Botryocella* sp. K Petrushevskaya (1975a) by not having an apical spine and long wings; from *Botryocella* sp. as illustrated in Riedel and Sanfilippo (1977, pl. 15, fig. 17) by having a tube off the postcephalic lobe instead of at the base of the antecephalic lobe.

Several authors have illustrated specimens that are herein synonymised with *B. pauciperforata* but gave no adequate description, eg. Petrushevskaya (1971b, figs. 82.V, VI), Riedel and Sanfilippo (1971, pl. 3F, figs. 9, 12, 1977, pl. 15, fig. 9). The specimen illustrated in Petrushevskaya and Kozlova (1972, pl. 39, fig. 4) as *Botryocella* aff. *cribrosa* group appears similar to *B. pauciperforata* and differs from *B. cribrosa* (Ehrenberg 1873, 1875) by possessing a tube off the postcephalic lobe.

Family CARPOCANIIDAE Haeckel 1881, emend. Riedel 1967b

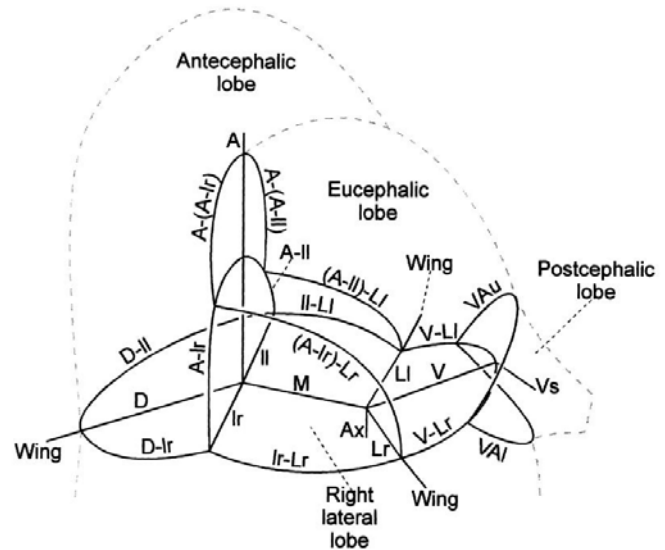
Genus CARPOCANOPSIS Riedel and Sanfilippo  
*Carpocanopsis* Riedel and Sanfilippo 1971, p. 1596.

*Type species:* *C. cingulatum* Riedel and Sanfilippo 1971, p. 1597, pl. 2G, figs. 17-21, pl. 8, fig. 8, (O.D.).

*Carpocanopsis ballisticum* O'Connor n. sp.  
Plate 2, figures 1-5; plate 5, figures 25a-28

?*Cryptoprora* cf. *ornata* Ehrenberg. - JOHNSON 1974, pl. 2, figs. 18-20.

*Cryptocarpium ornatum* (Ehrenberg). - HOLLIS et al. 1997, p. 66, pl. 6, figs. 23-25 (*partim*).



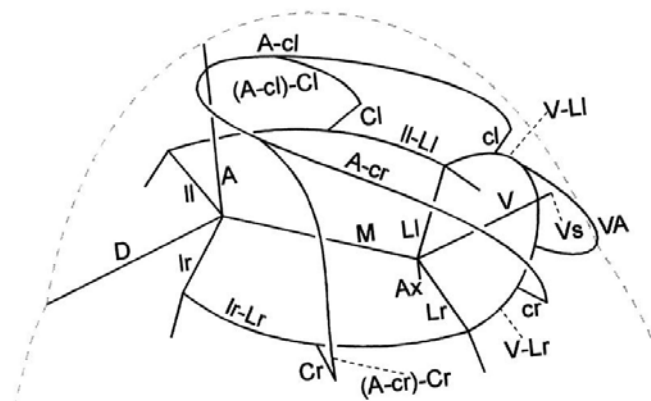
TEXT-FIGURE 4  
Schematic illustration of the internal skeleton of *Botryocella pauciperforata* (oblique lateral view, not to scale).

*Description:* Cephalis generally dome-shaped, rare specimens having very blunt point; pores circular to ovate, rarely subangular, generally irregular in size and distribution although some specimens show rough longitudinal alignment; collar stricture externally indistinct although on some specimens visible as slight contour change.

Thorax inflated cylindrical (wider distally than proximally) to inflated truncate-conical; generally greatest width reached above lumbar stricture; pores circular to subcircular, longitudinally aligned, rare pores may be out of alignment, may increase slightly in size to widest part of thorax then stay constant; longitudinal pore rows separated by low longitudinal ridges, on rare specimens ridges may extend onto cephalis; lumbar stricture generally externally indistinct, internally defined by transverse ring; ring may be porous, joined to shell by numerous bars.

Abdomen cylindroid (tapering slightly distally) to inverted truncate-conical; generally widest at or just below lumbar stricture; longitudinal pore rows and ridges continue from thorax; pores may become irregular in size and shape; ridges may continue to peristome but generally terminate above; when ridges terminate pores may become less regularly longitudinally aligned; peristome smooth, may have few irregularly sized and arranged dimples and/or circular to ovate pores; aperture slightly constricted; termination may be undulating (pl. 2, fig. 4) but generally consists of many distally pointed, lamellar feet irregular in length and width, proximally separated by arches.

Internal skeletal structure consists of bars **A**, **M**, **D**, **V**, **Ll**, **Lr**, **ll**, **lr**, **Cl**, **Cr**, **cl**, **cr**, arches **A-cl**, **A-cr**, (**A-cl**)-**Cl**, (**A-cr**)-**Cr**, **V-Ll**, **V-Lr**, **ll-Ll**, **lr-Lr**, **VA** and spines **Ax**, **Vs** (text-fig. 5; pl. 2, fig. 5); **A** extends freely upwards from **M** to top of cephalis, does not extend outside; **D** extends obliquely downwards from **M** to cephalic wall; bars **Ll**, **Lr**, **ll**, **lr** extend laterally to arches then continue to cephalic wall; **V** extends obliquely upwards from **M**



TEXT-FIGURE 5  
Schematic illustration of the internal skeleton of *Carpocanopsis ballisticum* (oblique lateral view, not to scale).

to arches; spine **Vs** extends into a cephalic pore from point where **V**, **V-Li** and **V-Lr** intersect; arch **VA** lies below **Vs**; bars **Cl**, **Cr**, **cl** and **cr** extend obliquely upwards from arches to cephalic wall; arches **ll-Li**, **lr-Lr**, **V-Li**, **V-Lr** form partial ring at base of cephalis, joined to cephalic wall by arch **VA**, bars **Cl**, **Cr**, **cl**, **cr** and extensions of bars **ll**, **lr**, **Li** and **Lr**; from point just below junction of **A** and cephalic wall arches **A-cl** and **A-cr** branch freely for a short way then fuse to cephalic wall and curve downwards to join **cl** and **cr** at cephalic wall; from point where **A-cl** and **A-cr** fuse to cephalic wall arches **(A-cl)-Cl** and **(A-cr)-Cr** branch and curve downwards, fused to cephalic wall, join to **Cl** and **Cr** at cephalic wall.

**Dimensions:** Range of 33 specimens (Holotype measurement given in parentheses): length of cephalis: 20-30µm (28µm); maximum width of cephalis: 40-48µm (42µm); length of thorax: 36-54µm (53µm); maximum width of thorax: 70-85µm (78µm); maximum number of pores on half equator of thorax: 13-16 (14); maximum number of pores in longitudinal pore row on thorax: 6-8 (8); length of abdomen: 44-105µm (105µm); maximum width of abdomen: 69-80µm (80µm); maximum number of pores in longitudinal pore row on abdomen: 5-9 (8).

**Etymology:** Derived from the Latin *ballista* (projectile) - refers to the projectile, or bullet-like, shape.

*Holotype and Type Locality:* R437, Flume Gully (J41/f8994), Oamaru.

**Discussion:** *Carpocanopsis ballisticum* is placed in *Carpocanopsis* because it is a robust carpoconiid with an abdomen separated from the thorax by an internally pronounced lumbar stricture (definition of Riedel and Sanfilippo 1971, p. 1596). It differs from other members of the genus in the following ways: from *C. bramlettei* Riedel and Sanfilippo 1971 by having a pored abdomen and a less well defined lumbar stricture; from *C. cingulatum* Riedel and Sanfilippo 1971 by having an abdomen that is not as sharply conical, longitudinally aligned abdominal pores proximally separated by longitudinal ridges, and a less densely pored cephalis; from *C. favosum* Haeckel 1887 (Riedel and Sanfilippo 1971) by not having a pronounced lumbar stricture and by having an abdomen that

narrows distally, rather than widening, and abdominal pores. The specimen illustrated in Sanfilippo et al. (1985, fig. 27.5) as *Carpocaniid* gen. *et* sp. indet. differs from *C. ballisticum* by having a distally tapering thorax. Hollis, in Strong et al. (1995, p. 208, figs. 11S, T), illustrated as *Cryptocarpium* cf. *ornatum* two specimens that have a "sparsely perforate hyaline fringe around the basal aperture" and an aperture that appears slightly constricted. They differ from *Carpocanopsis ballisticum* in the shape of the cephalis and the form of the peristome and termination.

*Carpocanopsis ballisticum* differs from *Cryptocarpium ornatum* (Ehrenberg) Sanfilippo and Riedel by having longitudinal ridges separating longitudinal pore rows, a distally narrowing abdomen, a peristome with a differentiated termination, and a definite carpocaniid internal cephalic structure (eg. see Petrushevskaya 1971a; Nishimura 1990; O'Connor 1997b). The internal cephalic structure of the Pterocorythidae is well documented (eg., Riedel 1958, Nigrini 1967, Petrushevskaya 1968, 1971a, b, 1975b, Nishimura 1990 [under the family Anthocorytidae], O'Connor 1997b), and its various elements are basically homologous between genera and species within the family. There are slight variations, with some species lacking bars **II** and **Ir**, and thus arches **D-II**, **D-Ir**, **II-LI** and **Ir-Lr**, and instead having arches **D-LI** and **D-Lr**. The distinguishing cephalic features of the family, the external cephalic lobes, are usually defined by furrows on the surface of the cephalis which are the external expressions of arches **A-LI** and **A-Lr**, which in turn are fused to the internal wall of the cephalis for their entire length. The internal skeleton of *Carpocanopsis ballisticum* is of an entirely different form to that of the Pterocorythidae. In addition to possessing several internal skeletal elements not present in pterocorythids it lacks arches **A-LI** and **A-Lr**, instead having arches **A-cl** and **A-cr** which are not fused to the cephalic wall for their entire length, are not expressed externally as furrows, and hence do not define external lobes. Instead, the cephalis of *C. ballisticum* is basically dome-shaped and externally unlobed.

The pterocorythid genus *Cryptocarpium* Sanfilippo and Riedel, from which all other members of the Pterocorythidae originate (see Sanfilippo and Riedel 1992), dies out in the Late Eocene with the extinction of *C. ornatum*. Near the end of its stratigraphic range the cephalis of *C. ornatum* becomes "as indistinct as in a typical carpocaniid" (Sanfilippo et al. 1985). Since in the Late Eocene *Carpocanopsis ballisticum* is definitely carpocaniid in form this may indicate that *C. ballisticum* originates directly from *Cryptocarpium ornatum*, and thus is the earliest member of the Carpocaniidae. The point where *C. ornatum* may become *Carpocanopsis ballisticum* is not known because detailed investigations of internal skeletal structures have not been carried out, but it is probably in the Late Eocene, as forms illustrated from earlier strata have a cephalis typical of *Cryptocarpium ornatum*, ie. spheroidal which may appear dome-shaped due to thickening of the encroaching thoracic walls cf. the definite dome-shaped cephalis with no thickened walls of *Carpocanopsis ballisticum*. Good examples of the spheroidal cephalis of *Cryptocarpium ornatum* are the mid-Eocene forms illustrated in Strong *et al.* (1995, figs. 11S, T) as *Cryptocarpium* cf. *ornatum*. The cephalis of these two illustrated forms can be plainly seen to be spheroidal, especially that of the second specimen (*ibid*, fig. 11T). Others are illustrated in Sanfilippo and Riedel (1992, pl. 2, figs. 18, 19), and Riedel and Sanfilippo (1971, pl. 3D, fig.10).



Johnson (1974, pl. 2, figs. 18-20) illustrated as *Cryptoprora* cf. *ornata* specimens which are tentatively synonymised with *Carpocanistrum ballisticum*, although they have a smooth surface and a cephalis that is more pointed and which appears poreless.

Family **Neosciadiocapsidae** Pessagno 1969, **emend.** herein

**Discussion:** In the erection of the family Neosciadiocapsidae Pessagno (1969) used several features as the basis for his family level classification (*ibid* p. 384), including the presence of a thoracic velum and the number of segments. It is agreed that the arrangement of cephalic elements, the presence of a vertical tube (cephalopyle of Pessagno) and the overall morphology (geometry of Pessagno) of the test are useful characteristics for classification at family level. However, the number of segments and the presence or absence of a velum are better suited to determinations at lower levels, as they are variable within families. The cephalic structure of the new genus *Verutotholus* is the same as that of the Neosciadiocapsidae as described in Pessagno (*ibid*, p. 392), with all the internal skeletal elements and a well developed vertical tube being present. The genus *Coniforma* Pessagno (*ibid*, p. 397) has a "prominent shelflike ridge which tends to frame the cardinal and cervical pores along the cephalic wall" and was only tentatively included in the family by Pessagno, partly because of this (see below). This "ridge" is actually the ring at the base of the cephalis formed by arches **V-LI**, **V-Lr**, **II-LI**, **Ir-Lr**, **D-II** and **D-Ir**. Many taxa assigned to the Neosciadiocapsidae by Pessagno have this ring (see *ibid*, *Petasiiforma glascoensis*, pl. 24, fig. 1, *P. formanae*, pl. 24, fig. 2, *Cassideus riedeli*, pl. 27, fig. 1, *Ewingella jonesi*, pl. 27, fig. 2, *Microsciadiocapsa lipmanae*, pl. 30, figs. 1, 2, *M. monticelloensis*, pl. 34, fig. 2, *M. madisonae*, pl. 36, fig. 2 and *Neosciadiocapsa diabloensis*, pl. 36, fig. 1 - in *M. madisonae* the arches are almost completely incorporated in the cephalic wall), although it is not nearly as prominent as in *Coniforma* (*ibid*, pl. 38, fig. 1), and it is also present in *Verutotholus*. A velum is not present in either *Verutotholus* or *Coniforma*, this being another reason for *Coniforma* only being tentatively assigned to the Neosciadiocapsidae. *Verutotholus* has three segments, with the thorax and abdomen being separated internally by a transverse ring. This transverse ring is present in some taxa assigned to the Neosciadiocapsidae, eg. *Ewingella guidaensis* Pessagno (*ibid*, pl. 29, figs. 7, 8) and *Sciadiocapsa ? baileyi* Pessagno (*ibid*, pl. 29, fig. 10), where it is described by Pessagno as a rim surrounding the thoracic mouth, and possibly in *Lipmanium sacramentoensis* Pessagno (*ibid*, pl. 26, figs. 11, 12), although it is described in the figure caption as a "crescent-shaped thoracic velum". In the opinion of the present author this makes these taxa tricyrtid, as the presence of this type of ring denotes internal segmentation, also externally expressed in these examples as a distinct change in shell contour. However, although Pessagno (*ibid*, p. 392) states in his definition of the family that members are dicyrtid, he does note (*ibid* p. 383) that "Whether or not the Neosciadiocapsidae are dicyrtid or tricyrtid is likely to remain a much debated issue". It appears that the family actually contains members of both morphologies.

In light of the above points it is herein proposed that the diagnosis of the family Neosciadiocapsidae be emended as follows - test of two or three segments, generally umbrella or helmet shaped; vertical tube present at base of cephalis; internal skeletal elements include bars **A**, **V**, **D**, **M**, **LI**, **Lr**, **II**, **Ir**, spine **Ax**,

and arches **A-LI**, **A-Lr**, **V-LI**, **V-Lr**, **II-LI**, **Ir-Lr**, **D-II**, **D-Ir** and possibly **VA** (eg. text-fig. 6; pl. 2, figs. 16, 20, 22b); post-cephalic segments internally separated by transverse ring, strictures may or may not be externally visible as distinct changes in shell contour; aperture may be covered by a velum. This emended definition allows *Verutotholus* to be accommodated in the Neosciadiocapsidae and also cements the position of *Coniforma* within the family. Both of these genera have the cephalic structure (internal skeletal elements and a vertical tube) of the Neosciadiocapsidae, and since cephalic structure may be considered the most important feature in family level radiolarian classification (eg., Riedel 1967a, 1967b, 1971; Foreman 1968; Goll 1968; Petrushevskaya 1971a; Takemura 1986; Nishimura 1990, etc.) they need to be included within that family. They also have the general gross morphology of the family, although lacking the pronounced distal "flair" of other members. The proposal that only forms with a vertical tube be included in the Neosciadiocapsidae, and not those with a vertical horn, excludes *Cassideus* Pessagno (*ibid*, p. 394), which appears synonymous with *Cycladophora* Ehrenberg (*sensu* Lombardi and Lazarus 1988, p. 101), but as a vertical tube is an important cephalic structural element then it must be considered an important feature in family level classification. The Artostrobiidae, also having a vertical tube, differ from the Neosciadiocapsidae by possessing bars **Vbl** and **Vbr** and hence arches **A-Vbl** and **A-Vbr**, rather than arches **A-LI** and **A-Lr** (see O'Connor 1997a & b for discussion on the internal skeletal structure of artostrobiids).

Foreman (1968) described and illustrated tentatively as *Clathrocyclas* three species - *C. ? diceros*, *C. ? lepta* and *C. ? hyronia*. All have the cephalic structural elements and overall morphology characteristic of the Neosciadiocapsidae. *Clathrocyclas ? diceros* and *C. ? hyronia*, having more than two segments and divisions in the form of internal rings (ledges of Foreman), may be related to *Verutotholus*. *Clathrocyclas ? lepta*, having only two segments, appears related to *Coniforma*, although it has thoracic ribs and wings. Close study of actual specimens would be needed to determine definite generic assignment.

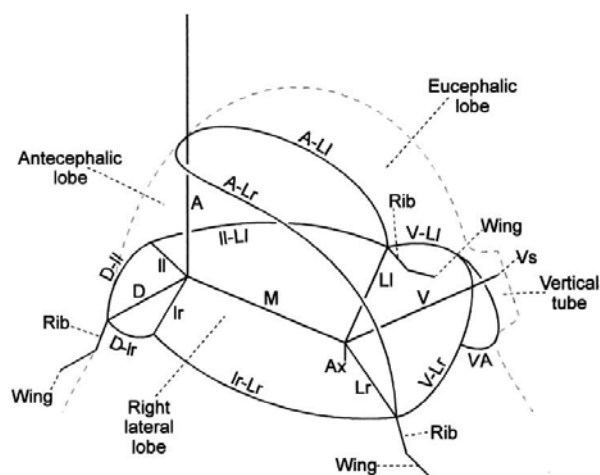
Genus **Verutotholus** O'Connor **n. gen.**

Plate 2, figures 12a-22b; plate 6, figures 1a-10b

**Description:** Shell of at least three segments; cephalis generally poreless and smooth-surfaced, externally inflated conical (internally variable), bearing stout apical horn and upwardly directed (usually), well developed vertical tube; has at least internal skeletal elements **M**, **A**, **V**, **D**, **LI**, **Lr**, **II**, **Ir**, **Vs**, **A-LI**, **A-Lr**, **V-LI**, **V-Lr**, **II-LI**, **Ir-Lr**, **D-II**, **D-Ir** and **VA** (text-fig. 6; pl. 2, figs. 16, 20, 22b); thorax inflated truncate-conical to truncate-ovoid, wider distally than proximally; three ribs corresponding to **D**, **LI** and **Lr** present in upper third, may extend outside as wings; abdomen variable; aperture not markedly constricted or covered by velum.

**Type Species:** *Verutotholus doigi* O'Connor **n. sp.**

**Species included:** *Verutotholus doigi* O'Connor **n. sp.** (described below); *V. edwardsi* O'Connor **n. sp.** (described below); *V. mackayi* O'Connor **n. sp.** (described below); possibly *Clathrocyclas ? diceros* Foreman; possibly *C. ? hyronia* Foreman.



TEXT-FIGURE 6

Schematic illustration of the internal skeleton of *Verutolithus doigi* (oblique lateral view, not to scale).

**Etymology:** Derived from the Latin *verutus* (provided with a dart), and *tholus* (cupola or dome) - refers to the general shape of the genus and its apical horn.

**Discussion:** *Verutolithus* is erected because no other genus possesses this combination of morphological characteristics, and it is placed in the Neosciadiocapsidae due to its cephalic structure and overall morphology. It differs from *Coniforma* Pessagno (1969, p. 397) by having three segments, with the thorax and abdomen being separated by an internal, transverse ring (the specimen illustrated in Petrushevskaya 1981, fig. 186, appears to have a ring but Pessagno 1969, p. 397, after "An examination of numerous well-preserved specimens of the type species of *Coniforma*" did not mention its presence), and by having thoracic ribs, and possibly wings, and a vertical tube that is directed upwards, rather than downwards. Although *Verutolithus* appears similar to the theoperid genera *Anthocyrtis*, *Clathrocyclas* and *Cycladophora*, it differs in the following ways: from *Anthocyrtis* Ehrenberg 1847a (chart to p. 54) by having a vertical tube (although Petrushevskaya 1971b, p. 177, fig. 93-3 illustrates a specimen of *A. mespilus* with a tube - see discussion for *Verutolithus edwardsi*, below) and thoracic ribs; from *Clathrocyclas* Haeckel 1881 (p. 434) by having a vertical tube and ribs in the thoracic wall (although Foreman 1968 described three species as *Clathrocyclas*, she did so doubtfully because they possessed vertical tubes and her usage is not followed here); from *Cycladophora* Ehrenberg 1872b (*sensu* Lombardi and Lazarus 1988) by having a vertical tube in place of a vertical horn and a thorax that is not differentiated into upper and lower parts by a contour change. *Verutolithus* has a cephalic structure similar to that of the artostrobiid genus *Plannapus* (see O'Connor 1997a) but possesses arches V-Li, V-Lr, A-Li and A-Lr and lacks bars Vbl and Vbr and arches A-Vbl and A-Vbr.

***Verutolithus doigi* O'Connor n. sp.**

Plate 2, figures 12a-16; plate 6, figures 1a-4

- ?*Pterocodon* ? *ampla* (Brandt), FOREMAN 1973, p. 438, pl. 5, figs. 3-5.  
 ?*Clathrocyclas universa* ? Clark and Campbell. - PETRUSHEVSKAYA 1975a, pl. 42, fig. 5.  
 ?*Clathrocyclas* sp. CAULET 1986, pl. 6, fig. 1.

**Description:** Cephalis internally spheroidal, externally inflated conical; surface smooth, poreless; bearing long, stout, three-bladed apical horn, often curved distally toward posterior, sometimes twisted; eucephalic lobe apically open into horn; horn generally proximally open toward posterior approx. 10µm-15µm above base (pl. 2, fig. 13a, b), if horn twisted opening directed laterally (pl. 2, fig. 12a); well developed, upwardly directed, posterior vertical tube at base of cephalis, circular to ovate in transverse section, externally expressed as short, cylindrical to truncate-conical protrusion; collar stricture often externally visible as change in shell contour.

Thorax inflated truncate-conical to truncate ovoid to bi-retta-shaped; uppermost part smooth and poreless, may be distally dimpled; remaining part porous, rough-surfaced due to nodes at pore bar junctions; pores circular to subcircular, hexagonally framed and arranged, increasing in size to widest part of thorax then decreasing slightly to lumbar stricture; rare specimens may have irregular pore arrangement and/or a few ovate pores; many specimens have centripetal growths within pores that, when broken, give pores rosette-shaped appearance; pores generally large with respect to pore bars; three ribs present in upper part (generally in smooth part), correspond to D, Li and Lr, may extend outside as very small wings from upper thorax (pl. 2, figs. 12b, c, 13b); lumbar stricture externally visible, defined internally by smooth, poreless ring.

Abdomen truncate-conical to inflated truncate-conical; generally smooth-surfaced; pores large, circular to subangular, generally arranged in rough transverse rows, pores in first transverse row may be smaller than those on thorax but rest generally larger than thoracic pores, generally increase in size distally then decrease again just before termination; termination smooth, may be slightly undulating; aperture not constricted or very slightly constricted by narrow, inward curved "lip" (pl. 2, fig. 13a).

Internal skeleton consists of bars A, M, V, D, Li, Lr, II, Ir, spines Vs, Ax, and arches A-Li, A-Lr, V-Li, V-Lr, II-Li, Ir-Lr, D-Li, D-Lr and VA (text-fig. 6; pl. 2, fig. 16); Ax reduced to a node; A extends freely upwards from M to join anterior wall of cephalis, continues outside as apical horn; bars D, Li and Lr extend obliquely downwards from M to join cephalic wall, continue as ribs in upper part of thorax, may extend outside as small wings; Li and Lr may bi- or trifurcate before joining cephalic wall; V extends obliquely upwards from M to juncture of V-Li and V-Lr; Vs projects freely into vertical tube from juncture of V, V-Li and V-Lr; bars II and Ir short; from juncture of A with cephalic wall arches A-Li and A-Lr curve downwards, fused to cephalic wall, join to bars Li and Lr at collar stricture; VA defines lower base of vertical tube and along with rest of arches forms ring at base of cephalis.

**Dimensions:** Range of 21 specimens (Holotype measurement given in parentheses): length of apical horn: 65-108µm (100µm); length of cephalis: 20-30µm (22µm); maximum width of cephalis: 28-40µm (35µm); length of thorax: 50-76µm (65µm); maximum width of thorax: 75-114µm (102µm); number of transverse pore rows on thorax: 5-7 (6); maximum number of pores on half equator of thorax: 8-11 (9); length of abdomen: 84-98µm, from 5 specimens (95µm); maximum width of abdomen: 105-156µm, from 6 specimens (130µm); number of transverse pore rows on abdomen: 5-6, from 5 speci-

mens (6); maximum number of pores on half equator of abdomen: 8-10, from 5 specimens (9).

**Etymology:** In honour of Mr A.J. Doig, well known amateur diatomist, for his considerable contribution to work on the Oamaru Diatomite.

**Holotype and Type Locality:** R456, Bain's Farm (J41/f8967), Oamaru.

**Discussion:** *Verutolithus doigi* differs from the similar looking theoperid *Theocyrtis ampla* Brandt (in Wetzel 1935; Clark and Campbell 1942 and Petrushevskaya 1971b, 1975a as *Clathrocyclas universa*; Sanfilippo and Riedel 1979 and Sanfilippo et al. 1985 (*partim*) as *Pterocodon ampla*) primarily by having a vertical tube, but also by having an apical horn that is more massive and always strongly three-bladed, a less well defined collar stricture, a smooth, poreless upper part to the thorax, more thoracic pores, larger abdominal pores, and a differentiated termination. Most specimens of *V. doigi* observed do not have a complete abdomen, rather it is broken so the aperture is surrounded by a row of tooth like projections, much like that of *T. ampla*, that are the remnants of the broken transverse pore row. *Calocyclas extensa* Clark and Campbell 1942, although similar in appearance to *V. doigi*, differs by having no vertical tube, and by having a less stout, conical apical horn, and abdominal pores similar in size and form to those on the thorax. *Verutolithus doigi* differs from *V. ? diceros* (Foreman) by having a bladed and single apical horn, a poreless cephalis, and an inflated truncate-conical to biretta shaped, rather than campanulate, thorax which is also much shorter; from *V. ? hyronia* (Foreman) by having only three segments, an upwardly, rather than downwardly, directed vertical tube, a poreless cephalis, and an inflated truncate-conical to biretta shaped, rather than campanulate, thorax.

The specimens illustrated in Foreman (1973, pl. 5, figs. 3-5), as *Pterocodon ? ampla*, are similar to *V. doigi* but differ by having a shorter and conical apical horn, often fewer thoracic pores, smaller abdominal pores, and a cylindrical abdomen. However, they are tentatively included in *V. doigi* as Foreman mentioned the presence of a vertical pore at the collar stricture. She also stated that they had only four collar pores, but the anterior pair (those separated by **D**) may have been overlooked as they are very small in *Verutolithus* (see pl. 2, figs. 16, 20, 22b).

Petrushevskaya (1975a, pl. 42, fig. 5) illustrated as *C. universa* ? with a "cephalo-tube in place of spine vert" a specimen which is herein tentatively included in *Verutolithus doigi*. It differs slightly by having a rough-surfaced cephalis and upper thorax.

The form illustrated in Caulet (1986, pl. 6, fig. 1) as *Clathrocyclas* sp. is also tentatively included in *Verutolithus doigi*. It differs by having a shorter apical horn, and a cylindrical abdomen, and it is not clear from the illustration whether it possesses a vertical tube.

***Verutolithus edwardsi* O'Connor n. sp.**

Plate 2, figures 17a-20; plate 6, figures 5a-8

**Description:** Cephalis externally inflated conical, internally lobed due to **A-Ll** and **A-Lr**, lobes generally externally defined by furrows on cephalic surface; surface smooth, poreless; bearing reasonably stout, proximally bladed apical horn, becomes distally conical, curved toward posterior; well developed, upwardly directed, posterior vertical tube at base of cephalis, circular to ovate in transverse section, externally expressed as

short, truncate-conical protrusion; collar stricture generally externally indistinct.

Thorax truncate-ovoid (wider distally than proximally) to inflated truncate-conical; maximum width generally at lower 2/3; uppermost part generally smooth, poreless, may be dimpled distally; remaining part porous, rough-surfaced due to nodes at pore bar junctions; pores circular to subcircular, generally hexagonally framed and arranged, increasing in size to widest part of thorax then decreasing slightly to lumbar stricture; occasionally few small pores may appear out of sequence; three ribs corresponding to **D**, **Ll** and **Lr** present in proximal part, become three long, stout, proximally bladed, downward curving wings extending from approx. 1/3 way down thorax; wings buttressed at base by pore bars; lumbar stricture externally visible, defined internally by transverse ring joined to shell by numerous extensions; transverse row of longitudinally elongate pores at lumbar stricture, upper half of each pore on thorax, lower half on abdomen.

Abdomen essentially narrow poreless band with lower half of transverse pore row at top; from base of abdomen extend many lamellar, straight or outwardly and/or downwardly curved, smooth, poreless, distally pointed feet, separated by arches.

Internal skeletal structure as for *Verutolithus doigi*, except that arches **A-Ll** and **A-Lr** are prominent inside cephalis (pl. 2, fig. 20), giving it lobed appearance internally, and are generally externally visible as furrows on cephalic surface; cephalis not apically open.

**Dimensions:** Range of 11 specimens (Holotype measurement given in parentheses): length of apical horn: 45-80µm, from 3 specimens; length of cephalis: 21-24µm (24µm); maximum width of cephalis: 30-36µm (32µm); length of thorax: 67-80µm (70µm); maximum width of thorax: 86-102µm (102µm); length of **D** wing: 50-100µm, from 2 specimens (100µm); length of **Ll** and **Lr** wings: 70µm, from 1 specimen; number of transverse pore rows on thorax: 7.5-9.5 (8.5); maximum number of pores on half equator of thorax: 10-12 (12); length of abdomen from internal ring to end of longest foot: 30-70µm (70µm); maximum width of abdomen between ends of diametrically opposed feet: 92-136µm (136µm); number of feet: 11-17 (17).

**Etymology:** In honour of A.R. Edwards, whose bulletin (Edwards 1991) guided the author to this present study, for his considerable contribution to work on the Oamaru Diatomite.

**Holotype and Type Locality:** R464, Flume Gully (J41/f8002), Oamaru.

**Discussion:** *Verutolithus edwardsi* differs from *V. doigi* in the form of the apical horn, by not having an apically open cephalis, by having three very conspicuous wings, and in the form of the abdomen; from *V. ? diceros* (Foreman) by having a single apical horn, a poreless cephalis, a truncate-ovoid to inflated truncate-conical, rather than campanulate, thorax, long thoracic wings, and a different form to the abdomen; from *V. ? hyronia* (Foreman) by having only three segments, a poreless cephalis, an upwardly, rather than downwardly, directed vertical tube, a truncate-ovoid to inflated truncate-conical, rather than campanulate, thorax, long thoracic wings, and a different form to the abdomen. *Verutolithus edwardsi* appears similar to *Anthocyrtis mespilus* Ehrenberg 1847 (Ehrenberg 1854; Petrushevskaya 1971b, 1981) but differs by having a vertical tube, a poreless cephalis and upper thorax, more and larger thoracic



pores, and three strong thoracic wings. One specimen of *A. mespilus* illustrated by Petrushevskaya (1971b, fig. 93 III) shows a vertical tube but the other two illustrated specimens do not. Petrushevskaya's specimens also have conical, rather than lamellar, feet, fewer thoracic pores, a pored cephalis, very short or no wings, and a conical base to the apical horn (they may not be specimens of *A. mespilus* as they differ somewhat from Ehrenberg's illustrations). *Verutotholus edwardsi* differs from similar *Clathrocyclas* taxa, eg. *C. principessa* Haeckel 1887, primarily by having a vertical tube and also by having wings. It differs from *Pterocodon campanella* Ehrenberg 1873, 1875; (Haeckel 1887) by having a vertical tube, a poreless cephalis and upper thorax, a wider thorax (with respect to its length), many more thoracic pores, proximally bladed wings, and in the form of the apical horn (Haeckel states "... short conical horn, half as long (as cephalis) ..." from a "...complete specimen examined by me, the apical horn, the three lateral wings and twelve terminal feet were well preserved").

***Verutotholus mackayi* O'Connor n. sp.**

Plate 2, figures 21a-22b; plate 6, figures 9a-10b

**Description:** Cephalis internally spheroidal, externally inflated conical; surface dimpled, poreless; bearing long, stout, three-bladed apical horn, often curved distally toward posterior, sometimes twisted; well developed, upwardly directed, posterior vertical tube at base of cephalis, circular to ovate in transverse section, externally expressed as short, cylindrical to truncate-conical protrusion; generally eucephalic lobe apically open into horn; base of horn, ie. where it joins cephalis, generally open proximally toward posterior, small blade divides opening (pl. 2, figs 21a, b); collar stricture generally indistinct.

Thorax inflated truncate-conical; greatest width reached at lumbar stricture; uppermost part smooth, poreless, may be distally dimpled; remaining part porous, rough-surfaced due to nodes at pore bar junctions; pores circular to subcircular, hexagonally framed and arranged, generally large with respect to pore bars, increasing in size to lumbar stricture; often transverse row of smaller pores just above lumbar stricture; many specimens have centripetal growths within pores that, when broken, give pores rosette-shaped appearance; three ribs present in upper part (generally in smooth part), correspond to **D**, **Ll** and **Lr**, may extend outside as very small wings from upper thorax (pl. 2, fig. 21b); lumbar stricture externally expressed as change in contour, internally as smooth, poreless ring.

Abdomen departs from thorax at 40°-60° angle (from vertical) then curves downward; only first three to four transverse pore rows preserved, surface generally smooth; pores large, circular to subangular, generally arranged in transverse rows, generally larger than thoracic pores although pores in first transverse row may be smaller than those on thorax, increase in size distally; termination ragged as though broken along pore row.

Internal skeletal structure as for *V. doigi* (pl. 2, fig. 22b).

**Dimensions:** Range of 9 specimens (Holotype measurement given in parentheses): length of apical horn: 30-61µm (40µm); length of cephalis: 22-25µm (25µm); maximum width of cephalis: 33-37µm (35µm); length of thorax: 60-71µm (60µm); maximum width of thorax: 95-110µm (100µm); number of transverse pore rows on thorax: 6-7 (6); maximum number of pores on half equator of thorax: 9-12 (11); width of abdomen: 140-166µm (140µm); number of pores on half equator of abdomen: 11-16 (12).

**Etymology:** Named for Mr A. McKay, the first person to recognise the Oamaru Diatomite as a distinct rock unit.

**Holotype and Type Locality:** R470, Jackson's Paddock (J41/f8914), Oamaru.

**Discussion:** *Verutotholus mackayi* appears similar to *V. doigi* but differs by having a dimpled cephalis, a shorter and less stout apical horn with a posterior opening that is situated at the base of the horn (not 10µm-15µm above the base) and is divided in two, the widest part of the thorax always at the lumbar stricture, a lumbar stricture expressed as a contour change, rather than a constriction, and a wider abdomen with more equatorial pores. The greatest width of the abdomen in *V. doigi* is generally reached at or near the termination, but in *V. mackayi* the abdomen is generally as wide as or wider than the maximum of *V. doigi* by the third pore row down from the lumbar stricture (the abdomen of *V. mackayi* is only preserved to about the third or fourth transverse pore row). In addition the abdomen of *V. mackayi* departs from the lumbar stricture at an angle of 40°-60° from the vertical, whereas that of *V. doigi* departs at 20°-30°. *Verutotholus mackayi* differs from *V. edwardsi* primarily by the form of the abdomen and by lacking the three large thoracic wings; from *V. ? diceros* (Foreman) by having a single and bladed apical horn, a poreless cephalis, an inflated truncate-conical, rather than campanulate, thorax, and a much shorter thorax; from *V. ? hyronia* (Foreman) by having only three segments, an upwardly, rather than downwardly, directed vertical tube, a poreless cephalis, an inflated truncate-conical, rather than campanulate, thorax, and an abdomen that flares markedly from the lumbar stricture.

Family PLAGONIIDAE Haeckel 1881, emend. Riedel 1967b

Genus *Lithomelissa* Ehrenberg, emend. O'Connor 1997a  
*Lithomelissa* EHRENBURG 1847b, p. 54.

**Type species:** *L. microptera* Ehrenberg 1854, pl. 36, fig. 2, 1873, p. 241, 1875, pl. 3, fig. 13, (by subsequent monotypy, *vide* Foreman and Riedel 1972).

***Lithomelissa lautouri* O'Connor n. sp.**

Plate 2, figures 23-27; plate 6, figures 11a-15

?*Lamptonium sanfilippae* Foreman, LING 1975, p. 729, pl. 9, fig. 23 (partim).

?*Lithomelissa* sp. CAULET 1986, pl. 2, fig. 6.

**Description:** Cephalis large, truncate-spheroidal, with short, inverted truncate-conical neck; bearing long, relatively stout, three-bladed, distally pointed, anteriorly offset apical horn; surface roughened by nodes at pore bar junctions; pores on spheroidal part circular to ovate, relatively large (average 8-9µm), roughly hexagonally framed and arranged, irregular in size although tending to be larger proximally; pores on neck generally more irregular in size, shape and distribution; often spongy overgrowth on neck; collar stricture externally distinct.

Thorax small, truncate-conical; surface relatively smooth; pores irregular in size, shape and distribution, some with small spines pointing towards pore centre; three straight, three-bladed, proximally buttressed, moderately long (approx. 40µm) wings project from upper thorax, correspond to **D**, **Ll** and **Lr** (pl. 6, fig. 11b); aperture not constricted; termination ragged as though broken through pores.

Internal skeletal elements consist of bars **A**, **D**, **M**, **V**, **LI**, **Lr**, **II**, **Ir**, **A<sub>1</sub>**, **II<sub>1</sub>**, **Ir<sub>1</sub>**, spine **Ax**, and arches **A-LI**, **A-Lr**, **D-II**, **D-Lr**, **II-LI**, **Ir-Lr** and **LI-Lr** (text-fig. 7; pl. 1, fig. 27); **A** very thin, extends straight upwards from **M** freely to top of cephalis, projects outside as apical horn; **D** extends obliquely downwards from **M** to thoracic wall, projects outside as wing; **LI** and **Lr** extend laterally to arches then obliquely downwards to thoracic wall, project outside as wings; **II** and **Ir** extend laterally to arches; **V** very thin, extends obliquely upwards from **M** to cephalic wall; spine **Ax** reduced to a node; from point approximately 1/5 up length of **A** arches **A-LI** and **A-Lr** extend laterally then curve downwards, free for their entire length, join **LI** and **Lr** at arches; from same point **A<sub>1</sub>** extends laterally in sagittal plane to join cephalic wall; approximately from points where **A-LI** and **A-Lr** begin to curve downwards bars **II<sub>1</sub>** and **Ir<sub>1</sub>** extend laterally to cephalic wall; arches **D-II**, **D-Lr**, **II-LI**, **Ir-Lr**, **LI-Lr** form ring at base of cephalis; **D-II** and **D-Lr** fused to cephalic wall; **II-LI**, **Ir-Lr** and **LI-Lr** generally joined to wall by short bars and extensions of bars **LI** and **Lr**; **LI-Lr** passes below **V**.

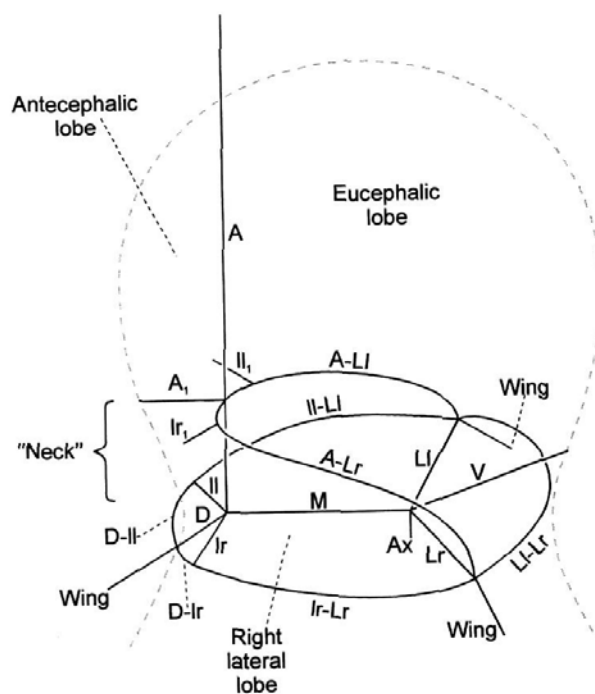
**Dimensions:** Range of 20 specimens (Holotype measurement given in parentheses): length of apical horn: 30-46, from 6 specimens; length of cephalis: 100-122µm (117µm); maximum width of cephalis: 97-120µm (100µm); maximum number of pores on half equator of cephalis: 14-19 (14); maximum number of pores on length of cephalis: 13-18 (14).

**Etymology:** Named for Dr H.A. de Lautour, the first person to recognise the siliceous microfossil content of the Oamaru Diatomite.

**Holotype and Type Locality:** R477, Bain's Farm (J41/f8964), Oamaru.

**Discussion:** This species is included in *Lithomelissa* because of its large spheroidal cephalis with bars **II** and **Ir** and in which **A** is free (see O'Connor 1997a). The thorax is always very short and has the appearance of being broken, probably because complete specimens have not been observed. This may mean that in life the thorax was larger and of a different form from that described above. Thoracic wings are also rarely seen, again, probably due to breakage.

*Lithomelissa lautouri* differs from morphologically similar taxa as follows: from *L. capito* Ehrenberg 1873, 1875, by being larger (Ehrenberg 1873 gives width of shell of *L. capito* as 59µm and length of cephalis as 68µm), and by having an apical horn, a generally more spheroidal cephalis with more and generally regularly arranged pores, a narrower collar structure, and longer, bladed wings; from *L. ehrenbergi* Bütschli 1882 (Haeckel 1887; Caulet 1986) by having a larger and more spheroidal cephalis with more and generally regularly arranged pores, and no vertical horn; from *L. buetschlii* Haeckel 1887 (Nishimura 1990) by having an apical horn, a larger cephalis with larger and fewer pores, no vertical horn, and no spines on the surface of the cephalis; from *Lophophaena capito* Ehrenberg 1873, 1875 (synonymised with *Lithomelissa ehrenbergi* in Haeckel 1887) by being larger (Ehrenberg 1873 gives width of cephalis as 66µm and length of cephalis as 60µm), and by having a more spheroidal cephalis with more and generally regularly distributed pores, and proximally buttressed, bladed wings; from *Dictyocryphalus capito* Ehrenberg 1872 by being larger (Ehrenberg 1872a gives length of cephalis as 62µm), and by having an apical horn, a generally more spheroidal cephalis



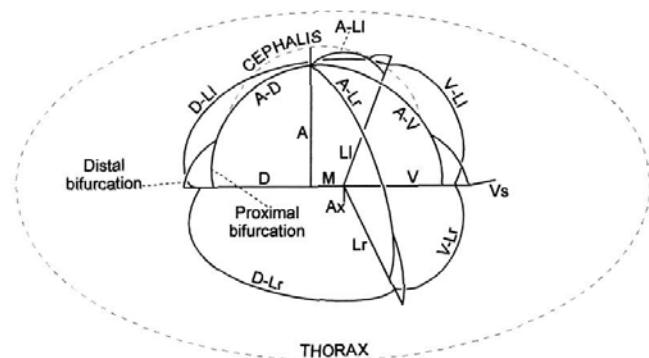
TEXT-FIGURE 7

Schematic illustration of the internal skeleton of *Lithomelissa lautouri* (oblique lateral view, not to scale).

with more, smaller and generally regularly arranged pores, a narrower upper thorax, and thoracic wings.

Four specimens illustrated in Petrushevskaya and Kozlova (1972, pl. 33, figs. 20-23) as *Lophophaena* ? *capito* group appear similar to *Lithomelissa lautouri* but have no apical horn or thoracic wings, and the specimens in figs. 20 and 21 are smaller than is normal for *L. lautouri*, although Petrushevskaya (in *ibid* p. 535) states that they differ from typical *Lophophaena capito* in their greater dimensions. Similarly, the specimen illustrated in Petrushevskaya (1975a, pl. 9, fig. 21) as *Lophophaena* ? *capito* group also resembles *Lithomelissa lautouri*, but is larger, has no apical horn or thoracic wings, and possesses a large thorax. The poor reproduction in both sets of illustrations makes it unclear whether the lack of apical horn and thoracic wings may be due to breakage, but all of the illustrated specimens differ from *Lophophaena capito* in the ways mentioned above, and the specimen in Petrushevskaya (1975a) shows no sign of thoracic wings even though it has a sizeable thorax. Petrushevskaya (1971b, figs. 56.XVII, XVIII) illustrated as *Lophophaena* sp. G two specimens which she later synonymised with the specimens in Petrushevskaya and Kozlova (1972). They differ from Petrushevskaya and Kozlova's specimens by being smaller and by having a distinct apical horn, and from *L. lautouri* by being smaller, and having generally smaller, fewer and irregularly arranged cephalic pores, smaller, more irregularly arranged thoracic pores, and the specimen in fig. 56.XVII has porous wings with a very broad base, rather than solid with a buttressed base. Ling (1975, pl. 9, fig. 23, as *Lamptonium sanfilippoae*) and Caulet (1986, pl. 2, fig. 6, as *Lithomelissa* sp.) both illustrated specimens that appear similar to *L. lautouri* (Ling's specimen is illustrated upside down), but Caulet's specimen is smaller than is usual for *L. lautouri*, and neither appear to have wings, al-





TEXT-FIGURE 8

Schematic illustration of the internal skeleton of *Velicucullus fragilis* (oblique lateral view, not to scale).

though this could be due to breakage. Since none of the above taxa have their internal structure described in any detail comparison on that basis is impossible.

Genus **VELICUCULLUS** Riedel and Campbell  
*Velicucullus* Riedel and Campbell 1952, p. 669.

*Type species: Soreuma magnificum* Clark and Campbell 1942, p. 51, pl. 4, fig. 15, (O.D.).

***Velicucullus fragilis* O'Connor n. sp.**

Plate 3, figures 1a-4b; plate 6, figures 16a-18

**Description:** Cephalis large, dome-shaped, indistinctly lobed, delicate; surface irregular, smooth; lobes may be externally defined by furrows; pores circular to subangular, irregular in size and distribution, not framed; pored growth at base of cephalis between bars **V**, **LI**, **Lr**, **M** and **D** (pl. 3, figs. 1a, b, 4b, pl. 6, fig. 16b); collar stricture externally distinct as sharp contour change.

Thorax almost discoidal; surface smooth; pores circular to subangular, roughly radially aligned, generally decreasing in size toward periphery; periphery ragged, probably due to breakage; very short velum generally positioned two pores in from periphery, spongy, distally tapering, not extending towards centre of shell (pl. 3, figs. 1a, b, c, 2, pl. 6, figs. 16a, b, 17).

Internal skeletal elements consist of at least bars **M**, **V**, **D**, **A**, **LI**, **Lr**, spines **Vs**, **Ax** and arches **A-D**, **A-V**, **A-LI**, **A-Lr**, **V-LI**, **V-Lr**, **D-LI** and **D-Lr** (text-fig. 8; pl. 3, fig. 4b); **M** very short; **A** extends freely upwards from **M** to join cephalic wall; bars **V**, **D**, **LI**, **Lr** extend laterally from **M** to join arches at collar stricture; **Vs** extends from intersection of **V**, **V-LI** and **V-Lr** as a pore bar then becomes free and may point obliquely upwards or straight outwards; **Ax** short; arches **V-LI**, **V-Lr**, **D-LI**, **D-Lr** form lobed ring at base of cephalis; from point just below junction of **A** with cephalic wall arches **A-D**, **A-V**, **A-LI**, **A-Lr** curve downwards freely at first then become fused to cephalic wall, bifurcate approximately 2/3 down their length, proximal branch of each arch joins to one of bars **D**, **V**, **LI**, **Lr** just prior to their junction with ring-forming arches, distal branch joins to pore bars adjacent to those bars; arches **A-D**, **A-V**, **A-LI**, **A-Lr**

define lobes, may be expressed externally as furrows on surface of cephalis where they are fused to cephalic wall.

**Dimensions:** Range of 26 specimens (Holotype measurement given in parentheses): maximum diameter of cephalis: 108-150µm (120µm); maximum diameter of thorax: 280-420µm (325µm); maximum number of pores in radial pore row on thorax: 8-10 (10); maximum number of pores on half circumference of thorax: 40-59 (49).

**Etymology:** Latin for fragile - refers to the fragile nature of the cephalis and thorax.

**Holotype and Type Locality:** R486, Flume Gully (J41/f8002), Oamaru.

**Discussion:** *Velicucullus fragilis* is placed in *Velicucullus* because it has a lobed cephalis, an almost discoidal thorax, and a spongy velum (definition of Riedel and Campbell 1952). Although a velum is generally regarded as covering the aperture of the thorax (eg., see Pessagno 1969), in the case of *Velicucullus* this does not appear to be the case, and in *V. fragilis* it is very reduced. No specimen of *V. fragilis* with an entire cephalis was seen in this study and generally all that remains is the upper part and the growth between bars at the base. The thorax is also probably incomplete so the periphery is ragged as though broken through pores. *Velicucullus fragilis* differs from *V. magnificum* (Riedel and Campbell 1952; Clark and Campbell 1942 as *Soreuma magnificum*) by having thoracic pores that decrease in size distally and are more numerous, no radial apophyses, and a smaller velum; from *Velicucullus* sp. (Sanfilippo and Riedel 1973, pl. 20, figs. 4-6; Blome 1992) by having thoracic pores that decrease in size distally, and no radial apophyses; from *Velicucullus* sp. (Sanfilippo and Riedel 1973, pl. 20, figs. 2, 3; Weaver and Dinkelman 1978) by having more thoracic pores and no radial apophyses; from *V. ? palaeocenica* Nishimura 1992 by lacking an apical horn, and by having a flatter thorax, thoracic pores that decrease in size distally and are more numerous, no radial apophyses, and a smaller velum; from *V. altus* Abelmann 1990 by having an almost discoidal thorax with pores that decrease in size distally; from *V. oddgurneri* Bjørklund 1976 by having a velum near the periphery, rather than more centrally located, and thoracic pores that decrease in size distally; from *Sethophormis umbrella* Haeckel 1887 by lacking a meshed surface to the cephalis, thoracic ribs and hexagonal thoracic pores.

Family **PTEROCORYTHIDAE** Haeckel 1881, emend. Moore 1972, *sensu* O'Connor 1997b

Genus **LAMPROCYCLAS** Haeckel, *sensu* Sanfilippo and Riedel 1992

*Lamprocyclas* Haeckel 1881, p. 434.

*Type species: L. nuptialis* Haeckel 1887, p. 1390, pl. 74, fig. 15, (S.D. Campbell 1954, p. D132).

***Lamprocyclas particollis* O'Connor n. sp.**

Plate 3, figures 5-11; plate 6, figures 19a-23

*Lamprocyclas "particollis"* O'Connor, HOLLIS et al. 1997, p. 66, pl. 7, figs. 1-7 (*nom. nud.*).

**Description:** Cephalis distinctly lobed, lobes may be externally visible as bulges; eucephalic lobe sits posteriorly above lateral lobes, opens apically into posterior of apical horn; apical horn anteriorly offset, stout, three-bladed, distally pointed, proximally open posteriorly, may distally curve towards posterior;

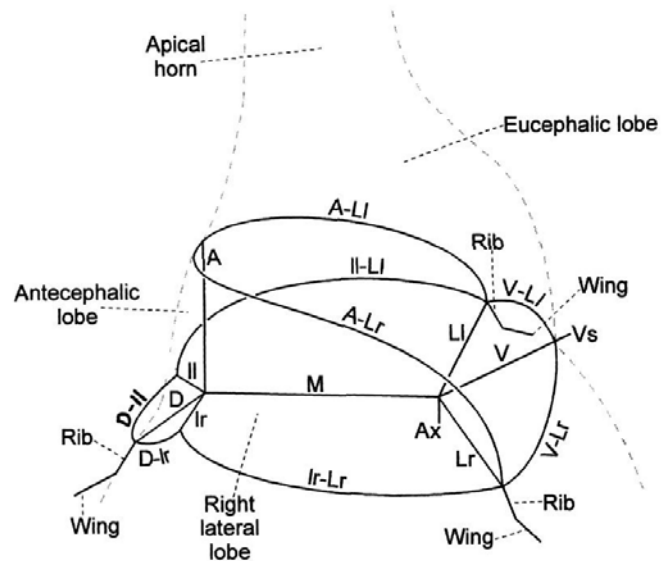
anterior blade of horn corresponds to **A**, longer than other two blades; pores circular to ovate, irregular in size distribution, although rough longitudinal alignment common; large pore sometimes present at anterior base of cephalis, bisected by **A** (pl. 3, fig. 10); two large, upwardly directed pores flank upper part of **A**, posterior bars of these pores form beginning of **A-Li** and **A-Lr** (pl. 3, fig. 10); very occasionally small vertical horn present (pl. 3, fig. 6); collar stricture externally distinct as change in shell contour.

Thorax inflated truncate-conical to campanulate; maximum width generally reached above lumbar stricture; pores circular to subcircular, rarely ovate, roughly longitudinally aligned on uppermost part of thorax, alignment becoming more regular distally and pores becoming generally quincuncially arranged; increase slightly in size distally to widest part of thorax then generally of constant size; longitudinal pore rows become separated by low longitudinal ridges approximately 1/4 to 1/3 down length of thorax; three short ribs corresponding to **D**, **Li** and **Lr** incorporated in upper thorax, occasionally project outside as one or two, rarely three, small wings on upper part of thorax (pl. 3, fig. 8); lumbar stricture may be externally visible as slight constriction, internally distinct as poreless transverse ring; at lumbar stricture many pores in lowermost pore row on thorax and uppermost row on abdomen indented due to pore bars being joined to internal transverse ring giving the appearance of transverse row of longitudinally elongate pores.

Abdomen variable, cylindrical (pl. 3, fig. 5, pl. 6, figs. 22, 23) to inverted truncate-conical (pl. 3, fig. 7, pl. 6, fig. 21) to inverted inflated truncate-conical (pl. 3, fig. 9); maximum width generally at or just below lumbar stricture; pores generally same size as those on thorax; longitudinal pore rows and ridges continue from thorax; ridges terminate at varying levels on abdomen below which pores may become irregular in size, shape and distribution, and surface of abdomen generally becomes smooth; peristome variable, may be smooth poreless band (pl. 3, fig. 7), or have tiny pores or dimples (pl. 3, fig. 6), or be only as wide as a pore bar (pl. 3, fig. 5); aperture generally slightly constricted; termination may be irregularly toothed (teeth small, not well developed) or undulating.

Internal skeletal structure consists of bars **A**, **D**, **M**, **V**, **Li**, **Lr**, **Il**, **Ir**, arches **A-Li**, **A-Lr**, **V-Li**, **V-Lr**, **Il-Li**, **Ir-Lr**, **D-Li**, **D-Lr** and spine **Ax**, occasionally small **Vs** (text-fig. 9; pl. 3, figs. 10, 11); **A** extends freely upwards to join cephalic wall, becomes anterior blade of apical horn; from point where **A** joins cephalic wall arches **A-Li** and **A-Lr** curve downwards, fused to cephalic wall, join to **Li** and **Lr** at collar stricture, define lateral lobes; rest of arches form ring at base of cephalis; **V** extends obliquely upwards from **M** to cephalic wall; **Vs**, if present, extends from intersection of **V**, **V-Li** and **V-Lr**, may extend outside as very short vertical horn; **D** extends obliquely downwards from **M** to thoracic wall, becomes rib incorporated in wall, may extend outside as small wing on upper thorax; **Li** and **Lr** extend laterally to cephalic wall, may trifurcate before joining wall, central branches become ribs incorporated in thoracic wall, may extend outside as small wings on upper thorax; **Ax** short.

**Dimensions:** Range of 70 specimens (Holotype measurement given in parentheses): length of apical horn: 55-102µm (90µm); length of cephalis: 35-52µm (40µm); maximum width of cephalis: 40-58µm (45µm); length of thorax: 58-90µm (80µm); maximum width of thorax: 100-135µm (120µm); maximum number of pores on half equator of thorax: 13-18 (17); maxi-



TEXT-FIGURE 9  
Schematic illustration of the internal skeleton of *Lamprocyclas particollis* (oblique lateral view, not to scale).

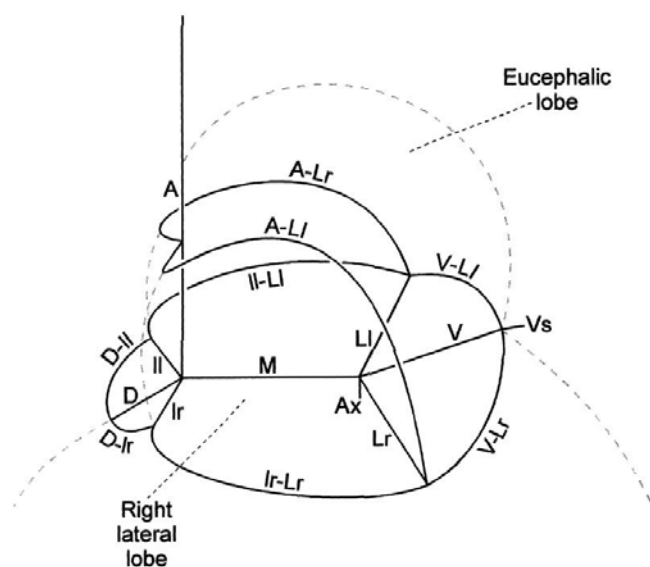
imum number of pores in longitudinal pore row on thorax: 7-11 (11); length of abdomen: 42-120µm (100µm); maximum width of abdomen: 107-142µm (125µm); maximum number of pores in longitudinal pore row on abdomen: 4-11 (8).

**Etymology:** Derived from the Latin *pars* (division), and *collis* (hill) - Latinisation of the type locality, used as a noun in apposition.

**Holotype and Type Locality:** R496, Division Hill (J41/f8996), Oamaru.

**Discussion:** This species has been placed in *Lamprocyclas* because of its distinct cephalic lobes, stout, bladed apical horn and differentiated peristome (definition of Sanfilippo and Riedel 1992). It is not included in *Albatrossidium* because it has a differentiated peristome and often exhibits appendages, and it differs from *Anthocyrtidium* Haeckel 1881 by not having an unusually elongate cephalis with the porous wall of the eucephalic lobe extending into the apical horn (definition of Sanfilippo and Riedel 1992). *Lamprocyclas particollis* differs from other, more typical *Lamprocyclas* by lacking an externally generally well defined lumbar stricture and well developed sub-terminal and/or terminal teeth, and by having an abdomen which is rarely much wider than the thorax, i.e. not very inflated, with pores generally the same size as those of the thorax.

*Lamprocyclas particollis* is a variable species, with only very rare specimens displaying the form seen to be characteristic of later members of the genus. The more typical form (pl. 3, fig. 6, pl. 6, figs. 19a, b) is of early *Lamprocyclas*, similar to that illustrated in Sanfilippo and Riedel (1992, pl. 1, fig. 10). One end member of its morphologic range resembles Late Eocene *Albatrossidium* (*ibid.* pl. 1, figs. 7, 12; pl. 3, fig. 5, pl. 6, figs. 22, 23), but differs by being more robust and by having low longitudinal ridges separating pore rows, and a differentiated peristome, rather than just peristomal teeth or a ragged termination. At the other end of the range are very rare specimens that more



TEXT-FIGURE 10  
Schematic illustration of the internal skeleton of *Artophormis fluminafauces* (oblique lateral view, not to scale).

closely resemble typical *Lamprocyclus* (pl. 3, fig. 9). All of these morphotypes have been included in the same taxon because they exhibit common features indicative of *Lamprocyclus*. They differ slightly in the shape of the abdomen and the general form of the peristome and termination but their cephalic and thoracic features are consistent with the diagnosis of *L. particollis*. The wide morphologic range seems to suggest an early form of *Lamprocyclus*, close to the point of origin of the genus from *Albatrossidium* in the Late Eocene *Lychnocanium bandyca* Zone (see Sanfilippo and Riedel 1992 for detailed discussion).

Family THEOPERIDAE Haeckel 1881, emend. Riedel 1967b

Genus *Artophormis* Haeckel

*Artophormis* Haeckel 1881, p. 438. Type species: *A. horrida* Haeckel 1887, p. 1458, pl. 75, fig. 2, (fide Campbell 1954, p. D139).

*Artophormis fluminafauces* O'Connor n. sp.

Plate 3, figures 12-16b; plate 6, figures 24a-27

**Description:** Cephalis internally spheroidal, externally truncate-spheroidal because lower part enveloped by upper thorax; surface smooth to roughened by small thorns at pore bar junctions; bearing thin, anteriorly offset, conical apical horn, generally longer than cephalis, may curve distally, may have few small thorns on distal part; pores circular to subcircular, irregular in size and arrangement, generally relatively large; collar stricture externally distinct.

Thorax inflated truncate-conical to hemispheroidal; surface rough due to nodes at pore bar junctions; greatest width reached just above lumbar stricture; pores circular to subcircular, generally hexagonally framed and arranged, rare pores have inwardly directed spines; generally transverse row of larger pores adjacent to collar stricture, pore bars of this row join cephalis to thorax; lumbar stricture externally distinct, defined internally as smooth, poreless, transverse ring attached to shell by numerous

short bars and also by pore bars of lowermost transverse pore row of thorax and uppermost transverse pore row of abdomen.

Abdomen truncate-conical to inflated truncate-conical; maximum width reached above stricture with post-abdominal segment, rarely narrower than thorax; surface as for thorax although often less rough; pores as for thorax, although on rare specimens may be irregular in size and arrangement; stricture externally visible as change in surface texture of shell, internally as smooth, peristome-like transverse ring; numerous short subterminal teeth originating from pore bars of last transverse pore row encircle base of abdomen.

Fourth segment cylindroidal, smooth-surfaced, thin-walled, very delicate; pores irregular in shape, size and distribution; transverse row of larger pores adjacent to stricture with abdomen; joined to abdomen by thin, delicate bars.

Internal skeletal elements consist of bars **A**, **M**, **V**, **D**, **Li**, **Lr**, **II**, **Ir**, spines **Ax**, **Vs**, and arches **A-Li**, **A-Lr**, **V-Li**, **V-Lr**, **II-Li**, **Ir-Lr**, **D-II** and **D-Ir** (text-fig. 10; pl. 3, figs. 16a, b); bar **A** extends upwards from **M** as distinct pore bar incorporated in anterior cephalic wall, projects outside as apical horn; bar **D** extends obliquely downwards from **M** as distinct pore bar incorporated in upper thoracic wall; bars **Li** and **Lr** extend laterally to arches; bars **II** and **Ir** extend laterally to arches as distinct pore bars incorporated in cephalic wall at collar stricture; bar **V** extends slightly obliquely upwards from **M** to arches; spine **Vs** conical, extends outside cephalis from junction of **V** with arches (pl. 6, fig. 26); spine **Ax** reduced to a node; from point approximately half way up length of **A** arches **A-Li** and **A-Lr** curve upwards then downwards, mostly incorporated in cephalic wall, join to bars **Li** and **Lr** at collar stricture; arches **D-II** and **D-Ir** incorporated in upper thoracic wall; rest of arches form partial ring at base of cephalis.

**Dimensions:** Range of 37 specimens (Holotype measurement given in parentheses): length of apical horn: 14-41µm (24µm); length of cephalis: 26-35µm (30µm); maximum width of cephalis: 30-40µm (38µm); length of thorax: 45-62µm (50µm); maximum width of thorax: 75-93µm (90µm); maximum number of pores on half equator of thorax: 11-15 (14); maximum number of pores on length of thorax: 5-7 (7); length of abdomen: 40-60µm (50µm); maximum width of abdomen: 85-112µm (105µm); maximum number of pores on half equator of abdomen: 13-18 (14); maximum number of pores on length of abdomen: 4-8 (6).

**Etymology:** From the Latin *fluminis* (stream), and *fauces* (narrow channel) - Latinisation of the type locality, used as a noun in apposition.

**Holotype and Type Locality:** R506, Flume Gully (J41/f8002), Oamaru.

**Discussion:** This species is included in *Artophormis* because it has four segments, a spheroidal cephalis, an ornamented apical horn, and a fourth segment generally more delicate and of different wall structure to the rest of the shell. In this context *Stichocorys coronata* (Carnevale, see O'Connor 1997b) and the species erected by Sanfilippo in Sanfilippo and Nigrini (1995), *Eucyrtidium plesiodiaphanes*, should probably be placed in *Artophormis*. Because of the delicate nature of the fourth segment of *A. fluminafauces* it is nearly always missing due to breakage or dissolution.

*Artophormis fluminafauces* differs from *A. gracilis* Riedel 1959 by having a cephalis with larger pores and in which **A**, **II** and **Ir** are incorporated as distinct pore bars (pl. 3, fig. 16a), a transverse row of large pores below the collar stricture, pores that are larger and more regularly arranged on the thorax and abdomen, abdominal and thoracic pores of the same size, a smoother-surfaced and thinner-walled shell, a truncate to inflated truncate-conical, rather than inflated annular, thorax, a more obvious lumbar stricture, a fourth segment lacking longitudinal ribs, and by the first three segments being generally longer than the 110-135µm reported by Sanfilippo *et al.* (1985). Specimens of *A. fluminafauces* that lack the fourth segment appear similar to late forms of *A. gracilis* (Late Oligocene-Early Miocene) but differ as above. *Artophormis fluminafauces* differs from *A. barbadensis* (Ehrenberg 1873) by having a large-pored cephalis with distinct **A**, **II** and **Ir**, a thin conical apical horn, thoracic and abdominal pores of the same size, an abdomen generally the same length as or shorter than the thorax, and a fourth segment that lacks proximal transverse bars connecting longitudinal spines; from *A. dominasinensis* (Ehrenberg 1873) by having a long thin conical apical horn, large-pored cephalis with distinct **A**, **II** and **Ir**, equal sized abdominal and thoracic pores, and an abdomen generally the same length as or shorter than the thorax; from *Stichocorys coronata* (Carnevale, see O'Connor 1997b) by having a large-pored cephalis, differently shaped thorax and abdomen, and by lacking a row of large pores adjacent to the lumbar stricture; from *Eucyrtidium plesiadiaphanes* Sanfilippo (in Sanfilippo and Nigrini 1995) as for *A. dominasinensis*, and by having, in addition, less distinct strictures. *Artophormis fluminafauces*, furthermore, first appears in older strata than do *A. gracilis*, *Stichocorys coronata* and *Eucyrtidium plesiadiaphanes*.

#### Genus *Eucyrtidium* Ehrenberg

*Eucyrtidium* EHRENBURG 1847a, p. 54. Type species: *Lithocampe acuminata* Ehrenberg 1844, p. 84; 1854, pl. 22, fig. 27 as *E. acuminatum*, (S.D. Frizzell in Frizzell and Middour 1951, p. 33)

**Discussion:** *Eucyrtidium* is a large genus comprising a wide variety of forms. It is applied herein partly in the sense of Petrushevskaya and Kozlova (1972) to forms where the upper part of the skeleton is broadly conical, because the lower part of the cephalis is enveloped by the upper thorax and the apical horn is relatively broad-based. It should be possible to subdivide this group to make the genus more manageable. For example forms with a well developed pore or small tube on the upper thorax may be transferred to *Phormocyrtis* Haeckel (as defined in Foreman 1973; see also O'Connor 1997b). It was noted during this study that some species of *Eucyrtidium* (*E. mariae* Caulet, *E. montiparum* Ehrenberg, *E. spinosum* Takemura, *Eucyrtidium* sp. below (pl. 9, figs. 14-17) and *E. ventriosum* O'Connor n. sp.) have a prominent, externally downwardly projecting **Vs** which may prove useful as a diagnostic character for generic definition. Further study is needed to confirm this.

#### *Eucyrtidium ventriosum* O'Connor n. sp.

Plate 3, figures 17-21b; plate 6, figures 28a-31

*Eucyrtidium* sp. A. LING 1975, p. 731, pl. 12, fig. 20.

*Eucyrtidium* sp. B. group O'CONNOR 1993, p. 73, pl. 8, fig. 11 (partim).

*Eucyrtidium montiparum* Ehrenberg, HOLLIS *et al.* 1997, p. 61, pl. 5, figs. 25-27 (partim).

**Description:** Cephalis internally spheroidal, externally hemispheroidal as lower part enveloped by upper thorax; surface smooth to slightly roughened by small nodes; generally shallow

anterior furrow corresponding to **A** (pl. 3, fig. 18); pores small, circular to subcircular, irregularly arranged, rare specimens poreless; bearing reasonably stout, conical, slightly anteriorly offset apical horn, at least as long as cephalis; horn may appear proximally bladed due to furrows caused by pores on uppermost cephalis extending onto proximal part of horn; collar stricture generally externally visible as change in contour.

Thorax inflated truncate-conical, widest at or just above lumbar stricture; surface rough due to nodes at pore bar junctions; pores circular to subcircular, generally hexagonally framed and arranged; three short ribs present in upper thorax corresponding to **D**, **LI** and **Lr**, may extend outside as small wings on upper thorax; lumbar stricture externally visible as contour change, internally as smooth, poreless, transverse ring joined to shell by numerous short bars.

Abdomen truncate-ovoid to inflated annular, widest at mid-height, generally slightly wider distally than proximally; surface and pores as for thorax; pores generally larger than those on thorax; stricture as for lumbar stricture.

Post-abdominal segments cylindroidal, surface smooth to slightly roughened by small nodes at pore bar junctions; pores circular to subcircular, may be larger than those on abdomen, generally longitudinally aligned, rare specimens have circular to ovate pores irregularly arranged; stricture between first and second post-abdominal segments generally externally indistinct, internally as for lumbar stricture although not always parallel to it; aperture not constricted; termination ragged as though broken along pore row.

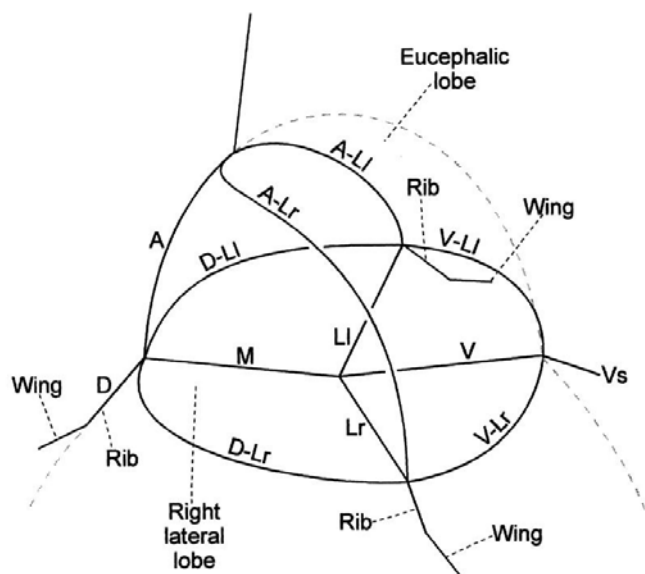
Internal skeletal elements consist of bars **A**, **M**, **D**, **V**, **LI**, **Lr**, spine **Vs** and arches **A-LI**, **A-Lr**, **V-LI**, **V-Lr**, **D-LI** and **D-Lr** (text-fig. 11; pl. 3, figs. 20a-21b); **A** incorporated in cephalic wall, generally externally expressed as shallow anterior furrow on cephalis (pl. 3, fig. 18), extends outside as apical horn; **D** extends obliquely downwards from **M** as rib in upper thoracic wall, may extend outside as small wing on anterior upper thorax; **LI** and **Lr** extend laterally to arches then continue downwards as ribs in upper thoracic wall, may extend outside as small wings on upper thorax; **V** extends obliquely upwards from **M** to arches; spine **Vs** stout, extends obliquely downwards from junction of **V** with arches, projects outside cephalis; from point where **A** exits shell arches **A-LI** and **A-Lr** curve downwards fused to cephalic wall to join to bars **LI** and **Lr**; rest of arches form ring at base of cephalis.

**Dimensions:** Range of 31 specimens (Holotype measurement given in parentheses): length of apical horn: 10-40µm (28µm); length of cephalis: 18-25µm (23µm); maximum width of cephalis: 25-34µm (26µm); length of thorax: 40-61µm (50µm); maximum width of thorax: 65-78µm (70µm); maximum number of pores on half equator of thorax: 10-13 (11); maximum number of pores on length of thorax: 6-8 (6); length of abdomen: 52-75µm (60µm); maximum width of abdomen: 95-115µm (100µm); maximum number of pores on half equator of abdomen: 13-15 (13); maximum number of pores on length of abdomen: 6-8 (7); length of first post-abdominal segment: 32-60µm (50µm); maximum width of first post-abdominal segment: 78-100µm (80µm).

**Etymology:** Latin for big-bellied - refers to the wide abdomen.

**Holotype and Type Locality:** R515, Flume Gully (J41/f8197), Oamaru.





TEXT-FIGURE 11  
Schematic illustration of the internal skeleton of *Eucyrtidium ventriosum* (oblique lateral view, not to scale).

**Discussion:** *Eucyrtidium ventriosum* differs from most members of *Eucyrtidium* by the abdomen being the widest part of the shell; from *E. buetschlii* Haeckel 1887 by having more than four segments, and a less distinct cephalis, and by lacking a constricted aperture and differentiated termination; from *E. cienkowskii* Haeckel 1887 by the abdomen being inflated annular to truncate-ovoid, rather than inflated truncate-conical, and by having better defined strictures; from *E. teuscheri* Haeckel 1887 by having generally smaller pores and a truncate-ovoid to inflated annular abdomen; from *E. calvertensis* Martin 1904 (as illustrated in Hays 1970) and *E. yatsuoensis* Nakaseko 1963 by having a larger apical horn and externally distinct strictures adjacent to the abdomen; from *E. apenninicum* Principi 1909 by being larger, and by having a pored cephalis, and more pores on all segments. Although superficially similar to some species of *Stichocorys*, *E. ventriosum* generally differs by having a less distinct cephalis, i.e. the collar stricture is much less distinct.

Ling (1975, pl. 12, fig. 20) illustrated, as *Eucyrtidium* sp. A, a specimen of *E. ventriosum* indicating its presence to the top of the *Cryptocarpium ornatum* zone, and it has also been encountered in the lower Oligocene of Northland, New Zealand (O'Connor, unpublished data).

Genus *Eurystomoskevos* Caulet, **emend.** herein  
*Eurystomoskevos* CAULET 1991, p. 536.

**Type species:** *E. petrushevskae* Caulet 1991, p. 536, pl. 3, figs. 14, 15, (O.D.).

**Discussion:** *Eurystomoskevos* is herein emended to accommodate a broader range of taxa than that allowed by the rigid definition of Caulet (1991). This is required to accommodate *E. cauleti* n.sp. (below) which, although similar to *E. petrushevskae*, differs by having a more distinct cephalis and a thorax that does not flare distally. The emended definition is: shell of two segments; pored cephalis may be indistinct or dis-

ting; bearing apical horn of varying stoutness; thorax variable, generally widening distally, pores large, termination ragged; three wings corresponding to **D**, **Li** and **Lr** present on upper thorax; internal skeletal structure consists of bars **A**, **D**, **V**, **M**, **Li**, **Lr**, **Il**, **Ir**, spine **Vs**, and arches **A-Li**, **A-Lr**, **V-Li**, **V-Lr**, **Il-Li**, **Ir-Lr**, **D-Li**, **D-Lr**; bars **D**, **Il** and **Ir** may be included in thoracic and cephalic walls as distinct pore bars; spine **Ax** present if **D**, **Il** and **Ir** free of cephalic wall.

Although *E. cauleti* n. sp. (below) is similar to some species assigned to *Diplocyclas*, it is not included in that genus because, as stated by Caulet (1991), its type species (*D. bicorona* Haeckel 1887) has a large vertical horn and a peristome, as do other taxa since assigned to *Diplocyclas* (eg. see Petrushevskaya 1975a).

*Eurystomoskevos cauleti* O'Connor n. sp.  
Plate 3, figures 22-26; plate 7, figures 1a-3

*Eurystomoskevos "cauleti"* O'CONNOR, Hollis et al. 1997, p. 61, pl. 5, figs. 4, 5 (nom. nud.).

**Description:** Cephalis internally subspheroidal, externally hemispheroidal as lower part enveloped by upper thorax; surface smooth, generally anteriorly furrowed, furrow corresponding to **A**; bearing thin, conical, anteriorly offset apical horn; pores circular to subcircular, irregular in size and arrangement, generally two large pores at anterior base of cephalis either side of **A**; collar stricture generally distinct as slight contour change.

Thorax variable, truncate-conical to inflated truncate-conical to truncate-ovate, may have slight distal flare, surface smooth; pores circular to subangular, large, rough transverse alignment common, may increase in size distally but generally irregular in size distribution; bars of pore row adjacent to cephalis join it to thorax; three short ribs corresponding to **D**, **Li** and **Lr** incorporated in upper thoracic wall, project outside as small wings on upper thorax; aperture generally not constricted, although slightly constricted on rare specimens; termination ragged.

Internal skeleton consists of bars **A**, **D**, **M**, **V**, **Li**, **Lr**, **Il**, **Ir**, spine **Vs**, and arches **A-Li**, **A-Lr**, **V-Li**, **V-Lr**, **Il-Li**, **Ir-Lr**, **D-Li** and **D-Lr** (text-fig. 12; pl. 3, figs. 23-26); **A** projects upwards from **M** as pore bar to anterior top of cephalis, extends outside as apical horn; **V** extends obliquely upwards from **M** to arches; spine **Vs** very short, projects freely from intersection of **V**, **V-Li** and **V-Lr**; bars **Li** and **Lr** extend obliquely downwards to join cephalic wall at collar stricture, become ribs incorporated in thoracic wall, project outside as small wings on upper thorax; **D** extends obliquely downwards from **M** as pore bar to collar stricture, becomes rib incorporated in thoracic wall, projects outside as small wing on upper thorax; bars **Il** and **Ir** extend laterally as pore bars; from about 2/3 up length of **A** arches **A-Li** and **A-Lr** curve downwards initially as pore bars then incorporated in cephalic wall, join to **Li** and **Lr** at collar stricture; rest of arches partially incorporated in cephalic wall as pore bars, internally define collar stricture.

**Dimensions:** Range of 35 specimens (Holotype measurement given in parentheses): length of apical horn: 4-25µm (20µm); length of cephalis: 15-23µm (18µm); maximum width of cephalis: 22-31µm (25µm); length of thorax: 55-95µm (70µm); maximum width of thorax: 60-96µm (60µm); maximum number of pores on half equator of thorax: 5-8 (6); maximum number of pores on length of thorax: 5-10 (7).



**Etymology:** In honour of Dr J.-P. Caulet, who erected the genus *Eurystomoskevos*, for his considerable contributions to radiolarian micropaleontology.

**Holotype and Type Locality:** R524, Division Hill (J41/f8196), Oamaru.

**Discussion:** *Eurystomoskevos cauleti* differs from *E. petrushevskae* Caulet (1991) by having a smaller apical horn, a more distinct cephalis, bars **D**, **II** and **Ir** as pore bars, and a thorax that generally does not flare.

Genus *Lophocyrtis* Haeckel  
*Lophocyrtis* HAECKEL 1887, p. 1410.

**Type species:** *Eucyrtidium stephanophorum* Ehrenberg 1873, p. 233, 1875, pl. 8, fig. 14 = *Lophocyrtis* (*L.*) *jacchia* (Ehrenberg 1873), Sanfilippo 1990, (S.D. Campbell 1954, p. D134).

Subgenus *Lophocyrtis* Haeckel

**Discussion:** Sanfilippo (1990) redescribed *Lophocyrtis* (*Lophocyrtis*) and defined it as a lineage consisting of two taxa. *Lophocyrtis* (*L.*) *haywardi* n. sp., below, is included because it is a three-segmented theoperid with a porous subspheroidal cephalis, a well developed, distally thorned apical horn and an abdomen with a proximal row of large pores (definition of Sanfilippo 1990).

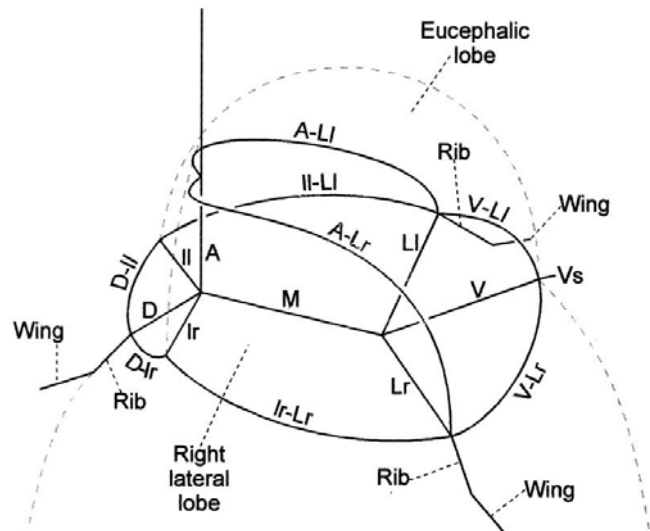
***Lophocyrtis* (*Lophocyrtis*) *haywardi* O'Connor n. sp.**  
Plate 3, figures 27-31; plate 7, figures 4a-7

*Lophocyrtis* (*Cyclampterium*) *hadra* Riedel and Sanfilippo, SANFILIPPO 1990, p. 304, pl. 1, fig. 12 (*partim*); O'Connor 1993, p. 74, pl. 8, fig. 17; Hollis et al. 1997, p. 62, pl. 6, fig. 18.  
*Lophocyrtis* (*Lophocyrtis*) cf. *jacchia* (Ehrenberg), Strong et al. 1995, p. 208, fig. 11Q (*partim*).

**Description:** Cephalis internally spheroidal, externally truncate-spheroidal as lower part enveloped by upper thorax; surface rough due to nodes, small spines and rare longer spines; bearing long, stout, conical apical horn upper half of which bears thorns that decrease in size distally; horn may be angled obliquely to cephalis or may have slight distal curve; pores circular to subcircular, few, irregular in size and distribution; collar stricture externally distinct.

Thorax inflated truncate-conical to hemispheroidal; surface rough due to nodes and occasional small thorns at pore bar junctions; greatest width reached before lumbar stricture; pores circular to subcircular, generally hexagonally framed and arranged; pores in row adjacent to cephalis often larger than those on rest of thorax and their bars join cephalis to thorax; lumbar stricture externally distinct, defined internally as smooth, pored transverse ring joined to thorax and abdomen by pore bars of adjacent rows.

Abdomen generally smooth-surfaced; uppermost part inflated cylindroidal, expanding and becoming inflated triangular in cross section where feet become distinct; greatest width generally reached just before feet terminate; pores circular to ovate, roughly longitudinally aligned, generally decrease in size distally; pore bars of row adjacent to thorax join abdomen to thorax; three equidistant, short, conical, subterminal feet project from mid or lower abdomen; abdomen narrows below feet to constricted aperture, generally circular in cross section; termi-



TEXT-FIGURE 12  
Schematic illustration of the internal skeleton of *Eurystomoskevos cauleti* (oblique lateral view, not to scale).

nation generally ragged (probably due to breakage) but some specimens have very narrow, smooth peristome with smooth to undulating termination (pl. 3, figs. 27, 28, pl. 7, figs. 4a, b).

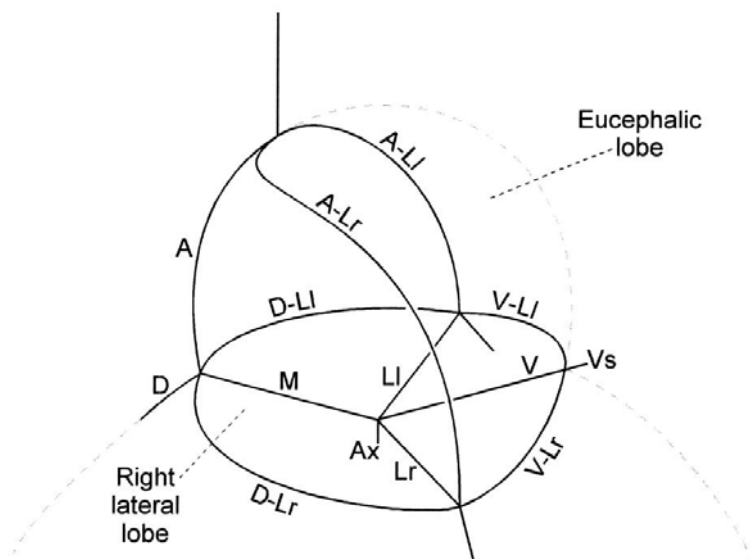
Internal skeleton consists of bars **A**, **D**, **M**, **V**, **LI**, **Lr**, spines **Ax**, **Vs**, and arches **A-LI**, **A-Lr**, **V-LI**, **V-Lr**, **D-LI** and **D-Lr** (text-fig. 13; pl. 3, fig. 31); **A** fused to cephalic wall, projects outside as apical horn; **D** extends obliquely downwards from intersection of **M**, **D-LI** and **D-Lr**, incorporated in thoracic wall; **Ax** reduced to a node; **V** extends obliquely upwards from **M** to arches; tiny **Vs** extends from intersection of **V**, **V-LI** and **V-Lr**; **LI** and **Lr** extend obliquely upwards to arches; from point where **A** projects outside arches **A-LI** and **A-Lr** curve downward fused to cephalic wall to join **LI** and **Lr** at collar stricture; rest of arches form ring at base of cephalis.

**Dimensions:** Range of 29 specimens (Holotype measurement given in parentheses): length of apical horn: 75-140µm (105µm); length from base of apical horn to first thorn: 30-52µm (45µm); length of cephalis: 25-38µm (33µm); maximum width of cephalis: 35-41µm (37µm); length of thorax: 60-85µm (70µm); maximum width of thorax: 106-130µm (112µm); maximum number of pores on half equator of thorax: 15-17 (16); maximum number of pores on length of thorax: 9-10 (10); length of abdomen including peristome: 45-95µm (90µm); maximum width of abdomen excluding feet: 100-130µm (110µm); maximum number of pores on length of abdomen: 5-10 (9).

**Etymology:** In honour of Dr B.W. Hayward for his contributions to New Zealand foraminiferal micropaleontology and biostratigraphy.

**Holotype and Type Locality:** R532, Bain's Farm (J41/f8965), Oamaru.

**Discussion:** *Lophocyrtis* (*Lophocyrtis*) *haywardi* differs from *L. (L.) exitelus* Sanfilippo 1990 by having more than one pore row



TEXT-FIGURE 13  
Schematic illustration of the internal skeleton of *Lophocyrtis* (*L.*) *haywardi* (oblique lateral view, not to scale).

on the abdomen, and only three feet, and by not having a delicate lattice attached to the ends of the feet; from *L. (L.) jacchia* (Ehrenberg) *jacchia* Sanfilippo and Caulet (1998) by not having the large arches at the base of the apical horn, and by having more pores on the thorax and abdomen, three short subterminal feet and an abdomen that is distally constricted; from *L. (L.) j. hapsis* Sanfilippo and Caulet (1998), with which it co-occurs (see Species List and pl. 9, fig. 32), by having a longer apical horn, **A** fused to the cephalic wall, rather than being partially free inside the cephalis, more and smaller thoracic pores, a more inflated abdomen that is not markedly thinner-walled than the thorax, and feet which are always subterminal and never arise from a narrow poreless band, and by not being endemic to the Antarctic; from *L. (Cyclampterium) hadra* Riedel and Sanfilippo 1986 by having more thoracic (15-17 pores on half equator cf. "14-22 pores around the thoracic circumference" as stated in Sanfilippo 1990) and abdominal pores (more than 24 on circumference cf. 8-18 stated in *ibid*), three subterminal feet, usually a much shorter abdomen, and an abdomen that is never closed.

Sanfilippo (1990, pl. 1, fig. 12) illustrated a specimen very similar to *L. (L.) haywardi*, suggesting it was a cold water variant of *L. (C.) hadra*, and a similar form was illustrated in O'Connor (1993, pl. 8, fig. 17). Strong et al. (1995, fig. 11Q) illustrated as *L. (C.) cf. jacchia* another form closely resembling these. All of these specimens are herein considered to belong in *L. (L.) haywardi*.

#### Genus *Lychnocanium* Ehrenberg, *sensu* O'Connor 1997a

*Lychnocanium* Ehrenberg 1847a, p. 385. Type species: *L. falciferum* Ehrenberg 1854, pl. 36, fig. 7, 1875, p. 160, (S.D. Campbell 1954, p. D124).

**Discussion:** Foreman and Riedel (1972, 1978) gave a different type species for *Lychnocanium* from that designated in Campbell (1954). Rather than *L. falciferum* they used *L. lucerna*

Ehrenberg 1847b, p. 55, unnumbered plate, fig. 5 (by subsequent monotypy). *L. lucerna* is pyramidal with a triangular cross-section, and in Ehrenberg's illustration appears to possess prominent (externally visible) thoracic ribs. Apparently Foreman (1973) raised *Lychnocanium* Haeckel (type species *Lychnocanium clavigerum* Haeckel, and previously a subgenus of *Lychnocanium*) to generic level because none of the lychnocaniid forms she encountered resembled *L. lucerna*, and she believed that *L. clavigerum* was a better representative. This author is of the opinion that all of the forms Haeckel (1887) described under *Lychnocanium* and its various subgenera correctly belong in the one genus, as his subgeneric distinctions merely involved the disposition of the feet. Nowhere in descriptions of *Lychnocanium* is there a mention of thoracic ribs, and in Haeckel's diagnoses of *Lychnocanium*, eg. Haeckel (1881, 1887), he requires that there be none. In my investigations I have found that there are in fact thoracic ribs in *Lychnocanium* but they are externally indistinct, ie. not externally expressed as in *L. lucerna*, but rather they take the form of alignment of pore bars, and on the inside wall of the thorax they may form slight ridges. As *L. lucerna* appears to have externally well defined thoracic ribs it does not seem to be a good representative of the genus, because these ribbed forms are now included in *Pterocanium* Ehrenberg (*sensu* Lazarus et al. 1985). Therefore *Lychnocanium* is used herein for lychnocaniid forms, and at present the type species designated by Campbell (1954) is retained.

Furthermore, it seems possible to define *Lychnocanium* on internal skeletal structure combined with external morphology. Investigations by the author have shown that several species of *Lychnocanium* have a very similar, if not identical, internal skeletal structure. The three taxa described below share a common internal structure, as do *L. neptunei* O'Connor 1997a, *L. tetrapodium* Ehrenberg (Bütschli 1882b, pl. XXX, fig. 7b), and *L. elongata* (Vinassa de Regny 1900; O'Connor unpublished data), although the latter lacks the rib corresponding to **D** and hence a third foot. A similar internal skeletal structure occurs in *Cyrtocapsa*, *Stichocorys*, *Theocorys* and *Lophocyrtis* (see O'Connor 1997a; *Lophocyrtis* (*L.*) *haywardi*, above), *Phormocyrtis* (see O'Connor 1997b), *Eucyrtidium* (see *E. ventriosum*, above), and *Sethochytris* (see *S. cavipodis*, below), and this structure could possibly be considered a typical theoperid one. Investigation of more *Lychnocanium* taxa is required to confirm the following diagnosis but based on available information the genus may be defined as follows: skeleton of two or three segments (skirt of other authors is herein considered an abdomen but is often very delicate and thus absent due to breakage/dissolution); cephalis bearing apical horn (developed to varying degrees); ribs corresponding to elements **D**, **LI** and **Lr** (**LI** and **Lr** only in *L. elongata*) incorporated in thoracic wall, externally indistinct (although pore bars may align along their length), generally internally visible, projecting outside from lowermost part of thorax as feet; internal skeletal structure consists of bars **A** (fused to cephalic wall), **D**, **M**, **V**, **LI**, **Lr**, arches **A-LI**, **A-Lr** (both fused to inner cephalic wall), **D-LI**, **D-Lr**, **V-LI**, **V-Lr** (which form ring at base of cephalis), and spines **Vs**, **Ax** (both developed to varying extents or lacking) (similar to text-fig. 13; pl. 4, figs. 5, 11, 15).

#### *Lychnocanium alma* O'Connor n. sp.

Plate 4, figures 1-5; plate 7, figures 8a-11

**Description:** Cephalis generally internally spheroidal although may appear internally lobed due to thickening of parts of inter-

nal wall by arches **A-LI** and **A-Lr**; externally truncate-spheroidal as lower part enveloped by upper thorax; surface roughened by irregularly distributed nodes; generally poreless although some specimens with few randomly scattered, tiny, circular to subcircular pores; bearing stout, conical apical horn of greater length than cephalis, generally with slight distal curve; surface of horn has fine longitudinal ridges; collar stricture externally defined as distinct contour change.

Thorax inflated truncate-conical to hemispheroidal, relatively thick-walled, greatest width generally at 2/3 length; surface rough due to large nodes at pore bar junctions; pores circular to subcircular, small, generally roughly hexagonally framed and arranged, although arrangement often irregular on parts of thorax, may be slight size increase to widest part of shell then slight decrease to lumbar stricture; lumbar stricture externally indistinct, defined internally as smooth, poreless transverse ring; three ribs corresponding to **D**, **LI** and **Lr** included in thoracic wall, not externally visible but pore bars generally aligned along their length; ribs extend outside shell approximately one to two pore rows up from lumbar stricture and combine with two pore bars to become three long, three-bladed, stout, generally straight, distally pointed feet; proximal parts of feet thinner because of fenestration where they meet abdomen, become thicker distally, ie. below abdomen; blades separated by pores at base of feet.

Abdomen generally robust; attached to lower thorax just above transverse ring and to upper 1/2 (approx.) of feet; attachment to feet distinct so feet have proximal spines if abdomen broken away from them and are proximally thinner; pores circular to ovate, irregular in size and distribution although those adjacent to feet tend to be larger; aperture not seen to be constricted; termination ragged, probably due to breakage.

Internal skeletal elements consist of bars **A**, **D**, **M**, **V**, **LI**, **Lr**, spines **Vs**, **Ax** and arches **A-LI**, **A-Lr**, **D-LI**, **D-Lr**, **V-LI** and **V-Lr** (similar to text-fig. 13; pl. 4, fig. 5); **A** fused to cephalic wall, extends outside as apical horn; **D** extends freely obliquely downwards from **M** to join thoracic wall, becomes rib; **LI** and **Lr** extend laterally to arches then become ribs; **V** extends slightly obliquely upwards from **M** to arches; spine **Vs** short, extends freely outside from junction of **V** with arches; spine **Ax** reduced to node; from approximately 3/4 up length of **A** arches **A-LI** and **A-Lr** curve downwards, fused to cephalic wall, join to **LI** and **Lr** at collar stricture; rest of arches form ring at base of cephalis.

**Dimensions:** Range of 24 specimens (Holotype measurement given in parentheses): length of apical horn: 40-60µm (50µm); length of cephalis: 26-33µm (32µm); maximum width of cephalis: 33-42µm (36µm); length of thorax: 54-70µm (68µm); maximum width of thorax: 80-102µm (80µm); maximum number of pores on half equator of thorax: 11-12 (12); maximum number of pores on length of thorax: 6-8 (6); length of abdomen: 60-115µm (70µm); length of feet: 125-190µm (160µm).

**Etymology:** After the Alma Group, which includes the Oamaru Diatomite. Alma is the name of a small town in the Oamaru area (see Text-fig. 1) and is used as a noun in apposition.

**Holotype and Type Locality:** R541, Flume Gully (J41/8197), Oamaru.

**Discussion:** *Lychnocanium alma* differs from most other members of *Lychnocanium* by having a robust abdomen that is gen-

erally always preserved, and if not then distinct spines are present on the upper parts of the feet showing where it was attached. Blome (1992) mentions and illustrates several similar taxa but *L. alma* differs from them in the following ways: from *Lychnocanium* sp. C (Blome 1992) by being larger, and by having a more stout apical horn, and longer feet; from *Lychnocanium* spp. D and E (Blome 1992) by being larger, and by having a stouter apical horn, longer feet, and an abdomen that does not become distally separated from the feet. It differs from *L. anacolum* (Foreman 1973) by having a generally poreless cephalis, and generally straight, rather than convexly curving, feet.

***Lychnocanium waiareka* O'Connor n. sp.**

Plate 4, figures 6-11; plate 7, figures 12a-15

*Lychnocanium tripodium* Ehrenberg, HOLLIS et al. 1997, p. 64, pl. 5, figs. 36, 37 (partim).

**Description:** Cephalis internally spheroidal, although may appear internally lobed because of thickening of parts of internal wall by arches **A-LI** and **A-Lr**; externally truncate-spheroidal, as lower part enveloped by upper thorax; surface may be slightly roughened by small nodes and/or irregularly distributed, small thorns; poreless, with irregularly distributed dimples; bearing long, moderately stout, conical apical horn, generally longer than cephalis; collar stricture externally distinct as marked contour change.

Thorax inflated truncate-conical to hemispheroidal; surface roughened by nodes at pore bar junctions; greatest width reached just below mid-length; pores small, circular to subcircular, generally hexagonally framed and arranged, may increase slightly in size to widest part of shell then decrease slightly to lumbar stricture; pores in uppermost transverse row may be slightly larger than others, bars from this row join to cephalis; lumbar stricture externally indistinct, defined internally as smooth, poreless transverse ring; three ribs corresponding to **D**, **LI** and **Lr** incorporated in thoracic wall, externally indistinct although pore bars may align along their length; ribs project outside shell approximately one to two pores up from lumbar stricture and combine with two pore bars to become long, three-bladed, distally pointed, reasonably stout, straight or slightly curved subparallel feet; at base of feet blades generally separated by pores.

Abdomen very delicate; attached to lowermost thorax and generally to central parts of feet; if abdomen missing attachment points generally visible as few short spines on central parts of feet (pl. 4, fig. 9, pl7, fig. 14) and ragged teeth around lower thorax; pores circular to ovate, irregular in size and distribution, some areas may be poreless; aperture not seen to be constricted; termination generally ragged, probably due to breakage.

Internal skeleton as for *L. alma*, except that arches **A-LI** and **A-Lr** branch approximately 2/3 to 3/4 up length of **A**; **LI** and **Lr** extend laterally to arches then extend obliquely downwards to thoracic wall where they become ribs (pl. 4, fig. 11).

**Dimensions:** Range of 50 specimens (Holotype measurement given in parentheses): length of apical horn: 32-54µm (53µm); length of cephalis: 36-42µm (42µm); maximum width of cephalis: 36-44µm (41µm); length of thorax: 68-88µm (85µm); maximum width of thorax: 80-105µm (89µm); maximum number of pores on half equator of thorax: 12-16 (14); maximum number of pores on length of thorax: 8-11 (8); length of abdo-



men: 50-89µm, from 8 specimens (65µm); length of feet: 80-177µm (115µm).

**Etymology:** After the Waiareka Volcanics, of which the Oamaru Diatomite is a member. Waiareka is a Maori name taken from a creek in the Oamaru area (see text-fig. 1), and is used as a noun in apposition.

**Holotype and Type Locality:** R551, Flume Gully (J41/f8197), Oamaru.

**Discussion:** *Lychnocanium waiareka* differs from similar appearing *Lychnocanium* species as follows: from *L. alma* by having a smaller apical horn, a dimpled cephalis, a different form to the abdomen, and subparallel, rather than diverging, feet; from *L. tripodium* Ehrenberg 1873 by being larger, and by having a relatively larger cephalis, a rougher surfaced and hemispheroidal thorax, and more widely diverging feet with attachment spines (abdominal remnants) on the central parts; from *L. conicum* Clark and Campbell 1942 by being slightly smaller, and by having a stouter apical horn, more thoracic pores, and much longer feet; from *L. grande rugosum* Riedel 1952 (Hays 1965; Weaver 1976, 1983) by being smaller, and by having a larger apical horn, and more thoracic pores; from *L. neptunei* O'Connor 1997a by having a poreless and larger cephalis, a smaller thorax with fewer pores, a different form to the abdomen, and abdominal attachment points on central parts of feet; from *L. n. nipponicum* Nakaseko 1963 by being older and smaller, and by having a longer apical horn, more and smaller thoracic pores, and generally longer feet; from *L. n. magnacornutum* (Sakai) 1980 by being older, and by having a less stout and shorter apical horn, and more thoracic pores; from *L. anacolum* (Foreman) 1973 by having a poreless cephalis, feet that are not markedly convex, and an abdomen not joined to the proximal parts of the feet; from *Lychnocanium* sp. (Johnson 1974) by being larger, and by having a less stout apical horn, more thoracic pores, and relatively longer feet; from *Lychnocanium* sp. (Chen 1975) by being larger, and by having a poreless cephalis, more thoracic pores, and bladed, rather than conical, feet; from *Lychnocanium* spp. A and C (Blome 1992) by being much larger, and by having more thoracic pores, relatively longer feet, and a different abdominal form.

***Lychnocanium waitaki* O'Connor n. sp.**

Plate 4, figures 12-15; plate 7, figures 16a-19

**Description:** Cephalis generally internally spheroidal although may appear slightly lobed due to thickening of wall along arches A-LI and A-Lr; externally truncate-spheroidal, as lower part enveloped by upper thorax; surface poreless, upper part with irregularly distributed dimples, may be few small thorns at dimple junctions (pseudo pore bar junctions), lower part generally smooth or ridged due to pore bars of uppermost transverse row on thorax extending upwards onto lower cephalis; bearing thin, conical apical horn, longer than cephalis, may curve distally, may appear bladed at base because of furrows caused by cephalic dimples extending onto proximal parts of horn; collar stricture externally distinct as marked contour change.

Thorax inflated truncate-conical to hemispheroidal; surface roughened by thorns at pore bar junctions; greatest width reached at approximately 2/3 length from cephalis; pores relatively large, circular to subcircular, generally hexagonally framed and arranged, increasing in size to widest part of shell then decreasing slightly to aperture; lumbar stricture defined internally as smooth, poreless transverse ring; three ribs corre-

sponding to D, LI and Lr incorporated in thoracic wall, internally visible, externally indistinct although pore bars generally align along their length; ribs project outside shell approximately one to two pores up from lumbar stricture and combine with two pore bars to form long, stout, three-bladed, distally pointed, divergent feet which may be straight or curve slightly outwards; at base of feet blades separated by pores.

Abdomen very delicate, generally only seen as small remnants (pl. 7, fig. 18); pores circular to ovate, irregular in size and arrangement; uppermost pore row generally consists of larger pores, pore bars of this row attach abdomen to lower thorax just above transverse ring; occasional specimens have small spines on proximal parts of feet that may also be evidence of attachment; termination ragged.

Internal skeleton as for *L. waiareka* except no Vs seen and A-LI and A-Lr begin approximately 4/5 up length of A (pl. 4, fig. 15).

**Dimensions:** Range of 34 specimens (Holotype measurement given in parentheses): length of apical horn: 38-62µm (38µm); length of cephalis: 38-45µm (40µm); maximum width of cephalis: 38-48µm (41µm); length of thorax: 80-105µm (95µm); maximum width of thorax: 118-140µm (130µm); maximum number of pores on half equator of thorax: 11-14 (13); maximum number of pores on length of thorax: 9-11 (9); length of feet: 110-185µm (>105µm).

**Etymology:** After the Waitaki Subdivision, the area which includes the strata mentioned in this report. Waitaki is the Maori name given to a small town and adjacent river approximately 20km NE of Oamaru, and is used as a noun in apposition.

**Holotype and Type Locality:** R559, Flume Gully (J41/8197), Oamaru.

**Discussion:** *Lychnocanium waitaki* differs from similar members of the genus as follows: from *L. tripodium* Ehrenberg 1873 (Petrushevskaya and Kozlova 1972) by being much larger, and by having shorter and more divergent feet; from *L. favosum* Haeckel 1887 by having a longer and conical apical horn, a poreless cephalis, and bladed, rather than conical, feet; from *L. fortipes* Haeckel 1887 by having a longer and conical apical horn, a poreless cephalis and feet without terminal serrations; from *L. sigmopodium* Haeckel 1887 by having a conical apical horn, a poreless cephalis and fewer and larger thoracic pores; from *L. g. grande* Campbell and Clark 1944 by having a longer apical horn, and a poreless cephalis, and by being larger overall, and older; from *L. g. rugosum* Riedel 1952 (Hays 1965; Weaver 1976, 1983) by being older, and by having a larger apical horn, more and generally larger thoracic pores, shorter feet (than those of the specimens illustrated in Hays 1965, pl. 3, fig. 5 and Weaver 1983, pl. 2, fig. 1), and a different form to the abdomen (*ibid*); from *L. aff. grande* Chen 1975 by being larger and rougher-surfaced, and by having longer feet, and a more distinct collar stricture; from *L. cf. grande* Reynolds 1977 and *L. cf. grande* Alexandrovich 1992 by being much larger, and by having more and larger thoracic pores; from *L. aff. grande* (Hollis in Strong et al. 1995) by having a longer apical horn, larger thoracic pores, and feet that are more divergent; from *L. korotzevi* (Dogiel in Dogiel and Reshetnyak 1952, 1955; Petrushevskaya 1962, 1981; Petrushevskaya and Kozlova 1972; Wang and Yang 1992) by being much larger and older, and by having feet that are generally straight, rather than outwardly curved, and a different form to the abdomen; from *L. neptunei* O'Connor 1997a



by having a poreless cephalis, fewer thoracic pores, feet that are more divergent, and by being generally larger overall; from *L. n. nipponicum* Nakaseko 1963 by being older, and by having a longer apical horn, more thoracic pores, and a generally hemispheroidal, rather than truncate-spheroidal, thorax; from *L. n. magnacornutum* (Sakai) 1980 by being older and larger, and by having a smaller apical horn, more thoracic pores, and a relatively shorter thorax; from *Lychnocanium* sp. Johnson 1974 by having a less stout apical horn, and by being much larger with longer feet; from *Lychnocanium* sp. (Weaver and Dinkelman 1978) by having a poreless cephalis, fewer and larger thoracic pores, and less stout feet; from *Lychnocanium* sp. (Sakai 1980) by being larger with a bigger apical horn; from *Lychnocanium* sp. B (Abelmann 1990) by being older, and by having a relatively shorter and wider thorax, and longer feet; from *Lychnocanium* sp. (Ling 1992) by having a less stout apical horn, a smaller, thinner-walled, and relatively shorter and wider thorax, and longer feet; from *Lychnocanium* sp. A (Hollis in Strong et al. 1995) by having a longer apical horn, a poreless cephalis, and more thoracic pores.

#### Genus *Pterosyringium* Haeckel

*Pterosyringium* Haeckel 1887, p. 1319. Type species: *Pterocorys tubulosa* Haeckel 1887, p. 1319, pl. 68, fig. 6, (S.D. Campbell 1954, p. D130).

**Discussion:** *Pterosyringium* Haeckel 1887, originally erected as a subgenus of *Pterocorys* Haeckel 1881, is herein raised to generic level to accommodate forms with a generally spheroidal cephalis, three simple (not fenestrated) thoracic wings, and an abdomen that narrows distally. Haeckel's diagnosis included only forms where the "...abdomen prolonged into a narrow cylindrical tube...", but forms without a tube are included here as the distal abdomen is often broken in many specimens making determination of this feature difficult. Subgenus *Pterosyringium* is raised to generic level because *Pterocorys* has since become the type genus of the Pterocorythidae, its type species being *P. campanula* Haeckel 1887. The forms here included in *Pterosyringium* do not have the distinctly lobed and usually elongate cephalis of pterocorythids, and as the type species also lacks this feature *Pterosyringium* is regarded as unrelated to the Pterocorythidae and seems better placed in the Theoperidae. The genus *Pterocyrtidium* Bütschli 1882 was treated by Haeckel (1887) as a subgenus of *Pterocorys* and was considered a junior objective synonym of *Pterocorys* (*Pterocorys*) by Campbell (1954). Foreman and Riedel (1978) mentioned that the type species designated for *Pterocyrtidium* by Campbell (1954), *Pterocorys campanula*, seemed inappropriate as it was not one of the species included in the genus at the time it was erected. Because of this confusion *Pterocyrtidium* is not used herein.

Species considered to belong to *Pterosyringium* as applied herein include *Pterocorys* (*Pterosyringium*) *tubulosa* Haeckel 1887, *Pterocorys* (*Pterocyrtidium*) *colomba* Haeckel 1887, *P. (P.) hirundo* Haeckel 1887, and *Pterosyringium hamata* (described below). Other species described by Haeckel (1887) probably also belong but as they were not illustrated they have not been formally included. *Pterosyringium* differs from *Lithornithium* Ehrenberg 1847 by not having a closed abdomen; from *Lipmanella* Loeblich and Tappan 1961 by the thoracic wings not being latticed.

#### *Pterosyringium hamata* O'Connor n. sp.

Plate 4, figures 16-21b; plate 7, figures 20a-23

Theoperid, gen. et sp. indet. JOHNSON 1974, pl. 2, figs. 14-17, pl. 6, fig. 11.

?Theoperid, gen. et sp. indet. JOHNSON 1974, pl. 5, fig. 17.

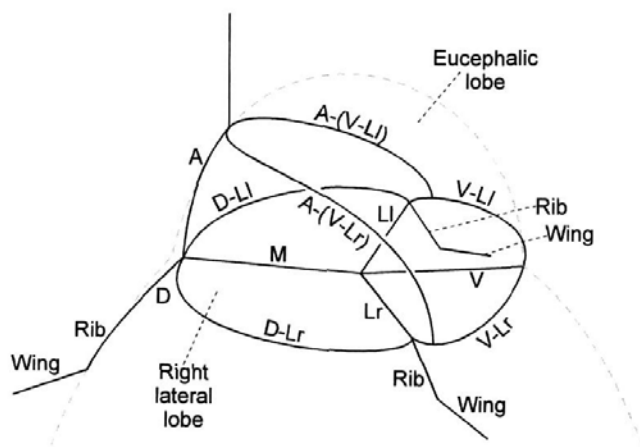
**Description:** Cephalis internally spheroidal to ovoid, may appear internally lobed because of thickening of parts of inner cephalic wall by arches **A-(V-Li)** and **A-(V-Lr)**; externally truncate-spheroidal to truncate-ovoid as lower part enveloped by upper thorax; externally indistinctly bi-lobed due to distinct anterior furrow corresponding to **A** (pl. 4, fig. 18), often pores line either side of furrow; surface smooth to roughened by irregularly distributed nodes; bearing conical, anteriorly offset apical horn of variable length and stoutness; pores few, generally very small, circular to subcircular, irregularly distributed; rare specimens have relatively large, circular to subcircular, irregularly distributed pores over entire surface of cephalis (pl. 4, fig. 21a); collar stricture variable, either externally distinct as contour change or externally indistinct as only slight contour change.

Thorax inflated truncate-conical to hemispheroidal, thick-walled; greatest width in the lower third; surface roughened by nodes of variable size at pore bar junctions; pores circular to subcircular, irregular in size and distribution, rarely roughly hexagonally arranged; three ribs corresponding to **D**, **Li** and **Lr** internally distinct, externally indistinct, although pore bars may align on some specimens, on others furrows may coincide with ribs; ribs project outside shell as three conical wings from varying levels on thorax although always from lower half; if wings long then generally proximally buttressed and buttressing may extend over lumbar stricture onto abdomen (pl. 4, fig. 16); lumbar stricture generally externally indistinct, defined internally as thick, smooth, poreless transverse ring joined to thorax and abdomen by pore bars of adjacent pore rows.

Abdomen cylindroid to truncate-ovoid, tapering distally, may be irregularly constricted, on rare specimens may curve slightly distally; wall proximally thick, thinning distally; surface generally smooth; pores circular to ovate, irregular in size and distribution, occasionally roughly longitudinally aligned; aperture constricted in form of short, narrow tube; termination irregular, rare specimens with few distally pointed, lamellar, curved feet.

Internal skeletal elements consist of bars **A**, **D**, **M**, **V**, **Li**, **Lr**, and arches **A-(V-Li)**, **A-(V-Lr)**, **D-Li**, **D-Lr**, **V-Li** and **V-Lr** (text-fig. 14; pl. 4, figs. 21a, b); **A** fused to and incorporated in cephalic wall thus creating anterior furrow and bi-lobed cephalis, projects outside as apical horn; **D** extends obliquely downwards from **M** to thoracic wall, becomes rib, projects outside as wing; **V** extends slightly obliquely upwards from **M** to arches; **Li** and **Lr** extend laterally to arches then extend obliquely downwards to thoracic wall, become ribs, project outside as wings; **A-(V-Li)** and **A-(V-Lr)** curve downwards from point where **A** exits shell, fused to cephalic wall, join to **V-Li** and **V-Lr** where they become fused to cephalic wall, i.e. adjacent to points where **Li** and **Lr** join arches; remaining arches form ring at base of cephalis.

**Dimensions:** Range of 80 specimens (Holotype measurement given in parentheses): length of apical horn: 5-36µm (8µm); length of cephalis: 20-26µm (23µm); maximum width of cephalis: 26-39µm (33µm); length of thorax: 42-57µm (50µm); maximum width of thorax: 60-77µm (69µm); length of thoracic wings: 9-34µm, from 43 specimens (10); maximum number of pores on half equator of thorax: 9-12 (9); maximum number of pores on length of thorax: 5-8 (6); length of abdomen: 54-105µm, from 13 specimens (90µm); maximum width of ab-



TEXT-FIGURE 14  
Schematic illustration of the internal skeleton of *Pterosyringium hamata* (oblique lateral view, not to scale).

domen: 60-86µm (70µm); maximum number of pores on half equator of abdomen: 9-13 (8).

**Etymology:** Latin for barbed - refers to the three downwardly-directed wings.

**Holotype and Type Locality:** R569, Flume Gully (J41/f8003), Oamaru.

**Discussion:** The abdomen of *Pterosyringium hamata* is rarely fully preserved and generally the termination is ragged as though broken along a pore row. On many specimens the wings are also broken or very short and difficult to see (pl. 4, figs. 19, 20, pl. 7, figs. 20a, b, 21). When reasonably complete specimens have been observed it is relatively easy to identify those that have suffered breakage.

*Pterosyringium hamata* differs from similar taxa as follows: from *P. tubulosa* Haeckel by having wings that do not lie along the thorax for their entire length, a different shaped thorax, and by not having an abdomen in the form of a long narrow tube; from *P. columba* (Haeckel) by having a generally sparsely pored cephalis, conical, rather than bladed, wings, and a less externally distinct lumbar stricture; from *P. hirundo* (Haeckel) by having a conical, rather than bladed, apical horn, conical, rather than bladed, thoracic wings, wings that are much shorter, a different shaped thorax, smaller thoracic and abdominal pores, and no spines on the thorax; from *Pterocyrtidium barbadense* (Ehrenberg) group Petrushevskaya and Kozlova (1972) by having an inflated truncate-conical to hemispheroidal, rather than truncate-spheroidal, thorax, wings that extend from the lower, rather than the upper (as in Ehrenberg 1875, pl. 17, fig. 6), half of the thorax, a rougher-surfaced thorax, thoracic and abdominal pores that are irregularly arranged, a distally tapering abdomen, and by being significantly larger (eg. width of thorax of Petrushevskaya and Kozlova's specimens approx. 55µm cf. 60-77µm for *Pterosyringium hamata*; length of thorax of Petrushevskaya and Kozlova's specimens approx. 34µm cf. 42-57µm for *P. hamata*); from *Pterocyrtidium* sp. Ling (1975) by having pores that are much more irregular in arrangement, and wings that originate much higher on the shell; from *Lipmanella* aff. *Theocorys redondoensis* Alexandrovich (1992)

by being smaller, and by having wings that are relatively more stout; from *Theocyrts* (*Theocorypha*) *diabloensis* Clark and Campbell, Chen (1975) by having a longer apical horn, a less well defined cephalis and collar stricture, a less well defined lumbar stricture, and thoracic and abdominal pores of approximately the same size.

Johnson (1974, pl. 2, figs. 14-17, pl. 5, fig. 17, pl. 6, fig. 11) illustrated as theoperid gen. et sp. indet. several specimens that closely resemble *Pterosyringium hamata*. They are smaller than, or at the small end of the range of, *P. hamata*, and none exhibits thoracic wings, although this may be due to breakage or under development as seen in some specimens of *P. hamata*. One of Johnson's specimens (1974, pl. 5, fig. 17) also has regularly arranged thoracic and abdominal pores, a feature not seen in *P. hamata*. Specimens of *P. hamata* have been observed in the early Oligocene of Northland, New Zealand (O'Connor, unpublished data).

#### Genus *Sethochytris* Haeckel

*Sethochytris* Haeckel 1881, p. 433. Type species: *S. triconiscus* Haeckel 1887, p. 1239, pl. 57, fig. 13, (fide Campbell 1954, p. D124).

**Discussion:** This genus is applied in the sense of Riedel and Sanfilippo (1970) who include *Sethochytris babylonis* (Clark and Campbell) group, the form of which is similar to *S. cavipodis*, ie. two-segmented, pyriform, possessing three feet, nearly identical internal skeletal structure (O'Connor, unpublished data). Ling (1975) included specimens of *S. babylonis* group in his *Lychnocanoma babylonis-turgidulum* (sic) group, but *Lychnocanoma*, a junior synonym of *Lychnocanium* (see O'Connor 1997a, and above), has feet extending from the lowermost part of a generally inflated truncate-conical to hemispherical to campanulate thorax, rather than subterminal feet and a pyriform thorax.

#### *Sethochytris cavipodis* O'Connor n. sp.

Plate 4, figures 22-27; plate 7, figures 24a-27

?Gen. et sp. indet., RIEDEL and SANFILIPPO 1970, pl. 8, fig. 10.  
?Lithochytris (*Lithochytrodes*) *turgidulum* (sic) (Ehrenberg),  
PETRUSHEVSKAYA and KOZLOVA 1972, p. 552, pl. 27, figs. 8, 9

**Description:** Cephalis thick-walled, internally subspheroidal, externally hemispheroidal to inflated truncate-conical as lower part enveloped by upper thorax, poreless, generally smooth-surfaced; bearing proximally broad and bladed, distally conical and pointed apical horn, generally shorter than cephalis; collar stricture generally externally indistinct although may be visible as slight contour change.

Thorax pyriform to inflated truncate-conical; greatest width reached at about 2/3 down length; surface rough due to nodes at pore bar junctions; pores circular to ovate, generally hexagonally framed and arranged although arrangement becomes less regular below feet, some specimens with very thick shells have rosette-shaped pores because of centripetal growth; three generally distinct ribs extend from bars D, LI and Lr through thorax; at approx. 3/4 to 4/5 down length of thorax ribs project outside as three equidistant, proximally bladed, distally conical and pointed, subterminal feet; each foot partially surrounds a large pore where it exits the thorax so appears proximally hollow (pl. 4, fig. 24b), becoming solid distally; feet may be straight or curve slightly inwards; aperture very constricted in form of pore at base of thorax (pl. 4, fig. 24b); basal pore may be slightly larger than other thoracic pores, circular to ovate, surrounded by

narrow, poreless area; on some specimens basal pore becomes short, smooth tube with ragged termination (pl. 4, fig. 25).

Internal skeletal elements consist of bars **A**, **M**, **D**, **V**, **LI**, **Lr**, spines **Ax**, **Vs**, and arches **A-LI**, **A-Lr**, **V-LI**, **V-Lr**, **D-LI**, **D-Lr** (see text-fig. 15; pl. 4, fig. 27); bar **A** extends freely upwards from **M** to cephalic wall, projects outside as apical horn; **D** extends obliquely downwards from **M** to join thoracic wall, becomes rib incorporated in wall, extends outside as subterminal foot on lower thorax; **LI** and **Lr** extend laterally to arches then continue downwards to join upper thoracic wall, become ribs incorporated in wall, extend outside as subterminal feet on lower thorax; **V** extends slightly obliquely upwards from **M** to arches; spine **Ax** reduced to node; spine **Vs** very broad, extends freely from intersection of **V**, **V-LI** and **V-Lr** towards pore on uppermost thorax; from intersection of **A** with cephalic wall arches **A-LI** and **A-Lr** curve downwards, fused to cephalic wall for most of their length, become free just before joining to **LI** and **Lr**; rest of arches form ring at base of cephalis, joined to cephalic wall at collar stricture by numerous short bars.

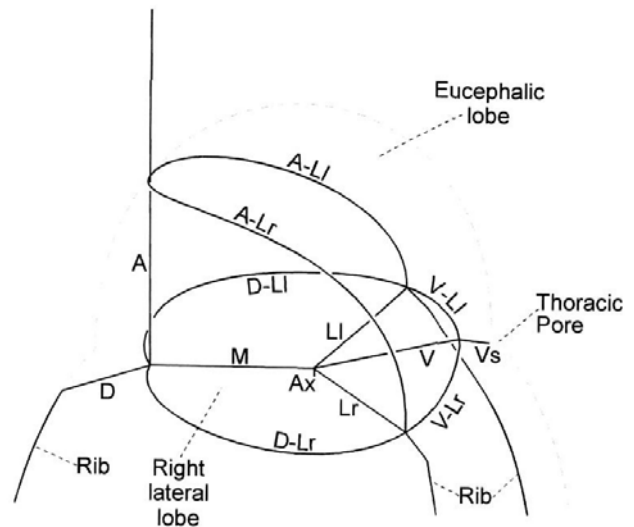
**Dimensions:** Range of 26 specimens (Holotype measurement given in parentheses): length of apical horn: 15-30µm (27µm); length of cephalis: 27-37µm (31µm); maximum width of cephalis: 35-45µm (40µm); length of thorax: 140-172µm (160µm); maximum width of thorax: 117-150µm (140µm); maximum number of pores on half equator of thorax: 13-15 (14); maximum number of pores on length of thorax: 13-19 (16); maximum length of feet: 46-70µm (62µm).

**Etymology:** Derived from the Latin *cavi* (hole), and *pedes* (foot) - refers to the pore enveloped by the proximal part of each foot.

**Holotype and Type Locality:** R579, Flume Gully (J41/f8004), Oamaru.

**Discussion:** *Sethochytris cavipodis* differs from *S. triconiscus* Haeckel 1887 by having poreless, rather than pored tube-like, feet; from *S. babylonis* (Clark and Campbell 1942) group by being larger and generally more inflated, and by having an apical horn that is generally shorter than the cephalis, shorter feet in relation to the rest of the shell, and an aperture in the form of a pore, rather than a larger opening (cf. pl. 9, fig. 40); from the similar appearing *Lychnocanium turgidum* Ehrenberg 1873 by having a larger apical horn, an internally subspheroidal cephalis, a generally pyriform thorax, and longer feet; from *L. ventricosum* Ehrenberg 1873 by being larger, and by having a less pronounced cephalis and smaller aperture; from *Lithomelissa ventricosa* Ehrenberg 1873 (Bütschli 1882b as *Lychnocanium ventricosum*) by being larger, and by having a longer, stouter apical horn, three, rather than two, feet, and a pyriform to inflated truncate-conical, rather than ovate, thorax; from *Lychnocanium pyriforme* Haeckel 1887 by having a shorter apical horn, a poreless cephalis, a generally pyriform thorax, and pores at the base of the feet.

Riedel and Sanfilippo (1970, pl. 8, fig. 10) illustrated a specimen as Gen. et sp. indet. that is herein tentatively synonymised with *S. cavipodis*. They excluded it from *S. babylonis* group because of its size, degree of inflation, and at least partially bladed feet, but it differs only slightly from *S. cavipodis* by having a longer apical horn (the aperture is not visible in their illustration so its form is unknown, hence its tentative inclusion in *S. cavipodis*). Petrushevskaya and Kozlova (1972, p. 552) synonymise Riedel and Sanfilippo's specimen with *Lithochytris* (*Lithochytrodes*) sp. T, which in turn differs from *S. cavipodis*



TEXT-FIGURE 15  
Schematic illustration of the internal skeleton of *Sethochytris cavipodis* (oblique lateral view, not to scale).

primarily by having a large aperture, rather than a basal pore. In fact several of the specimens illustrated by Petrushevskaya and Kozlova (1972) under the genus *Lithochytris* Ehrenberg are better placed in *Sethochytris* as they are only two-segmented. *Lithochytris* (*Lithochytrodes*) aff. *tripodium* Ehrenberg (Petrushevskaya and Kozlova 1972, p. 552, pl. 27, fig. 5) differs from *S. cavipodis* by having very broad feet, fewer thoracic pores and a less inflated thorax. The species that they illustrated and mentioned (Petrushevskaya and Kozlova 1972, p. 552, pl. 27, figs. 8, 9) as *Lithochytris* (*Lithochytrodes*) *turgidulum* (sic) (Ehrenberg) is herein tentatively included in *Sethochytris cavipodis* because it has the characteristic basal pore and pyriform thorax, although the illustrations are not clear enough to discern pores at the base of the feet.

#### Genus *Thyrsochyrtis* Ehrenberg

*Thyrsochyrtis* Ehrenberg 1847b, chart to p. 54. Type species: *T. rhizodon* Ehrenberg 1873, p. 262, 1875, pl. 12, fig. 1, (fide Campbell 1954, p. D130).

#### Subgenus *Thyrsochyrtis* Ehrenberg

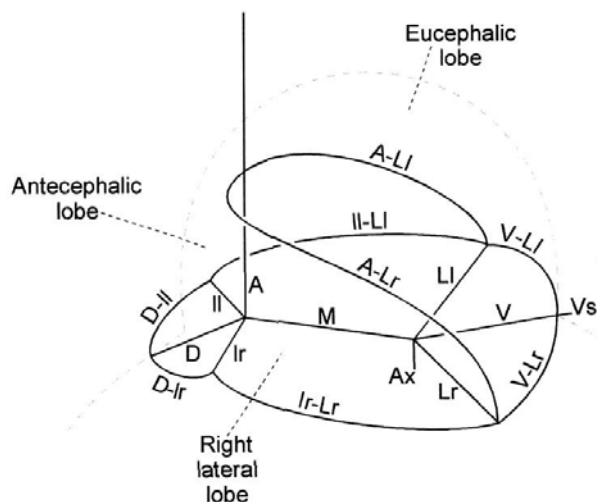
**Discussion:** The following species is only tentatively included in *Thyrsochyrtis* (*Thyrsochyrtis*) because its position in the phylogenetic lineage represented by that genus (see Sanfilippo and Riedel 1982) is unclear. It does, however, conform to the morphologic definition given in Sanfilippo and Riedel (1982), although it lacks the terminal feet common to other members of the genus.

#### *Thyrsochyrtis* (*Thyrsochyrtis* ?) *pinguicoides* O'Connor n. sp. Plate 4, figures 28-32; plate 7, figures 28a-31

?*Thyrsochyrtis* sp. DINKELMAN 1973, p. 788, pl. 3, figs. 7, 8  
*Theocotyle* "pinguicoides" O'Connor, HOLLIS et al. 1997, p. 65, pl. 6, figs. 10-12 (nom. nud.).

**Description:** Cephalis internally spheroidal, externally truncate-spheroidal as lower part enveloped by upper thorax; surface rough due to small nodes and spines; bearing long, stout,





TEXT-FIGURE 16  
Schematic illustration of the internal skeleton of *Thyrsocyrtis* (*T. ?*) *pinguicoides* (oblique lateral view, not to scale).

proximally bladed, distally conical apical horn, although some specimens have entirely bladed horn and others conical; pores circular to subcircular, irregular in size and arrangement; pores on uppermost cephalis extend onto base of horn forming furrows; collar stricture externally distinct as contour change.

Thorax inflated truncate-conical to hemispheroidal; surface rough due to nodes at pore bar junctions; greatest width reached before lumbar stricture; pores circular to subcircular, roughly hexagonally framed and arranged; pore bars of uppermost pore row join cephalis to thorax; lumbar stricture externally distinct, defined internally as smooth, transverse ring joined to thorax and abdomen by numerous short bars.

Abdomen inflated cylindroidal; surface rough due to nodes at pore bar junctions; greatest width reached at approximately mid-length; pores circular to ovate, larger and more irregularly hexagonally framed and arranged than those on thorax; peristome generally smooth, porous, narrow, may have appearance of a transverse ring surrounding aperture, or may project downwards; very rare specimens have wide, longitudinally ridged peristome (pl. 4, fig. 31); aperture constricted; termination smooth to finely undulating.

Internal skeleton consists of bars **A**, **D**, **M**, **V**, **LI**, **Lr**, **II**, **Ir**, spines **Ax**, **Vs**, and arches **A-LI**, **A-Lr**, **V-LI**, **V-Lr**, **II-LI**, **Ir-Lr**, **D-II** and **D-Ir** (text-fig. 16; pl. 4, fig. 32); **A** extends freely straight upwards from **M** to anterior top of cephalis, projects outside as apical horn; **D** extends obliquely downwards from **M** to collar stricture; **V** extends obliquely upwards from **M** to arches; spine **Vs** short, extends from intersection of **V**, **V-LI** and **V-Lr**; spine **Ax** short, pointed; **LI** and **Lr** extend obliquely downwards to collar stricture; **II** and **Ir** short, extend laterally to collar stricture; from about 2/3 up length of **A** arches **A-LI** and **A-Lr** curve downwards, free at first then fused to cephalic wall, join **LI** and **Lr** at collar stricture; rest of arches form ring at base of cephalis.

**Dimensions:** Range of 31 specimens (Holotype measurement given in parentheses): length of apical horn: 80-120µm (90µm); length of cephalis: 27-35µm (35µm); maximum width of cephalis: 43-50µm (45µm); length of thorax: 60-70µm (65µm); maximum width of thorax: 110-130µm (113µm); maximum number of pores on half equator of thorax: 12-14 (14); maximum number of pores on length of thorax: 6-7 (6); length of abdomen: 65-95µm (75µm); maximum width of abdomen: 125-155µm (140µm); width of aperture: 70-92µm (85µm); maximum number of pores on half equator of abdomen: 11-13 (13); maximum number of pores on length of abdomen: 5-7 (5).

**Etymology:** Derived from the Latin *pinguis* (stout), and *sica* (dagger) - refers to the stout apical horn.

**Holotype and Type Locality:** R588, Flume Gully (J41/f8197), Oamaru.

**Discussion:** *Thyrsocyrtis* (*Thyrsocyrtis* ?) *pinguicoides* differs from similar taxa as follows: from other *Thyrsocyrtis* species, with the exception of *T. (T.) bromia*, primarily by not having terminal feet; from *T. (T.) bromia* Ehrenberg by having more pores on the half equator of the abdomen, thoracic and abdominal pores that are closer in size, and by never having terminal feet; from *Theocotyle venezuelensis* Riedel and Sanfilippo by having a longer, stouter apical horn, a longer thorax with respect to the abdomen, and a shorter and generally narrower abdomen; from *T. conica* Foreman and *T. cryptocephala* (Ehrenberg) by having a longer, stouter apical horn, a more distinct lumbar stricture and a more inflated abdomen with larger pores; from *Theocotylissa ficus* (Ehrenberg) by having a longer, stouter apical horn, a hemispheroidal, rather than conical, thorax, a distinct lumbar stricture, and a smaller abdomen with respect to the thorax.

The specimens illustrated in Dinkelman (1973, pl. 3, figs. 7, 8), as *Thyrsocyrtis* sp., have more irregularly arranged thoracic pores, a differently shaped thorax, and a wider abdomen with respect to the thorax, and so are only tentatively included within *T. (T. ?) pinguicoides* here. Sanfilippo and Riedel (1982) synonymised the aforementioned specimens of Dinkelman with *T. (T.) bromia* and revised the definition of that species, saying that early specimens have 12 pores on the half equator of the abdomen. The earliest specimen of *T. (T.) bromia* that they illustrate, however (Sanfilippo and Riedel 1982, pl. 1, fig. 17), has fewer pores on the half equator of the abdomen (approx. 10). Their specimen further differs from Dinkelman's specimens by having terminal feet, and from *T. (T. ?) pinguicoides* by having a wider abdomen with respect to the thorax, a different shape to the thorax, and terminal feet. In addition, other reports illustrate specimens of *T. (T.) bromia* that occur early in its stratigraphic range, and these have the typical *T. (T.) bromia* form, eg., Riedel and Sanfilippo (1971, pl. 8, fig. 6), Dinkelman (1973, pl. 3, figs. 1, 2, 4, 6), Johnson (1974, pl. 5, fig. 7), Holdsworth (1975, pl. 1, figs. 19-21). Furthermore, the *Thyrsocyrtis* sp. illustrated by Dinkelman co-occurs with typical *T. (T.) bromia* in the same drill hole (DSDP Hole 163). Hollis et al. (1997) document *T. (T. ?) pinguicoides* from the mid-part of the range of *T. (T.) bromia*, and the forms herein are also from that part of its range, so it cannot simply be an early form of that species.

*Thyrsocyrtis* (*T. bromia*) appears to be a tropically restricted species (Sanfilippo et al. 1985). Caulet (1986) noted its presence in the Southwest Pacific, but provided no illustration, and said that "...their skeletons are somewhat different from tropical forms." Weaver (1983, p. 679) referred to a species from the



Southwest Atlantic as *Thyrsoyrtis* aff. *bromia* but did not illustrate it. The forms illustrated by Dinkelman (1973, pl. 3, figs. 7, 8, as *Thyrsoyrtis* sp.) are tropical, and range lower than *T. (T. ?) pinguicoides* as recorded in Hollis et al. (1997). As no other *Thyrsoyrtis* taxa were recorded from Site 277 (*ibid*) the origin of *T. (T. ?) pinguicoides* is unknown. It is possible that it is an offshoot of either *T. (T.) rhizodon* Ehrenberg, the ancestor of *T. (T.) bromia* and also a tropical species, or *T. (T.) bromia* from the early part of its range, which migrated southwards and became extinct after a short time leaving no descendants. The short stratigraphic range of *T. (T. ?) pinguicoides* may make it useful as a Late Eocene (late Kaiatan to early Runangan) marker for future southern high latitude studies.

## SPECIES LIST

This list is in strict alphabetical order. The distribution of the following taxa in the studied samples is presented in Table 2.

*Actinommidae* gen. et sp. indet. (Plate 8, figs. 1, 2; plate 10, figs. 1-6). Grouped here are several spherical forms with a varying number of medullary shells and variable cortical shell features. Also included are forms with six orthogonally spines (Plate 10, figs. 4-6) which probably fit into one of *Hexastylus* Haeckel, *Hexacantium* Haeckel or *Hexalanche* Haeckel, but due to the artificial nature of these genera (based on the number of medullary shells, an uncertain criteria due to the susceptibility of these shells to dissolution, see Caulet 1972) are placed here.

*Amphicraspedum murrayanum* Haeckel 1887, p. 523, pl. 28, fig. 1. (Plate 10, fig. 7).

*Amphicraspedum prolixum* Sanfilippo and Riedel group, Sanfilippo and Riedel 1973, p. 524, pl. 11, figs. 1-5, pl. 28, fig. 5. (Plate 8, fig. 3).

*Amphisphaera* aff. *spinulosa* (Ehrenberg), Crouch and Hollis 1996, p. 26; Hollis et al. 1997, p. 43, pl. 1, figs. 1, 2. (Plate 10, fig. 8).

*Amphisphaera* sp. A. (Plate 10, fig. 9). Cortical shell spheroidal, rough-surfaced due to small thorns at pore bar junctions, pores circular to subcircular; two medullary shells, outer one spheroidal, connected to cortical shell by numerous radial bars, pores circular to ovate, irregular in size and distribution; polar spines bladed, long, unequal in length.

*Amphisphaera* sp. B. (Plate 10, figs. 11, 12). Cortical shell spheroidal, thick-walled, relatively smooth-surfaced, pores rosette-shaped due to centripetal growths; two medullary shells, outer one spheroidal to ovoidal, connected to cortical shell by equatorial bars, pores circular to subcircular, generally hexagonally arranged; polar spines, bladed, one long, one very short, rare specimens have double long spine (Plate 10, fig. 11). Probably conspecific with *Amphisphaera* sp. Hollis et al. (1997, pl. 1, figs. 16, 17).

*Amphymenium splendarmatum* Clark and Campbell 1942, p. 46, pl. 1, figs. 12, 14. (Plate 8, fig. 4).

*Anthocyrtidium stenum* Sanfilippo and Riedel 1992, p. 24, pl. 1, figs. 16, 17, pl. 4, fig. 3. (Plate 9, fig. 2).

*Axoprimum pierinae* (Clark and Campbell), sensu Hollis et al. 1997, p. 44, pl. 1, figs. 7-13. (Plate 10, fig. 12).

*Bathropyramis magnifica* (Clark and Campbell), Hollis et al. 1997, p. 57, pl. 6, fig. 22. (Plate 9, fig. 3).

*Callimitra atavia* Goll 1979, p. 388, pl. 5, figs. 1, 5-9, 11. (Plate 9, fig. 4).

*Calocyclus* ? sp. (Plate 9, fig. 7). Test of three segments; cephalis spheroidal, poreless, dimpled, bearing conical apical horn; collar stricture externally distinct; thorax inflated truncate-conical, rough-surfaced due to small spines at pore bar junctions, pores large, generally hexagonally framed and arranged; lumbar stricture externally

distinct, expressed internally as transverse ring; abdomen truncate-conical (although appears broken so full form unknown), termination ragged, surface smooth, pores as for thorax but larger.

*Ceratocyrtis mashae* ? Bjørklund 1976, p. 1125, pl. 17, figs. 1-5. (Plate 9, fig. 9). This form is older than the mid-Oligocene age given as the oldest occurrence of this species in Bjørklund (1976).

*Ceratocyrtis robustus* ? Bjørklund 1976, p. 1125, pl. 17, figs. 6-10. (Plate 9, fig. 8). This form is older than the mid-Oligocene age given as the oldest occurrence of this species in Bjørklund (1976).

*Ceratocyrtis* sp. A. (Plate 9, fig. 10). Cephalis partly to mostly buried within thorax, pores large, bearing short, bladed apical and vertical horns; thorax widely flaring truncate-conical, pores large, irregular in size, shape and distribution, tend towards longitudinal alignment on some specimens; termination ragged.

*Ceratocyrtis* ? sp. B. (Plate 9, fig. 1). Test slightly inflated conical; cephalis rough surfaced due to short, stout spines originating at pore bar junctions, pores circular to ovate, irregularly arranged, bearing short, bladed apical horn; collar stricture externally indistinct, internally expressed as ring formed by arches **D-Li**, **D-Lr**, **V-Li** and **V-Lr**; pores of thorax as for cephalis but larger; three basally-butressed, short wings extend from uppermost thorax (correspond to **D**, **Li** and **Lr**); aperture constricted by pored ring near base of thorax; termination ragged. The generic assignment is questionable because of the presence of thoracic wings, and the lack of a long, branched **Ax**.

*Clathrocyclas* sp. (Plate 9, fig. 11). Test of three segments; cephalis spheroidal, rough-surfaced, pored, bearing large, conical, anteriorly offset apical horn; collar stricture externally distinct; thorax inflated truncate-conical, pores hexagonally arranged, increasing in size distally, three small wings on upper part correspond to **D**, **Li** and **Lr**; lumbar stricture externally distinct, internally expressed as transverse ledge; abdomen broken so form unclear but flares from lumbar stricture before beginning to curve downwards, pores smaller than those of thorax; termination ragged.

*Cornutella californica* Campbell and Clark, emend. Foreman 1968, p. 21, pl. 3, figs. 1a-c. (Plate 9, fig. 12).

*Dendrosyris* aff. *anthocyrtoides* (Bütschli), Goll 1968, p. 1419, pl. 174, figs. 9, 11-14. (Plate 10, fig. 29). Differs from *D. anthocyrtoides* primarily by having larger and fewer lattice pores.

*Dendrosyris* aff. *binapertonis* Goll 1968, p. 1420, pl. 173, figs. 5, 6, 10, 11. (Plate 10, fig. 30). Differs from *D. binapertonis* by being older, and by having a large apical horn and larger lattice pores; appears similar to the specimen illustrated in de Weaver (1981, pl. 3, fig. 4).

*Dendrosyris inferispina* Goll 1968, p. 1421, pl. 174, figs. 5-8, 10. (Plate 10, fig. 37).

*Dendrosyris tumidula* (Kozlova). *Petalosyris tumidula* Kozlova in Kozlova and Gorbovetz 1966, p. 97, pl. 15, figs. 10, 11. (Plate 10, fig. 41).

*Dendrosyris* sp. A. (Plate 10, fig. 31). Lattice shell smooth; lattice bars relatively thick; lattice pores large and ovate adjacent to sagittal ring, much smaller and circular to subcircular away from sagittal ring; apical horn short, thin, conical; three stout, distally branching basal feet.

*Dendrosyris* sp. B. (Plate 10, fig. 32). Lattice shell smooth; lattice bars relatively thin; lattice pores circular to ovate, approximately equal in size; apical horn short, thin, conical; three basal feet, bladed with distal thorns (possibly broken branches).

*Dendrosyris* sp. C. (Plate 10, fig. 33). Lattice shell rough-surfaced due to tubercles on lattice bars, and short

- thorns projecting from some lattice bar junctions; lattice bars relatively stout; lattice pores large, circular to subcircular; three conical, thorned basal feet.
- Dendrospyrus* sp. D. (Plate 10, fig. 34). Lattice shell smooth, irregular; lattice pores large and ovate adjacent to sagittal ring, circular to subcircular and irregular in size away from sagittal ring; apical horn short, thin, conical; three basal feet, bladed and expanding slightly distally (although generally broken so difficult to discern actual form).
- Dictyophimus* ? aff. *constrictus* Nishimura 1992, p. 338, pl. 10, fig. 16, pl. 13, fig. 10. *Dictyophimus* sp. B O'Connor 1993, p. 72, pl. 8, figs. 1, 2. (Plate 9, fig. 13). This species differs from that described in Nishimura (1992) primarily by having bladed and often more than two cephalic horns (which appear to correspond to either A or D, and L1 and Lr), much smaller pores on the cephalis and upper thorax, and short, conical thorns projecting from pore bar junctions on the cephalis and upper thorax. It is also larger significantly larger (eg., max. width of thorax 154-194µm cf. 116-130µm for *D. ? constrictus*).
- Dictyoprora urceolus* (Haeckel), Nigrini 1977, p. 251, pl. 4, figs. 9, 10 (Plate 9, fig. 44).
- Doradospyris argisca* (Ehrenberg), Goll 1969, p. 336, pl. 56, figs. 9-11. (Plate 10, fig. 35).
- Doradospyris costatascens* Goll 1969, p. 337, pl. 57, figs. 1-4. (Plate 10, fig. 36).
- Doradospyris* sp. (Plate 10, fig. 38). Lattice shell smooth, overgrowth on some areas, several small thorns project from top; pores circular to ovate, irregular in size and distribution; apical horn conical, extremely short; lattice skirt smooth-surfaced; pores circular to ovate, irregular in size and distribution; termination thorny, some thorns long (possibly feet).
- Eucyrtidium mariae* Caulet 1991, p. 536, pl. 4, figs. 3, 4. (Plate 9, fig. 14).
- Eucyrtidium montiparum* Ehrenberg 1873, p. 230, 1875, pl. 9, fig. 11. (Plate 9, fig. 15).
- Eucyrtidium spinosum* Takemura 1992, p. 746, pl. 5, figs. 5-8. (Plate 9, fig. 16).
- Eucyrtidium* sp. (Plate 9, fig. 17). Test of three segments; cephalis spheroidal with long, stout, bladed apical horn, prominent, downwardly-directed Vs, and small, irregularly distributed pores; thorax inflated truncate-conical, long, pores hexagonally framed and arranged, lumbar stricture externally distinct; abdomen generally cylindroidal, may be constricted or inflated in parts, pores as for thorax, surface smoother than that of thorax; aperture not constricted; termination ragged.
- Ewingella* ? sp. (Plate 9, fig. 18). Cephalis with tiny, irregularly distributed, circular to subcircular pores, or poreless and dimpled (probably overgrown); bearing narrow, conical apical horn (broken in illustrated specimen) and prominent vertical tube; collar stricture externally distinct as contour change; thorax inflated truncate-conical, pores circular to ovate, generally hexagonally arranged, generally increasing in size distally, may be overgrown; lumbar stricture externally distinct as contour change, internally expressed as thin ring; abdomen discoidal, pores circular to subangular, arranged in concentric rings, increase in size to approximately centre ring then decrease to periphery; termination ragged; typical neosciadiocapsid internal skeletal structure (see Neosciadiocapsidae, above). Differs from *Ewingella* by having a conical, rather than basally pored and bladed, apical horn, and by lacking a velum.
- Flustrella charlestonensis* (Clark and Campbell). *Porodiscus* (*Trematodiscus*) *charlestonensis* Clark and Campbell 1945, p. 23, pl. 3, figs. 11-16. (Plate 8, fig. 5). *Flustrella* Ehrenberg 1838 is applied because it has precedence over the more commonly used *Porodiscus* Haeckel 1881.
- Heliodiscus inca* Clark and Campbell, *sensu* Hollis et al. 1997, p. 45, pl. 1, figs. 25, 26. (Plate 10, fig. 13).
- Lamptonium* ? aff. *pennatum* Foreman 1973, p. 436, pl. 6, figs. 3-5, pl. 11, fig. 13. (Plate 9, fig. 19). Differs from *L. pennatum* by having a poreless cephalis, conical apical horn and wings that extend from the lower, rather than mid, thorax. In addition it is smaller than *L. pennatum* (length of cephalis and thorax: approx. 97µm cf. 125-150 for *L. pennatum*; maximum width of thorax: approx. 89µm cf. 100-140 for *L. pennatum*), and has a much younger occurrence than other members of the genus.
- Liriospyris clathrata* (Ehrenberg), Goll 1968, p. 1426, pl. 175, figs. 12, 13, 16, 17. (Plate 10, fig. 39).
- Liriospyris* ? sp. (Plate 10, fig. 40). Lattice shell rough-surfaced due to tubercles at lattice bar junctions; delicate meshed network present across surface of lattice shell (often broken away in many areas leaving short thorns where it was joined to shell); lattice bars relatively stout; lattice pores circular to ovate, irregular in size and distribution, although tend to be larger adjacent to sagittal ring; at least five conical, thorned basal feet.
- Lithelius minor* Jörgensen 1900, p. 65, pl. 5, fig. 24. (Plate 8, fig. 6; plate 10, fig. 14).
- Lithelius nautiloides* Popofsky 1908, p. 230, pl. 27, fig. 4 (only). (Plate 8, fig. 7; plate 10, fig. 15).
- Lithelius* ? sp. (Plate 8, fig. 24). Test fusiform, consisting of single spiral of many closely spaced whorls; rare forms have spongy "arms", as in the illustration. Similar forms have been encountered in the Oligocene (O'Connor 1993, p. 37, pl. 10, fig. 6) and Early Miocene (O'Connor 1997b, p. 114, pl. 3, fig. 4) of Northland, but only Eocene forms have been seen with "arms".
- Lithomelissa ehrenbergi* Bütschli 1882a, p. 517-519, pl. 33, figs. 21a, b. (Plate 9, fig. 20).
- Lithomelissa* aff. *ehrenbergi* Bütschli 1882a, p. 517-519, pl. 33, figs. 21a, b. (Plate 9, fig. 21). Differs from *L. ehrenbergi* by having a poreless cephalis, a more prominent Vs, and a less externally distinct collar stricture.
- Lithomelissa* cf. *gelasinus* O'Connor 1997a, p. 71 pl. 2, figs. 3-6, pl. 6, figs. 6-9. (Plate 9, fig. 22). Differs from the original description of *L. gelasinus* by having a pored, rather than spongy, abdomen.
- Lithomelissa* cf. *haeckeli* Bütschli 1882a, p. 517-519, pl. 33, figs. 23a, b. (Plate 9, fig. 23). The long wings of Bütschli's species are not seen (probably broken), and the collar stricture is more defined, but the internal skeletal structure of this species is similar to that in Bütschli's illustration. It differs from *L. haeckeli* as illustrated in Petrushevskaya and Kozlova (1979, figs. 283, 284, 472-474) by having much larger cephalic pores, a distinctly bladed apical horn, and smaller thoracic pores (cf. *ibid*, figs. 472-474), and by lacking a row of larger pores at the collar stricture (as in *ibid*, figs. 283, 284). Although similar in appearance to *L. lautouri* O'Connor n. sp., the internal skeletal structure is quite different.
- Lithomelissa* cf. *hertwigi* Bütschli 1882a, p. 517-519, pl. 33, figs. 22a, b. (Plate 9, fig. 24). Has a relatively shorter cephalis than that illustrated by Bütschli, but the internal skeletal structure is similar to that in Bütschli's illustration.
- Lithomelissa* cf. *mitra* Bütschli 1882a, p. 517-519, pl. 33, fig. 24. (Plate 9, fig. 25). Differs from Bütschli's specimen by having a poreless cephalis.
- Lophocyrtis* (*Apoplanus*) *aspera* (Ehrenberg), Sanfilippo and Caulet 1998. (Plate 9, fig. 5)
- Lophocyrtis* (*Lophocyrtis*) *jacchia* (Ehrenberg) *hapsis* Sanfilippo and Caulet 1998. (Plate 9, fig. 32). The illustrated specimen is virtually identical to the species de-

TABLE 2

Distribution of radiolarian species. "+" denotes presence, "?" denotes uncertain presence due to breakage. CQ - Capsize Stone Quarry, BN - Bain's Farm, JP - Jackson's Paddock, FH - Forrester's Hill, DH - Division Hill, FG - Flume Gully, CS - Cormack's Siding (Taylor's Quarry).

	CQ1	BN1	BN2	BN3	BN4	BN5	BN6	BN7	BN8	JP1	JP2	FH1	FH2	FH3	DH1	DH2	DH3	FG1	FG2	FG3	FG4	FG5	CS1
<i>Actinomyces</i> gen. et sp. indet.	+	+	+	+	+	+	+	+	+	+	+	+	+	+	+	+	+	+	+	+	+	+	+
<i>Amphicraspedum murrayanum</i>			+																	?	+	+	+
<i>Amphicraspedum proluxum</i> gr.																							
<i>Amphisphaera</i> aff. <i>spinulosa</i>	+	+	+	+	?	+				+	+	+	+	+	+	+	+	+	+	+	+	+	+
<i>Amphisphaera</i> sp. A	+	+	+							+	+	+	+	+				+	+	+	+	?	
<i>Amphisphaera</i> sp. B										+	+							+	+	+			
<i>Amphymenium splendens</i>				+						+	+								+				+
<i>Anthocyrtidium stenium</i>				?	+					+	+	+											
<i>Axoprunum pierinae</i>			+	?	+	+				+	+	+	?	?				+	+	+			
<i>Bathropyramis magnifica</i>				+							+	+						+	+			+	
<i>Callimitra atavia</i>				+						+					?			+					?
<i>Calocyclus</i> ? sp.			+								+					+		+					
<i>Ceratocyrtis muthae</i>	?	?									+												
<i>Ceratocyrtis robustus</i>	+	?									+							?			+		
<i>Ceratocyrtis</i> sp. A	?																	?	+	+			
<i>Ceratocyrtis</i> ? sp. B														+									
<i>Clathrocyclus</i> sp.		+	?												+								
<i>Cornutella californica</i>				+							+												
<i>Dendrosyrinx</i> aff. <i>anthocyrtoides</i>				+	+					+					+			+					
<i>Dendrosyrinx</i> aff. <i>binapertensis</i>						+	+			+	?	+				+		+	+	+	+	+	+
<i>Dendrosyrinx inferospina</i>		+	+															+	+	+	+	+	+
<i>Dendrosyrinx tumidula</i>	+	+	+	+									+	?				+	+	+	+	+	+
<i>Dendrosyrinx</i> sp. A		?	+									+						+	+	+	+	+	+
<i>Dendrosyrinx</i> sp. B				+	+							+			+			+	+	+	+	+	+
<i>Dendrosyrinx</i> sp. C	+	+		+								+			?			+	+	+	+	+	+
<i>Dendrosyrinx</i> sp. D	+																						
<i>Dictyophimus</i> ? aff. <i>constrictus</i>													+										
<i>Dorcadopsyrinx argus</i>		+	+			+					+	+	+					+	+	+	+	+	+
<i>Dorcadopsyrinx costatensis</i>	+			+																			
<i>Dorcadopsyrinx</i> sp.	+	+	+	+							+	+			+			+	+	+	+	+	+
<i>Eucyrtidium mariae</i>											+												
<i>Eucyrtidium montiparum</i>			+												+								
<i>Eucyrtidium spinosum</i>	+	+	+	+						+	+			+	+	+	+	+	+	+	+	+	+
<i>Eucyrtidium</i> sp.			+									+						+					
<i>Ewingella</i> ? sp.		+																					
<i>Flustrella charlestonensis</i>	+	+	+	+	+	+	+	+	+	+	+				+	+	+	+	+	+	+	+	?
<i>Heliodiscus inca</i>	+	+	+																	?		+	
<i>Lampetium</i> ? aff. <i>pernatum</i>																		+	+				
<i>Liriosyrinx clathrata</i>	+			+																+	+		
<i>Liriosyrinx</i> ? sp.		+	+								+												
<i>Lithelium minor</i>	+	+	+	+	?	+				?	+				+	+	+	+	+	+	+	+	+
<i>Lithelium nautiloides</i>	+	+	+	+	+	+	+	+	+	+	+	+	+	+	+	+	+	+	+	+	+	+	+
<i>Lithelium</i> ? sp.		+	+		+	+								+									
<i>Lithomelissa ehrenbergi</i>	+	+	+	+	+	+							+	?	+			+	?			+	
<i>Lithomelissa</i> aff. <i>ehrenbergi</i>	+		+	+																			
<i>Lithomelissa</i> cf. <i>gelasimus</i>	+	+	+	+									+										
<i>Lithomelissa</i> cf. <i>haeckeli</i>	+	+								?													
<i>Lithomelissa</i> cf. <i>herwigii</i>	+														+			+					+
<i>Lithomelissa</i> cf. <i>mitra</i>										+	+	+						+	+				
<i>Lophocyrtis (Apoplanus) aspera</i>	+	+				+	+									+	+	+	+	+	+	+	+
<i>Lophocyrtis (Lophocyrtis) jacchia hapsis</i>																							
<i>Lophocyrtis (Lophocyrtis) ? semipolita</i>	+	+	+	+	?	+				+	+	+	+	+	+	+	+	+	+	+	+	+	+
<i>Lophocyrtis (Paralampetium) ? longiventer</i>	+	+	+	+	?	+				+	+	+	+	+	+	+	+	+	+	+	+	+	?
<i>Lophophaena</i> sp. A	+	+	+	+							+	+	+	+	+	+	+	+	+	+	+	+	+
<i>Lophophaena</i> sp. B		+	+	+				+	+			?											
<i>Lychnocampana amphitrite</i>	+			+	+	+	+	+	+		+	+						+	+	+	+	+	+
<i>Orosphaeridia</i> gen. et sp. indet.											+	+						+					
<i>Peridium</i> sp.	+	+	+	+	+					+	+				+			+	+	+	+	+	+
<i>Periphaena heliastericus</i>	+	+	+					+			+	+						+	+	+	+	+	+
<i>Peripyramis</i> sp.	+	+	+							+	+	+						+	+	+	+	+	+
<i>Plagiomyx</i> gen. et sp. indet. A			+																				
<i>Plagiomyx</i> gen. et sp. indet. B		?										+	+										
<i>Plectopyramis</i> sp.																							
<i>Prunopyle fragilis</i>	+	+	+	+	+	+	+			+	+	+	+	+				+	+	+	+	+	+
<i>Prunopyle polyacantha</i>		+	+	+	+	+				+	+	+	+	+				+	+	+	+	+	+
<i>Prunopyle</i> aff. <i>polyacantha</i> ?		+	+	+																+	+	+	+
<i>Prunopyle</i> cf. <i>titian</i>	+	+										?							+	+	+	+	+
<i>Prunopyle</i> sp.		+																					
<i>Pseudodictyophimus gracilipes</i>	+	+	+	+	+	+				+	+				+			+			?	+	+
<i>Pteropilum</i> sp.											+												
<i>Sethocyrtis babytonis</i>		+			?	+				+								+	+	+	+	+	+
<i>Siphocampe</i> cf. <i>acephala</i>			+																				
<i>Siphocampe nodosaria</i>																	+						
<i>Siphocampe</i> aff. <i>nodosaria</i>							+																
<i>Spongodiscus cruciferus</i>		+		?						+	+						?	+	+	?	+	+	+
<i>Spongodiscus</i> cf. <i>cruciferus</i>										+	+									+	+	+	+
<i>Spongodiscus maculatus</i>	+	+	+	+		+	+			+	+	+	+	+	+	+	+	+	+	+	+	+	+
<i>Spongodiscus nitidus</i>	+	+	+	+	+	?	+			+	+	+	+	+	+	+	+	+	+	+	+	+	+
<i>Spongodiscus pulcher</i>	+	+	+	+	?	+	+			+	+	+	+	+	+	+	+	+	+	+	+	+	+
<i>Spongodiscus rhabdosyllus</i>	+	+	+		+	+				+	+							+	+	+	+	+	+
<i>Spongodiscus</i> aff. <i>rhabdosyllus</i>		+											?										
<i>Spongodiscus</i> sp.	+	+	+	+	+	+	+			+	+	+	+	+	+	+	?	+	+	+	+	+	+
<i>Spongopyle spiralis</i>		+	?							+	?	+						+	+				
<i>Spongopyle</i> sp.		+																					
<i>Stylodictya targaeformis</i>								+		+	+	+	+	+	+	+	+	+	+	+	+	+	+
<i>Stylodictya</i> cf. <i>variabilis</i>	?	+	+	+	+	+	+	+	+	+	+	+	+	+	+	+	+	+	+	+	+	+	+
<i>Stylodictya</i> sp.	+	+	+	+	+	+	+	+	+	+	+	+	+	+	+	+	+	+	+	+	+	+	+
<i>Stylasphaera hexazyphophora</i>	+	+	+	+	?					+	+				+			+	+	+	+	+	+
<i>Stylasphaera minor</i>	+	+	+												+			+	+	+	+	+	?
<i>Theocampe urceolus</i>	+						+			+								+	+	+	+	+	+
<i>Theoperidae</i> gen. et sp. indet.																		+					
<i>Tholosyrinx</i> ? sp.										+	+				?								
<i>Triaplosyrinx tricerus</i>		+																					?
<i>Veratoholus</i> cf. <i>doiigi</i>		+																					
<i>Zeolithium mitra</i>	+	+	+	+	+	+	+											+	+	+	+	+	+
<i>Zygocircus buetschlii</i>		+	+	+	+	+	+			+					+	+	+	+	+	+	+	+	+

- scribed and illustrated as *Calocyclas* sp. C. in Takemura (1992), a form which has been subsequently synonymised with *Lophocyrtis* (*L.*) *jacchia hapsis* by Sanfilippo and Caulet (1998). Although the feet are difficult to discern on the illustrated specimen, due the angle, one can be seen on the lower left hand part of the abdomen.
- Lophocyrtis* (*Lophocyrtis* ?) *semipolita* (Clark and Campbell), Sanfilippo and Caulet 1998. (Plate 9, fig. 6).
- Lophocyrtis* (*Paralampterium* ?) *longiventer* (Chen), Sanfilippo 1990, p. 309, pl. 3, figs. 1-5. (Plate 9, figs. 26-29). Several forms are grouped here, ranging from relatively smooth specimens to very spiny ones.
- Lophophaena* sp. A. (Plate 9, fig. 30). Cephalis relatively large, pores large, circular to subcircular, irregularly arranged, bearing thin, bladed, anteriorly offset apical horn and short, bladed vertical horn; collar stricture externally well defined; thorax inflated cylindrical, wider than cephalis, pores as for cephalis; termination ragged.
- Lophophaena* sp. B. (Plate 9, fig. 31). Cephalis relatively small, pores circular to ovate, irregularly arranged, bearing short, bladed, anteriorly offset apical horn and short, bladed vertical horn; collar stricture externally well defined; thorax relatively large, inflated truncate-conical, pores as for cephalis; termination ragged. This species has not been included in *Ceratocyrtis* because it lacks a long, branched Ax.
- Lychnocanium* *amphitrite* (Foreman), Hollis et al. 1997, p. 63, pl. 6, figs. 1-4. (Plate 8, fig. 25; plate 9, fig. 33). Abdomen generally missing or only remnants seen.

- Orosphaeridae gen. et sp. indet. (Plate 10, fig. 16). Included here are unidentifiable orosphaerid fragments.
- Peridium* sp. Similar to *Peridium* aff. *spinipes* Haecckel, Funakawa (1994), but cephalic pores are smaller and more numerous, and the maximum shell diameter is approximately 60µm (cf. 76-80µm for Funakawa's species). It is also somewhat older as Funakawa's specimens are from the Late Miocene. A well-developed but irregular thorax is present on well preserved specimens.
- Periphaena heliastericus* (Clark and Campbell), Sanfilippo and Riedel 1973, p. 523, pl. 9, figs. 1-6. (Plate 10, fig. 17).
- Peripyramis* sp. (Plate 9, fig. 34). Included here are plectopyramids in which the pores are not transversely aligned.
- Plagoniidae gen. et sp. indet. A. (Plate 9, fig. 35). Cephalis large, poreless, relatively smooth-surfaced; bearing relatively long, stout, bladed apical horn, pored at base; collar stricture generally externally indistinct; thorax short, no wider than thorax, pores small, circular to ovate, irregularly scattered; three relatively long and stout, downwardly directed wings/feet? extend from lower thorax; internal skeletal structure complex. Although externally similar to members of *Lithomelissa*, the complex internal skeletal structure of this species excludes it from that genus.
- Plagoniidae gen. et sp. indet. B. (Plate 9, fig. 36). Cephalis large, irregularly spheroidal, pores irregular in size, shape and distribution; bearing long, bladed, basally fenestrated apical horn; collar stricture externally distinct; thorax

# PLATE 1

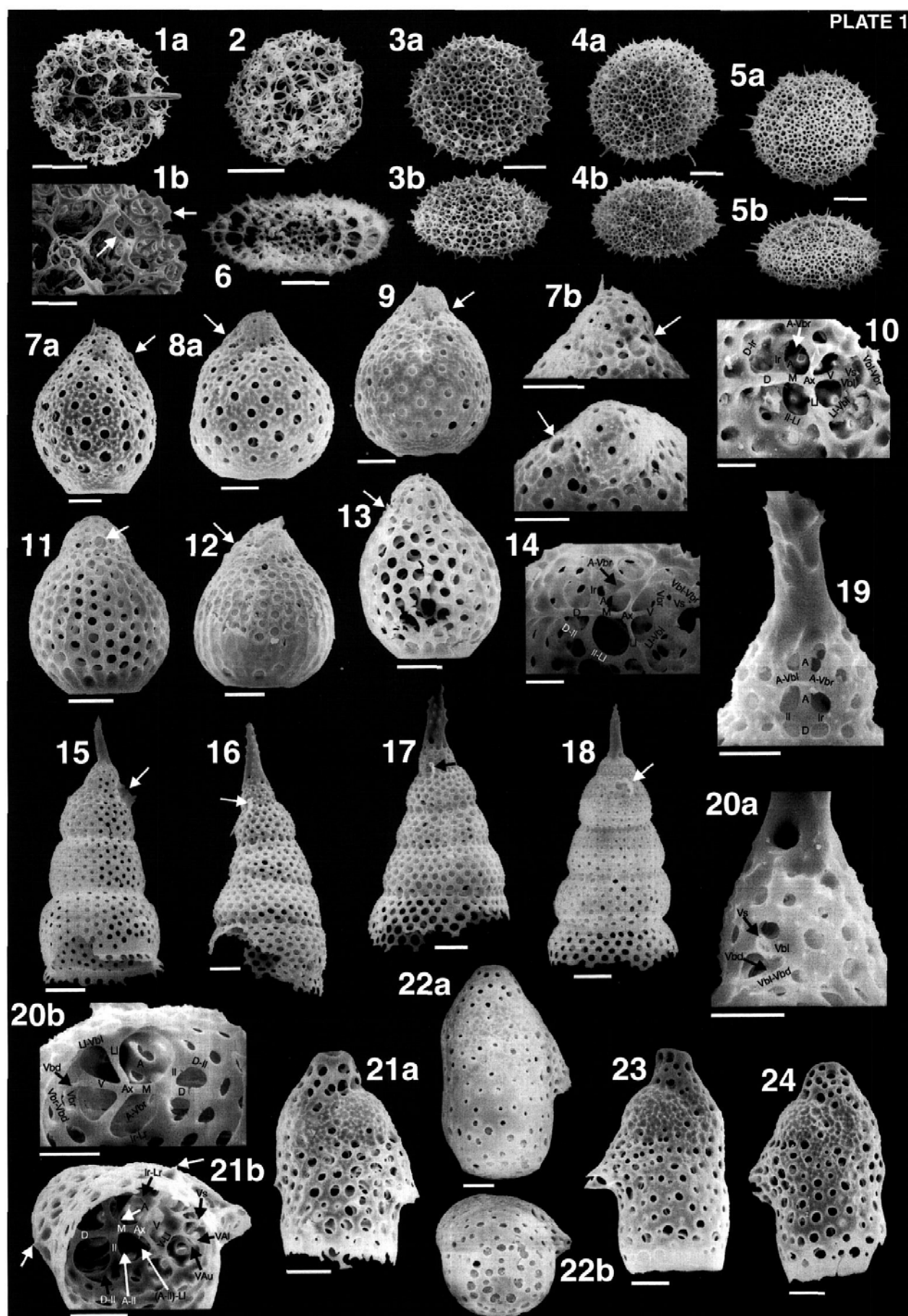
All illustrations are scanning electron micrographs. Illustrated specimens are from the following samples (see Table 1 for locality information): figs. 1a, b - JP1; figs. 11, 13 - JP2; figs. 4a, b, 22a, b - DH1; figs. 2, 5a-6, 16, 19-20b - DH2; figs. 3a, b, 12, 21a, b, 23, 24 - CQ1; figs. 7a-8b, 9, 14 - BN1; fig. 10 - CS1; figs. 15, 17, 18 - FH1. Scale bars for figs. 1a & 2 are 100µm; scale bars for figs. 1b & 3a-6 are 50µm; scale bars for figs. 7a-9, 11-13, 15-18 & 21a-24 are 20µm; scale bars for figs. 10, 14 & 19-20b are 10µm.

- 1a-2 *Tricorporisphaera bibula* O'Connor n. sp. - 1a, b) paratype, R384, 1b) enlargement of central area, oblique arrow indicates outer medullary shell, horizontal arrow indicates cortical shell, 2) paratype, R385.
- 3a-6 *Plectodiscus runanganus* O'Connor n. sp. - 3a-5b) paratypes R389-R391, 3a, 4a, 5a) view perpendicular to equatorial plane, 3b, 4b, 5b) oblique view, 6) paratype, R392, cross-sectional view.
- 7a-10 *Plannapus hornibrooki* O'Connor n. sp. - 7a, b) paratype, R397, 7a) right lateral view, arrow indicates vertical tube, 7b) enlargement of oblique right lateral view, arrow indicates vertical tube, 8a, b) paratype, R398, 8a) left lateral view, arrow indicates vertical tube, 8b) enlargement of oblique apical view, arrow indicates vertical tube, 9) paratype, R399, right lateral view, arrow indicates vertical tube, 10) paratype, R400, basal view of cephalis showing internal skeletal structure.
- 11-14 *Plannapus mauricei* O'Connor n. sp. - 11-13) paratypes R405-R407, 11) slightly oblique posterior view, arrow indicates vertical tube, 12, 13) left lateral

views, arrows indicate vertical tubes, 14) paratype, R408, basal view of cephalis showing internal skeletal structure.

- 15-20b *Spirocyrtis greeni* O'Connor n. sp. - 15-18) paratypes R413-R416, 15) right lateral view, arrow indicates vertical tube, 16, 17) slightly left oblique posterior views, arrows indicate remnants of vertical tubes, 18) posterior view, arrow indicates remnants of vertical tube, 19) paratype, R417, close-up of anterior view of cephalis showing structural elements, 20a, b) paratype, R418, 20a) close-up of slightly oblique posterior view of cephalis showing structural elements, 20b) basal view of cephalis showing internal skeletal structure.
- 21a-24 *Botryocella pauciperforata* O'Connor n. sp. - 21a, b) paratype, R423, 21a) right lateral view, 21b) basal view showing internal skeletal structure, upwardly-directed arrow indicates wing associated with D, downwardly-directed arrow indicates wing associated with Lr, 22a, b) paratype, R424, 22a) right lateral view, 22b) basal view showing closed thorax, 23, 24) paratypes R425 & R426, left lateral views.



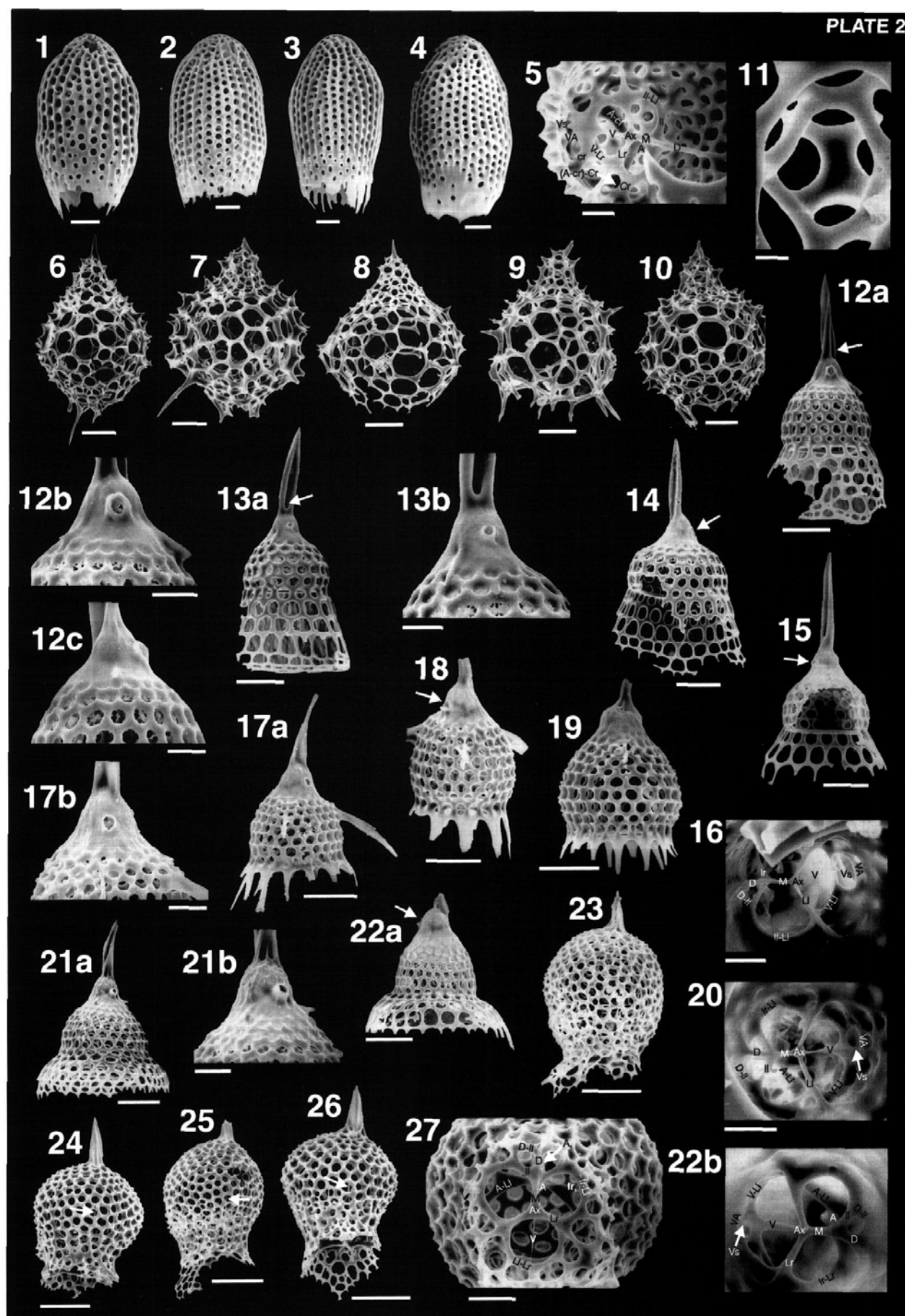


- short, irregular, pores as for cephalis; three relatively long, straight, bladed, basally fenestrated wings/feet? extend from uppermost thorax; termination ragged; internal skeletal structure complex.
- Plectopyramis* sp. (Plate 9, fig. 37). Large, conical test; cephalis with two long, stout, conical horns (corresponding to A and V ?); pores subangular, longitudinally and transversely aligned, markedly increasing in size distally; proximal pores may be subdivided by fine meshwork.
- Prunopyle fragilis* (Stöhr), Crouch and Hollis 1996, p. 26; Hollis et al. 1997, p. 47, pl. 2, figs. 28, 29. (Plate 8, fig. 8).
- Prunopyle polyacantha* Campbell and Clark 1944, p. 30, pl. 5, figs. 4-6 (only). (Plate 10, fig. 18).
- Prunopyle* aff. *polyacantha* ? Campbell and Clark 1944, p. 30, pl. 5, figs. 4-6 (only). (Plate 10, fig. 19). Shell ovoidal; pores of outermost layer circular to ovate, irregular in size and distribution; surface roughened by irregularly distributed thorns originating at pore bar junctions; several long spines surround pylome; internal structure irregular.
- Prunopyle* cf. *titan* Campbell and Clark, O'Connor 1993, p. 33, pl. 1, figs. 16, 17, pl. 10, fig. 1. (Plate 8, fig. 9). Differs from *P. titan* by being older and generally smaller.
- Prunopyle* sp. (Plate 8, fig. 10). Test ovoidal, outermost shell thick-walled, generally smooth-surfaced, pores small, circular to subcircular, irregularly distributed; inner structure indiscernible; long spines surround pylome.
- Pseudodictyophimus gracilipes* (Bailey), Petrushevskaya 1971b, p. 93, figs. 47-49. (Plate 9, fig. 38).
- Pteropilium* sp. (Plate 9, fig. 39). Test of at least five segments; cephalis subspheroidal, irregularly pored, bearing massive, bladed, anteriorly offset apical horn; collar stricture distinct; thorax truncate ovoid, pores small, hexagonally arranged; two massive, bladed, proximally fenestrated, downwardly curved wings extend from mid-thorax (one anterior, one posterior); lumbar stricture externally distinct; post-thoracic segments shorter than thorax, pores as for thorax but larger; termination ragged (possibly due to breakage).
- Sethochytris babylonis* (Clark and Campbell) group, Riedel and Sanfilippo 1970, p. 528, pl. 9, figs. 1-3. (Plate 9, fig. 40).
- Siphocampe* cf. *acephala* (Ehrenberg), Nigrini 1977, p. 254, pl. 3, fig. 5. (Plate 9, fig. 41). Differs slightly from *S. acephala* by having a centred cephalis, but falls within the boundaries of *S. acephala* (Ehrenberg) group of Hollis et al. (1997).
- Siphocampe nodosaria* (Haeckel), Nigrini 1977, p. 256, pl. 3, fig. 11. (Plate 9, fig. 42).
- Siphocampe* aff. *nodosaria* (Haeckel), Nigrini 1977, p. 256, pl. 3, fig. 11. (Plate 9, fig. 43). Differs from *S. nodosaria* by having well-defined, rounded abdominal strictures.
- Spongodiscus cruciferus* Clark and Campbell 1942, p. 50, pl. 1, figs. 1-6, 8, 10, 11, 16-18. (Plate 10, fig. 20).
- Spongodiscus* cf. *cruciferus* Clark and Campbell 1942, p. 50, pl. 1, figs. 1-6, 8, 10, 11, 16-18. (Plate 10, fig. 23). Differs from *S. cruciferus* by having a small, solid?, spherical part in the centre of the shell.

## PLATE 2

All illustrations are scanning electron micrographs. Illustrated specimens are from the following samples (see Table 1 for locality information): figs. 14, 16, 23-27 - BN1; figs. 12a-13b - BN2; figs. 1, 2 - BN6; figs. 3, 5 - BN7; fig. 6 - BN8; figs. 4, 9, 10, 17a-21b - FG1; figs. 7, 8, 11, 15, 22a, b - JP1. Scale bars for figs. 6-10, 12a, 13a, 14, 15, 17a, 18, 19, 21a, 22a & 23-26 are 50µm; scale bars for figs. 1-4, 12b, c, 13b, 17b, 21b & 27 are 20µm; scale bars for figs. 5, 16, 20 & 22b are 10µm; scale bar for fig. 11 is 5µm.

- 1-5 *Carpocanopsis ballisticum* O'Connor n. sp. - 1-4) paratypes R432-R435, 4) specimen with undulating termination, 5) paratype, R436, basal view of cephalis showing internal skeletal structure.
- 6-11 *Zealithapium oamaru* O'Connor n. sp. - 6-11) paratypes R441-R446, 11) basal view of apical horn showing lack of internal skeletal structure.
- 12a-16 *Verutotholus doigi* O'Connor n. sp. - 12a-c) paratype, R451, 12a) posterior view, arrow indicates posterior proximal opening of apical horn (twisted in this specimen so opening lateral), 12b) close-up of cephalis and upper thorax showing vertical tube and small wings, 12c) right lateral close-up of cephalis and upper thorax, vertical tube to right, 13a, b) paratype, R452, 13a) slightly right oblique posterior view, arrow indicates posterior proximal opening of apical horn, 13b) close-up of cephalis and upper thorax, 14) paratype, R453, right lateral view, 15) paratype, R454, left lateral view, 16) paratype, R455, basal view of cephalis showing internal skeletal structure.
- 17a-20 *Verutotholus edwardsi* O'Connor n. sp. - 17a, b) paratype, R460, 17a) posteriorly oblique right lateral view, 17b) posterior view, close-up of cephalis and upper thorax showing vertical tube, 18, 19) paratypes R461 & R462, 18) posteriorly oblique left lateral view, arrow indicates vertical tube, 20) paratype, R463, basal view of cephalis showing internal skeletal structure.
- 21a-22b *Verutotholus mackayi* O'Connor n. sp. - 21a, b) paratype, R468, 21a) posteriorly oblique right lateral view, 21b) close-up of cephalis and upper thorax showing vertical tube and small wings, 22a, b) paratype R469, 22a) left lateral view, arrow indicates vertical tube, 22b) basal view of cephalis showing internal skeletal structure.
- 23-27 *Lithomelissa lautouri* O'Connor n. sp. - 23-26) paratypes R472-R475, 24-26) arrows indicate A, 27) paratype, R476, basal view of cephalis showing internal skeletal structure.



- Spongodiscus maculatus* Clark and Campbell, emend. Blueford 1988, p. 254, pl. 7, figs. 6, 7. (Plate 8, fig. 11).
- Spongodiscus nitidus* (Sanfilippo and Riedel). *Stylotrochus nitidus* Sanfilippo and Riedel 1973, p. 525, pl. 13, figs. 9-14, pl. 30, figs. 7-10. (Plate 8, fig. 16). This form is included in *Spongodiscus* because of the spongy, discoidal nature of its shell. The distinguishing feature which led Sanfilippo and Riedel (1973) to place it in *Stylotrochus*, ie. greater ring spacing, is not considered distinct enough to separate it generically from other spongodiscids with internal rings, eg. *S. pulcher* (see Plate 8, figs. 12, 13).
- Spongodiscus pulcher* Clark and Campbell, emend. Blueford 1988, p. 252, pl. 7, figs. 2, 3. (Plate 8, figs. 12, 13).
- Spongodiscus rhabdostylus* (Ehrenberg), Sanfilippo and Riedel 1973, p. 525, pl. 13, figs. 1-3, pl. 30, figs. 1, 2. (Plate 8, fig. 14).
- Spongodiscus* aff. *rhabdostylus* (Ehrenberg), Sanfilippo and Riedel 1973, p. 525, pl. 13, figs. 1-3, pl. 30, figs. 1, 2. (Plate 10, fig. 21). Differs from *S. rhabdostylus* by having thick central and outer parts to the disk, separated by a thinner part (cf. *S. americanus* Kozlova in Kozlova and Gorbovetz 1966).
- Spongodiscus* sp. (Plate 8, fig. 15; plate 10 fig. 22). Test discoidal with slightly thickened centre, entirely spongy, no concentric rings; numerous thin bars extend from the centre of the shell and become conical marginal spines.
- Spongopyle spiralis* Bjørklund and Kellogg 1972, p. 392, pl. 1, figs. 4, 10. (Plate 8, fig. 17; plate 10, figs. 24a, b).

- Spongopyle* sp. (Plate 8, fig. 18; plate 10, figs. 25a, b). Lenticular test, subcircular in outline; cortical shell densely covered with small, irregularly arranged, circular to subcircular pores; surface relatively smooth with short, irregularly distributed, conical spines which are continuations of radial beams extending from centre of shell; 5-7 inner shells with large circular to ovate, irregularly distributed pores; pylome relatively large, circular in cross section, surrounded by conical spines.
- Stylodictya targaeformis* (Clark and Campbell), Petrushevskaya and Kozlova 1972, p. 526, pl. 18, fig. 10. (Plate 8, fig. 21; plate 10, fig. 27).
- Stylodictya* cf. *variabilis* Bjørklund and Kellogg 1972, p. 391, pl. 1, figs. 5, 9a, b. (Plate 8, fig. 19). Differs from *S. variabilis* by being smaller.
- Stylodictya* sp. (Plate 8, fig. 20; plate 10, fig. 26). Shell consisting of at least seven concentric chambers, distance between last two chambers much larger than that between any others; smooth-surfaced; many radial bars extend outside as long, conical, marginal spines.
- Stylosphaera hexaxypophora* (Clark and Campbell), Blueford 1988, p. 248, pl. 4, figs. 7-9. (Plate 8, fig. 22). Spines generally very short or broken in specimens encountered here.
- Stylosphaera minor* Clark and Campbell 1942, p. 16, pl. 1, figs. 13, 14. (Plate 8, fig. 23; plate 10, fig. 28).
- Theoperidae gen. et sp. indet. (Plate 9, fig. 45). Test of at least five segments; cephalis spheroidal, surface relatively smooth, pores small, circular to subcircular, irregularly distributed, bearing two, stout, bladed horns (correspond-

### PLATE 3

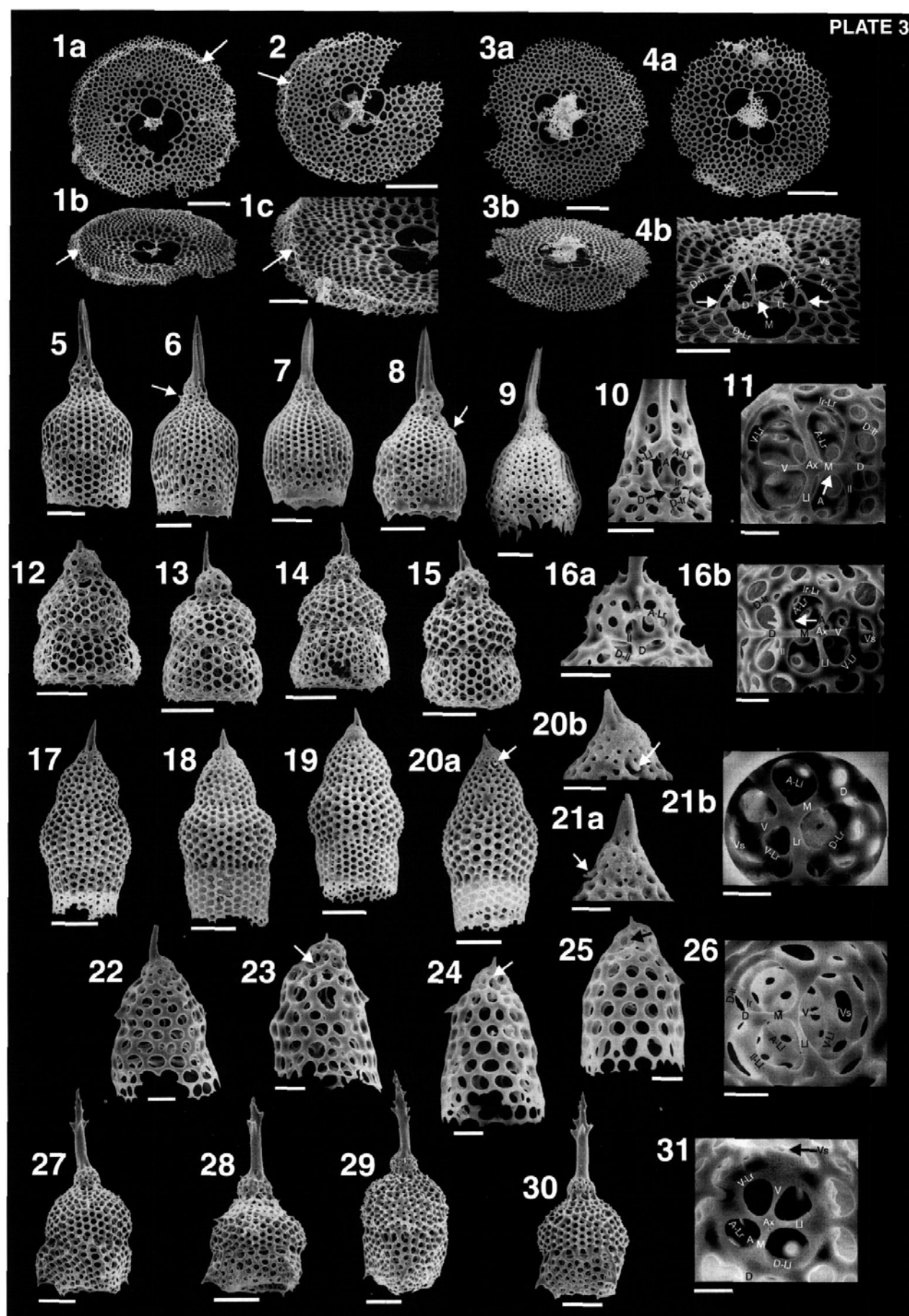
All illustrations are scanning electron micrographs. Illustrated specimens are from the following samples (see Table 1 for locality information): figs. 5, 6, 10, 27-31 - BN1; figs. 12-15 - BN2; fig. 9 - BN3; figs. 1a-c, 3a, b - BN6; figs. 2, 4a, b, 18 - JP1; fig. 19 - FH2; figs. 7, 8 - FH3; figs. 11, 22-26 - CQ1; figs. 16a-17, 21a, b - CS1; figs. 20a, b - DH2. Scale bars for figs. 1a, b & 2-4a are 100µm; scale bars for figs. 1c, 4b-9, 12-15, 17-20a & 27-30 are 50µm; scale bars for figs. 10, 16a, 20b, 21a & 22-25 are 20µm; scale bars for figs. 11, 16b, 21b, 26 & 31 are 10µm.

- 1a-4b *Velicucullus fragilis* O'Connor n. sp. - 1a-2) paratypes R482 & R483, arrows indicate velum, 1a, 2) basal views, 1b) oblique basal view, 1c) enlargement of oblique basal view, 3a-4b) paratypes R484 & R485, 3a, 4a) apical views, 3b) oblique apical view, 4b) oblique apical close-up of cephalis showing internal skeletal structure, unlabelled arrows indicate bifurcations.
- 5-11 *Lamprocyclas particollis* O'Connor n. sp. - 5-11) paratypes R489-R495, 5, 7) slightly left oblique anterior view, 6) left lateral view, arrow indicates large Vs, 8) right lateral view, arrow indicates small wing associated with Lr, 9) right lateral view, 10) anterior close-up of cephalis showing structural elements, 11) basal view of cephalis showing internal skeletal structure.
- 12-16b *Artophormis fluminafauces* O'Connor n. sp. - 12-15) paratypes R501-R504, 13) right lateral view, 14) left lateral view, 16a, b) paratype, R505, 16a) anterior close-up of cephalis showing structural elements,

16b) basal view of cephalis showing internal skeletal structure.

- 17-21b *Eucyrtidium ventriosum* O'Connor n. sp. - 17-19) paratypes R510-R512, 20a, b) paratype, R513, 20a) slightly right oblique posterior view, arrow indicates Vs, 20b) close-up of cephalis, arrow indicates Vs, 21a, b) paratype, R514, 21a) left lateral close-up of cephalis, arrow indicates Vs, 21b) basal view of cephalis showing internal skeletal structure (A hidden below junction of M, D and arches)
- 22-26 *Eurystomoskevos cauleti* O'Connor n. sp. - 22-26) paratypes R519-R523, 22) anteriorly oblique right lateral view, 23) slightly right oblique anterior view, arrow indicates II, 24) slightly left oblique anterior view, arrow indicates A-LI, 25) slightly right oblique anterior view, arrow indicates A, 26) basal view of cephalis showing internal skeletal structure (A hidden below junction of M, D, II and Ir).
- 27-31 *Lophocyrtis (Lophocyrtis) haywardi* O'Connor n. sp. - 27-31) paratypes R527-R531, 31) basal view of cephalis showing internal skeletal structure.





ing to **A** and **V**?); collar stricture externally indistinct due to wings; thorax slightly inflated truncate-conical, thick-walled, pores circular to subcircular, generally longitudinally aligned, three? stout, bladed wings (corresponding to **D**, **L** and **Lr**?) extend from uppermost thorax just below collar stricture (extend onto stricture and obscure it); lumbar stricture generally externally indistinct, internally expressed as a ring; abdomen short, slightly inflated cylindrical, wider than thorax, pores as for thorax; post abdominal segments as for abdomen but narrower, strictures as for lumbar stricture; termination ragged.

*Tholospyris* ? sp. (Plate 10, fig. 42). Lattice shell rough-surfaced due to short thorns projecting from lattice bars; lattice bars relatively thin; pores very large and subangular adjacent to sagittal ring, circular to ovate and irregular in size and distribution away from sagittal ring; at least five conical, thorned basal feet.

*Tristyluspyris tricerus* (Ehrenberg), Haeckel 1887, p. 1033; Sanfilippo *et al.* 1985, p. 665, figs. 10.3a, b. (Plate 8, fig. 26).

*Verutotholus* cf. *doigi* O'Connor n. sp., pl. 2, figs. 12a-16, pl. 6, figs. 1a-4. (Plate 9, fig. 46). Differs from *V. doigi* by having a stouter, relatively shorter, conical apical horn, rough-surfaced cephalis, and a relatively narrower abdomen that flares distally.

*Zealithapium mitra* (Ehrenberg). *Lithapium mitra* (Ehrenberg), Riedel and Sanfilippo 1970, p. 520, pl. 4, figs. 6, 7. (Plate 9, fig. 47). See *Zealithapium* O'Connor n.gen., above.

*Zygocircus buetschlii* Haeckel 1887, p. 948; Petrushevskaya and Kozlova 1972, p. 534, pl. 41, figs. 8-11. (Plate 10, fig. 43).

## ACKNOWLEDGMENTS

Many thanks are due to Associate Professor J.A. Grant-Mackie, University of Auckland, for advice, proof reading, and help with Latin names, and to Dr Chris Hollis, Institute of Geological and Nuclear Sciences, for advice, references, and samples. Thanks also to John Nowak for help with computer related problems. This study was funded in part by a University of Auckland Doctoral Scholarship, and the McKee Trust Post Graduate Scholarship.

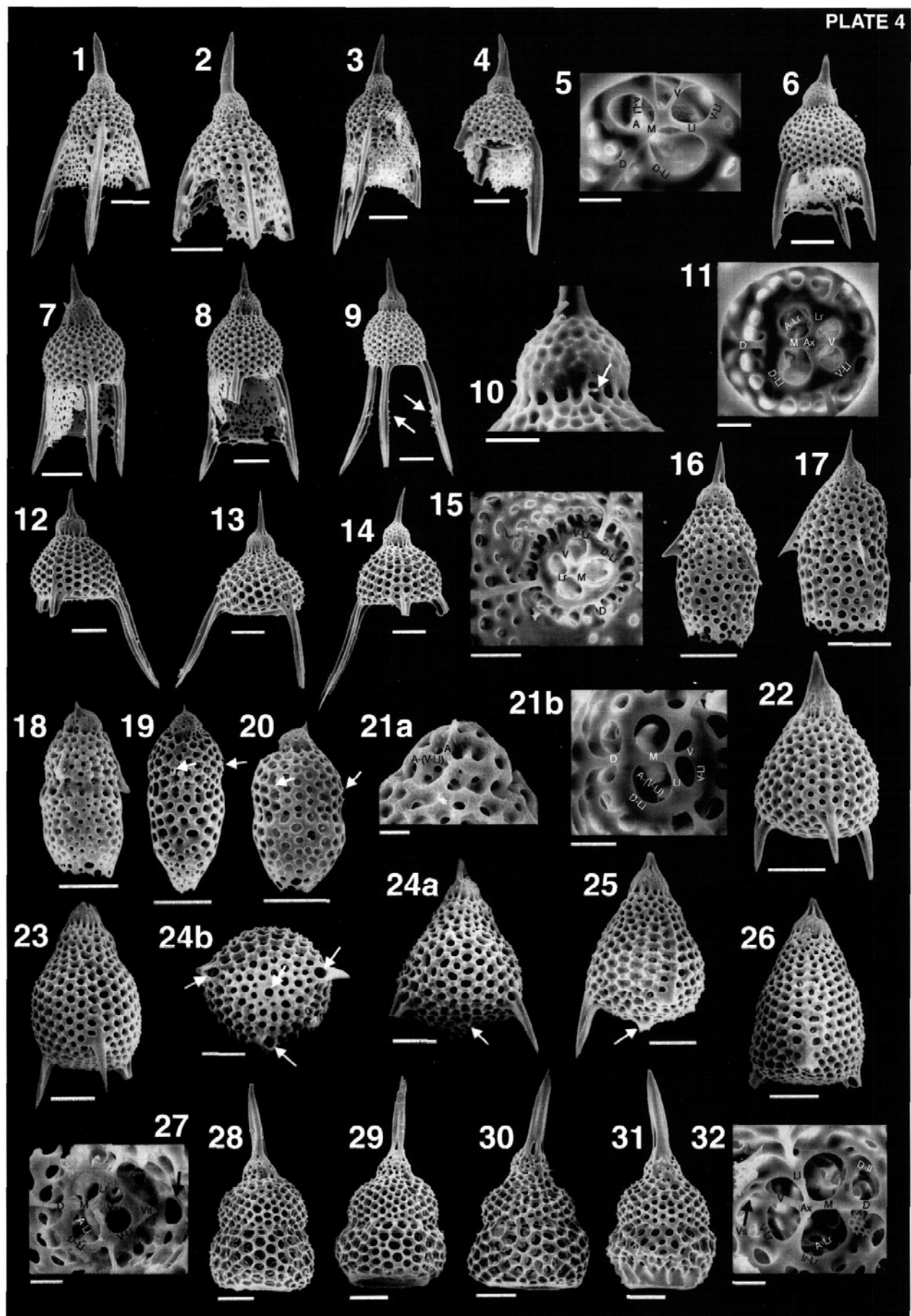
## REFERENCES

- ABELMANN, A., 1990. Oligocene to middle Miocene radiolarian stratigraphy of southern high latitudes from Leg 113, Sites 689 and 690, Maud Rise. In: Barker, P.F. *et al.* Proceedings of the Ocean Drilling Program, Scientific Results, Volume 113:675-708. College Station, Texas: Ocean Drilling Program.
- ALEXANDROVICH, J. M., 1992. Radiolarians from sites 794, 795, 796 and 797 (Japan Sea). In: Pisciotto, K.A. *et al.* Proceedings of the Ocean Drilling Program, Scientific Results, Volume 127/128, Part 1:291-307. College Station, Texas: Ocean Drilling Program.
- BENGSTON, P., 1988. Open Nomenclature. *Paleontology*, 31:223-227.
- BJØRKLUND, K. R., 1976. Radiolaria from the Norwegian Sea, Leg 38 of the Deep Sea Drilling Project. In: Talwini, M. *et al.* Initial Reports of the Deep Sea Drilling Project, Volume 38:1101-1168. Washington, DC: US Government Printing Office.
- BJØRKLUND, K. R. and KELLOGG, D. E., 1972. Five new Eocene radiolarian species from the Norwegian Sea. *Micropaleontology*, 18:386-396.

## PLATE 4

All illustrations are scanning electron micrographs. Illustrated specimens are from the following samples (see Table 1 for locality information): figs. 1, 2, 12-15, 28-30 - BN1; figs. 19-21b - BN7; figs. 3-5, 7-11, 23-24b - FG1; figs. 25-27 - FG4; fig. 6 - JP1; figs. 16, 17 - CQ1; fig. 18 - DH1; fig. 22 - FH3; figs. 31, 32 - CS1. Scale bars for figs. 1-4, 6-9, 12-14, 16-20, 22-26 & 28-31 are 50µm; scale bars for figs. 10 & 15 are 20µm; scale bars for figs. 5, 11, 21a, b, 27 & 32 are 10µm.

- 1-5 *Lychnocanium alma* O'Connor n. sp. - 1-5) paratypes R536-R540, 2) all feet broken, 5) basal view of cephalis showing internal skeletal structure.
- 6-11 *Lychnocanium waiareka* O'Connor n. sp. - 6-11) paratypes R545-R550, 9) specimen with abdomen missing, arrows indicate attachment points of abdomen to feet, 10) close-up of slightly right oblique posterior view of cephalis, arrow indicates **Vs**, 11) basal view of cephalis showing internal skeletal structure (**A** hidden below junction of **D**, **M** and arches).
- 12-15 *Lychnocanium waitaki* O'Connor n. sp. - 12-15) paratypes R555-R558, 15) basal view of cephalis showing internal skeletal structure (**A** hidden below junction of **D**, **M** and arches).
- 16-21b *Pterosyringium hamata* O'Connor n. sp. - 16-20) paratypes R563-R567, 19, 20) arrows indicate wing remnants, 21a, b) paratype, R568, 21a) close-up of right oblique anterior view showing structural elements, 21b) basal view of cephalis showing internal skeletal structure (**A** hidden below junction of **D**, **M** and arches).
- 22-27 *Sethochytris cavipodis* O'Connor n. sp. - 22, 23) paratypes R573 & R574, 23) apical horn broken, 24a, b) paratype, R575, 24a) arrow indicates basal pore, 24b) basal view, white arrows indicate pores at base of feet, black arrow indicates basal pore, 25-27) paratypes R576-R578, 25) arrow indicates basal pore in form of short tube, 26) feet broken, 27) basal view of cephalis showing internal skeletal structure (**A** hidden below junction of **D**, **M** and arches), arrow indicates large pore.
- 28-32 *Thyrsoyrtis* (T. ?) *pinguisoides* O'Connor n. sp. - 28-32) paratypes R583-R587, 31) specimen with unusually large peristome, 32) basal view of cephalis showing internal skeletal structure (**A** hidden below junction of **D**, **M**, **Il** and **Ir**).



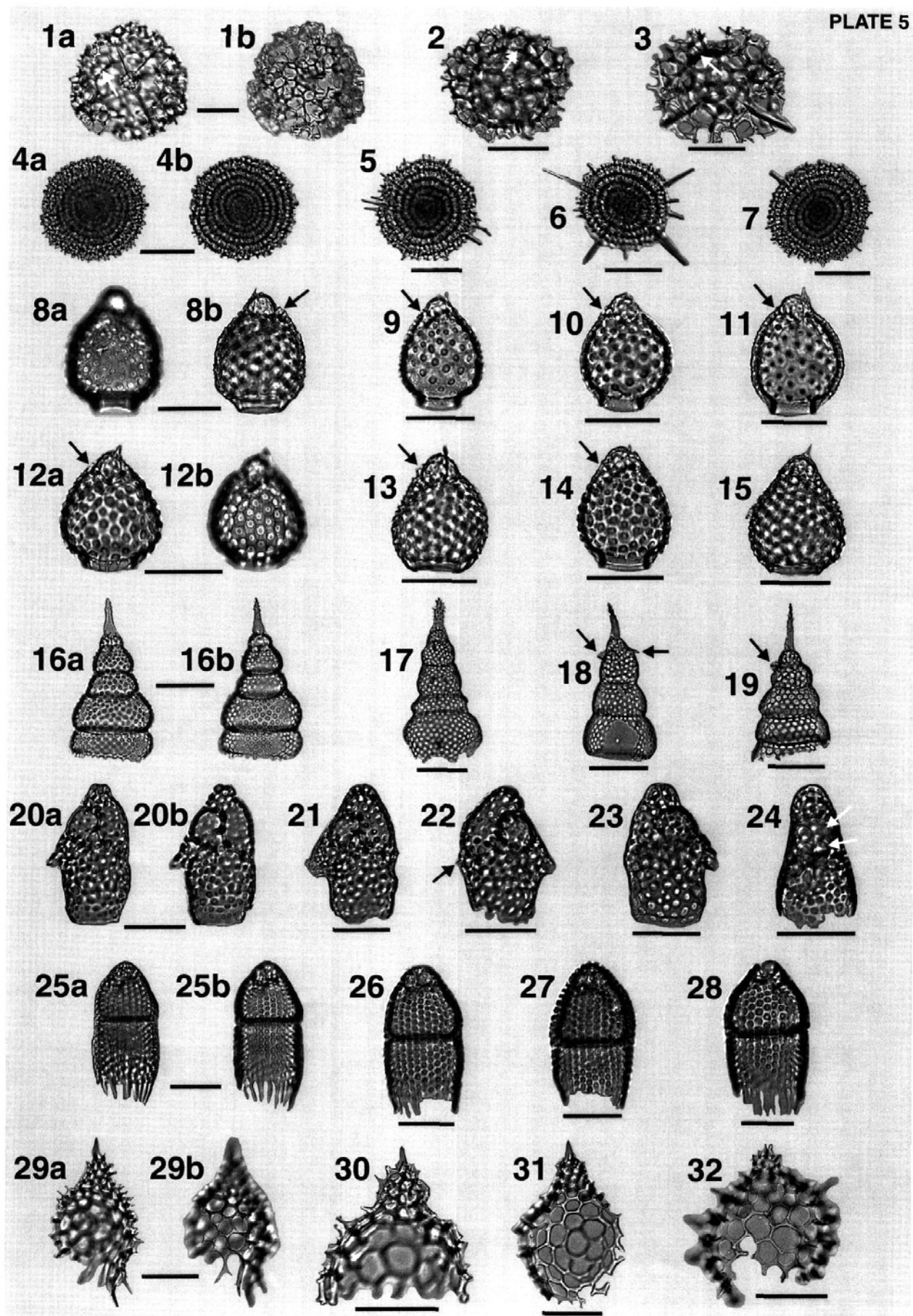
- BLOME, C. D., 1992. Radiolarians from Leg 122, Exmouth and Wombat Plateaus, Indian Ocean. In: von Raud, U. et al. Proceedings of the Ocean Drilling Program, Volume 122:633-652. College Station, Texas: Ocean Drilling Program.
- BLUEFORD, J. R., 1988. Radiolarian biostratigraphy of siliceous Eocene deposits in central California. *Micropaleontology*, 34:236-258.
- BURY, Mrs., 1862. Figures of remarkable forms of polycystins, or allied organisms, in the Barbados chalk deposit. 4pp., 26pls. London.
- BÜTSCHLI, O., 1882a. Beiträge zur Kenntnis der Radiolarienskelette, insbesondere der der Cyrtida. *Zeitschrift für Wissenschaftliche Zoologie*, 36:485-540, pls.31-33.
- , 1882b. Radiolaria. In: Bronn, H.G. (ed). *Klassen und Ordnungen des Thier-Reichs, wissenschaftlich dargestellt in Wort und Bild*, Volume 1, Part 1:332-478, pls.17-32.
- CAMPBELL, A. S., 1954. Radiolaria. In: Moore, R.C. (ed.) *Treatise on Invertebrate Paleontology. Part D, Protista 3. Protozoa (chiefly Radiolaria and Tintinnia)*. Geological Society of America & University of Kansas Press, pp.11-163.
- CAMPBELL, A. S. and CLARK, B. L., 1944. Miocene radiolarian faunas from southern California. *Special Paper of the Geological Society of America*, 51:1-76.
- CARNEVALE, P., 1908. Radiolarie e silicoflagellati di Bergonzano (Reggio Emilia). *Reale Istituto Veneto di Scienze, Lettere ed Arti, Memoire*, 28(3):1-46, pls.1-4.
- CAULET, J.-P., 1972. Premières observations sur la dissolution progressive des squelettes de Sphaerellaires (Radiolaires) en voie de sédimentation dans les vases de la Méditerranée. Incidences sur la systématique de ces formes. *Comptes Rendus Hebdomadaires des Séances de l'Académie des Sciences, serie D, Sciences Naturelles*, 274:2759-2762.
- , 1986. Radiolarians from the Southwest Pacific. In: Kennett, J.P. et al. *Initial Reports of the Deep Sea Drilling Project, Volume 90:835-861*. Washington, DC: US Government Printing Office.
- , 1991. Radiolarians from the Kerguelen Plateau, Leg 119. In: Barron, J. et al. *Proceedings of the Ocean Drilling Program, Scientific Results, Volume 119:513-546*. College Station, Texas: Ocean Drilling Program.

## PLATE 5

All illustrations are transmitted light photomicrographs. Illustrated specimens are from the following samples (see Table 1 for locality information): figs. 1a-2, 26, 27, 29a-32 - FG1; figs. 6, 7 - FG2; figs. 8a, b, 15, 25a, b - FG3; fig. 5 - FG4; figs. 3, 12a-13, 16a-17 - FG5; figs. 4a, b - CS1; figs. 20a, b - CQ1; figs. 9-11, 14 - BN2; fig. 28 - BN6; figs. 21-24 - DH1; figs. 18, 19 - DH2. Scale bars for figs. 1a-7 & 29a-32 are 100µm; scale bars for figs. 8a-28 are 50µm.

- 1a-3 *Tricorporisphaera bibula* O'Connor n. sp. - 1a, b) holotype, R386, 1a) specimen focused through centre, arrow indicates outer medullary shell, 1b) specimen focused on surface of cortical shell, 2, 3) paratypes R387 & R388, arrows indicate outer medullary shells.
- 4a-7 *Plectodiscus runanganus* O'Connor n. sp. - 4a, b) holotype, R393, 4a) specimen focused on equatorial plane, 4b) specimen focused near surface, 5-7) paratypes R394-R396.
- 8a-11 *Plannapus hornibrooki* O'Connor n. sp. - 8a, b) holotype, R401, right lateral view, 8a) specimen focused on surface of thorax, 8b) specimen focused on sagittal plane, arrow indicates vertical tube, 9-11) paratypes R402-R404, left lateral views, specimens focused on or near sagittal planes, arrows indicate vertical tubes.
- 12a-15 *Plannapus mauricei* O'Connor n. sp. - 12a, b) holotype, R409, left lateral view, 12a) specimen focused on sagittal plane, arrow indicates vertical tube, 12b) specimen focused on surface of thorax, 13-15) paratypes R410-R412, 13, 14) left lateral views, specimens focused on sagittal planes, arrows indicate vertical tubes.
- 16a-19 *Spirocyrtes greeni* O'Connor n. sp. - 16a, b) holotype, R419, posterior view, 16a) specimen focused through centre of cephalis, 16b) specimen focused on surface of abdomen, 17-19) paratypes R420-R422, 18) left lateral view, specimen focused on sagittal plane, downwardly-directed arrow indicates vertical tube, horizontal arrow indicates small wing associated with D, 19) left lateral view, specimen focused on sagittal plane, arrow indicates vertical tube.
- 20a-24 *Botryocella pauciperforata* O'Connor n. sp. - 20a, b) holotype, R427, right lateral view, 20a) specimen focused on sagittal plane, 20b) specimen focused on surface of cephalis, 21-24) paratypes R428-R431, 21) left lateral view, specimen focused above sagittal plane, 22) right lateral view, specimen focused above sagittal plane, arrow indicates small wing associated with D, 23) right lateral view, specimen focused above sagittal plane, 24) posterior view, downwardly-directed arrow indicates A-(A-II), near horizontal arrow indicates A-II.
- 25a-28 *Carpocanopsis ballisticum* O'Connor n. sp. - 25a, b) holotype, R437, 25a) specimen focused on sagittal plane, 25b) specimen focused on surface of thorax and abdomen, 26-28) paratypes R438-R440, specimens focused above sagittal plane.
- 29a-32 *Zealithapium oamaru* O'Connor n. sp. - 29a, b) holotype, R447, 29a) specimen focused on surface of narrow conical upper part, 29b) specimen focused on surface of wide lower part, 30-32) paratypes R448-R450, 30) specimen broken below greatest width.



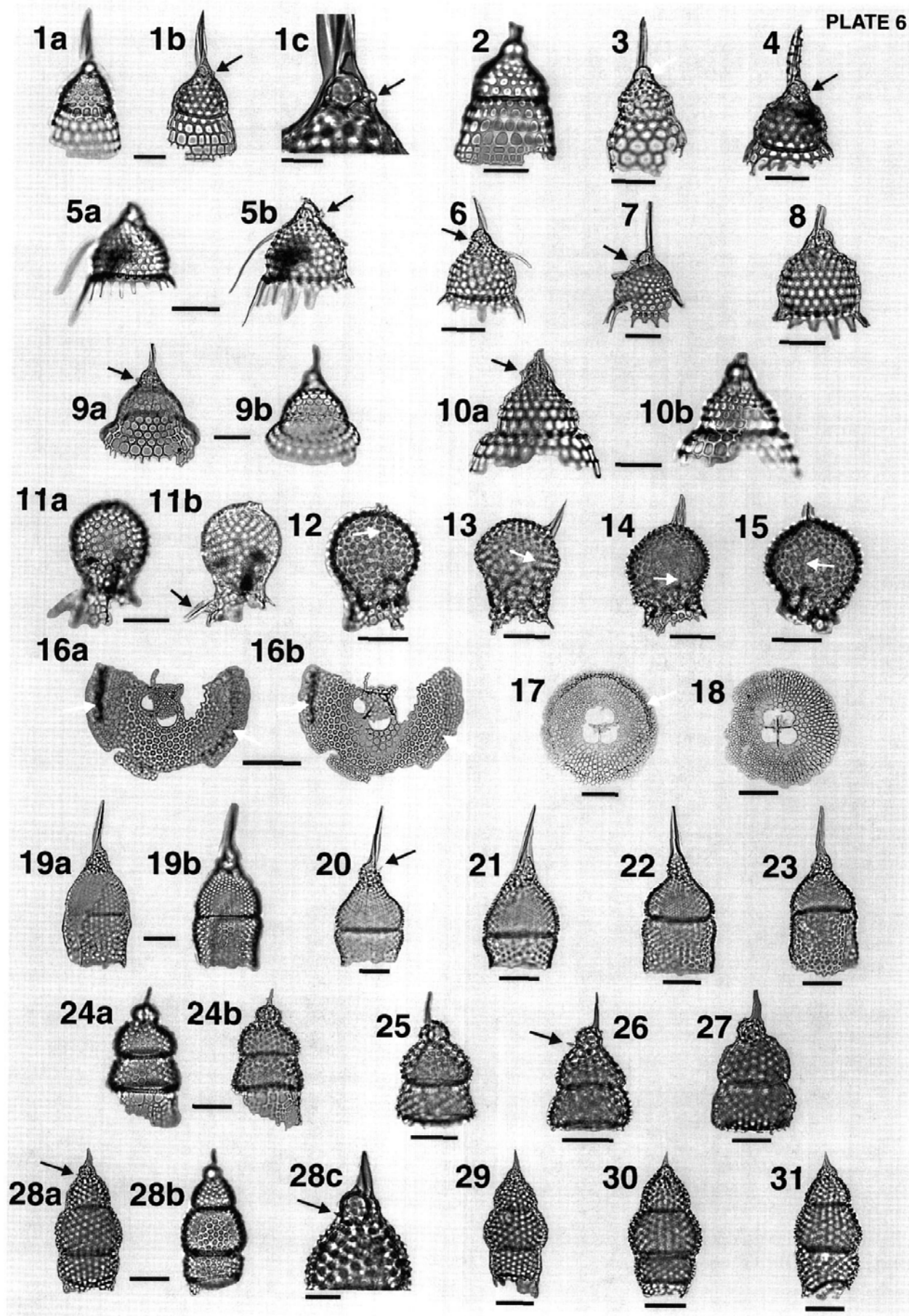


- CAYEUX, L., 1897. Contribution à l'étude micrographique de terrains sédimentaires. 1. Étude de quelques dépôts siliceux secondaires et tertiaires de Bassin de Paris et de la Belgique. 2. Craie du Bassin de Paris. Soc. Géol. Nord., Mém., Lille., 4(2):1-591, pl. 1-10.
- CHEN, PEI-HSIN, 1975. Antarctic Radiolaria. In: Hayes, D.E. et al. Initial Reports of the Deep Sea Drilling Project, Volume 28:437-513. Washington, DC: US Government Printing Office.
- CLARK, B. L. and CAMPBELL, A. S., 1942. Eocene radiolarian faunas from the Mt. Diablo area, California. Special Paper of the Geological Society of America, 39:1-112.
- , 1945. Radiolaria from the Kreyenhagen Formation near Los Banos, California. Geological Society of America Memoir, 10:1-66.
- CROUCH, E. M. and HOLLIS, C. J., 1996. Paleocene palynomorph and radiolarian biostratigraphy of DSDP Leg 29, sites 280 and 281, South Tasman Rise. Institute of Geological and Nuclear Sciences, Science Report 96/19. Lower Hutt. 46pp.
- De WEVER, P., 1981. Spyrids, artostrobiids, and Cretaceous radiolarians from the western Pacific, Deep Sea Drilling Project Leg 61. In: Moberly, R. et al. Initial Reports of the Deep Sea Drilling Project, Volume 61:507-520. Washington, DC: US Government Printing Office.
- DINKELMAN, M. G., 1973. Radiolarian stratigraphy: Leg 16, Deep Sea Drilling Project. In: van Andel, T.H. et al. Initial Reports of the Deep Sea Drilling Project, Volume 16:747-813. Washington, DC: US Government Printing Office.
- DOGIEL, V. A. and RESHETNYAK, V. V., 1952. Materialy po radiolarii severo-zapadnoi chasti Tikhogo okeana (Material on radiolarians of the northwestern part of the Pacific Ocean). Issled.

## PLATE 6

All illustrations are transmitted light photomicrographs. Illustrated specimens are from the following samples (see Table 1 for locality information): figs. 3-8, 14-18, 24a-25, 30, 31 - FG1; figs. 12, 13, 28a-29 - FG2; figs. 11a, b - BN1; figs. 22, 23, 26, 27 - BN2; figs. 1a-2 - BN4; figs. 9a-10b - JP1; fig. 21 - FH2; figs. 19a-20 - DH2. Scale bars for figs. 16a-18 are 100µm; scale bars for figs. 1a, b, 2-15, 19a-28b & 29-31 are 50µm; scale bars for figs. 1c & 28c are 20µm.

- 1a-4 *Verutotholus doigi* O'Connor n. sp. - 1a-c) holotype, R456, right lateral view, 1a) specimen focused on surface of thorax, 1b) specimen focused on sagittal plane, arrow indicates vertical tube, 1c) close-up of cephalis and upper thorax, arrow indicates vertical tube, 2-4) paratypes R457-R459, 2) anterior view, specimen focused on surface of thorax and abdomen, 3) posterior view, specimen focused on vertical tube, arrow indicates vertical tube, 4) right lateral view, specimen focused on sagittal plane, arrow indicates vertical tube.
- 5a-8 *Verutotholus edwardsi* O'Connor n. sp. - 5a, b) holotype, R464, right lateral view, 5a) specimen focused on surface of thorax, 5b) specimen focused on sagittal plane, arrow indicates vertical tube, 6-8) paratypes R465-R467, 6, 7) left lateral views, specimens focused on sagittal planes, arrows indicate vertical tubes, 8) specimen focused through centre of cephalis.
- 9a-10b *Verutotholus mackayi* O'Connor n. sp. - 9a, b) holotype, R470, left lateral view, 9a) specimen focused on sagittal plane, arrow indicates vertical tube, 9b) specimen focused on surface of thorax, 10a, b) paratype, R471, left lateral view, 10a) specimen focused on sagittal plane, arrow indicates vertical tube, 10b) specimen focused on surface of thorax.
- 11a-15 *Lithomelissa lautouri* O'Connor n. sp. - 11a, b) holotype, R477, 11a) specimen focused on surface of cephalis, 11b) specimen focused below centre of cephalis, arrow indicates wing, 12-15) paratypes R478-R481, specimens focused through centre of cephalis, arrows indicate A.
- 16a-18 *Velicucullus fragilis* O'Connor n. sp. - 16a, b) holotype, R486, basal view, arrows indicate velum, 16a) specimen focused on remains of cephalic wall, 16b) specimen focused on lower surface of thorax, 17, 18) paratypes R487 & R488, specimens focused on surface of thorax, 17) arrow indicates velum.
- 19a-23 *Lamprocyclus particollis* O'Connor n. sp. - 19a, b) holotype, R496, right lateral view, 19a) specimen focused on sagittal plane, 19b) specimen focused on surface of thorax and abdomen, 20-23) paratypes R497-R500, 20) left lateral view, specimen focused on sagittal plane, arrow indicates large Vs, 21) left lateral view, specimen focused on sagittal plane, 22) posterior view, specimen focused through centre of cephalis, 23) right lateral view, specimen focused on sagittal plane.
- 24a-27 *Artophormis fluminafauces* O'Connor n. sp. - 24a, b) holotype, R506, anterior view, 24a) specimen focused on surface of thorax and abdomen, 24b) specimen focused through centre of cephalis, 25-27) paratypes R507-R509, 25) right lateral view, specimen focused above sagittal plane, 26) left lateral view, specimen focused above sagittal plane, arrow indicates large Vs, 27) left lateral view, specimen focused on sagittal plane.
- 28a-31 *Eucyrtidium ventriosum* O'Connor n. sp. - 28a-c) holotype, R515, slightly anteriorly oblique left lateral view, 28a) specimen focused on sagittal plane, arrow indicates Vs, 28b) specimen focused on surface of abdomen, 28c) close-up of cephalis and thorax, arrow indicates Vs, 29-31) paratypes R516-R518, specimens focused near centre of cephalis.





- dalnevostochnykh morei SSSR. t. III (Investigations of the Far East Seas of the USSR, Publ.3).
- , 1955. Subclass Radiolaria. In: Atlas of the Invertebrates of the Far East Seas of the USSR. Institute of Zoology, Academy of Sciences, USSR, pp. 31-39, 1 pl.
- EDWARDS, A. R., 1991. The Oamaru Diatomite. New Zealand Geological Survey Paleontological Bulletin, 64. 260pp.
- EHRENBERG, C. G., 1838. Über die Bildung der Kreidefelsen und des Kreidemergels durch unsichtbare Organismen. Königlich Preussische Akademie der Wissenschaften zu Berlin, Abhandlungen, Jahre 1838, pp.59-147, pls.1-4, 3 tables.
- , 1844. Über 2 neue Lager von Gebirgsmassen aus Infusorien als Meeres-Absatz in Nord-Amerika und eine Vergleichung derselben mit den organischen Kreide-Gebilden in Europa und Afrika. Königlich Preussische Akademie der Wissenschaften zu Berlin, Bericht, Jahre 1844, pp.57-97.
- , 1847a. Über eine halibolithische, von Herrn R. Schomburgk entdeckte, vorherrschend aus mikroskopischen Polycystinen gebildete, Gebirgsmasse von Barbados. Königlich Preussische Akademie der Wissenschaften zu Berlin, Bericht, Jahre 1846, pp.382-385, chart to p. 385.
- , 1847b. Über die mikroskopischen kieselschaligen Polycystinen als mächtige Gebirgsmasse von Barbados und über das Verhältniss der aus mehr als 300 neuen Arten bestehenden ganz eigenthümlichen Formengruppe jener Felsmasse zu den jetzt lebenden Thieren und zur Kreidebildung. Eine neue Anregung zur Erforschung des Erdlebens. Königlich Preussische Akademie der Wissenschaften zu Berlin, Bericht, Jahre 1847, pp.40-60, chart to p. 54, 1 pl.
- , 1854. Mikrogeologie. Das Erden und Felsen schaffende Wirken des unsichtbar kleinen selbständigen Lebens auf der Erde. Voss, Leipzig. 374pp., Atlas 31pp., 41pls. Fortsetzung (1856) 88pp.
- , 1872a. Mikrogeologische Studien als Zusammenfassung seiner Beobachtungen des kleinsten Lebens der Meeres-Tiefgründe aller Zonen und dessen geologischen Einfluss. Königlich Preussische Akademie der Wissenschaften zu Berlin, Monatsbericht, Jahre 1872, pp.265-322.
- , 1872b. Mikrogeologischen Studien über das kleinste Leben der Meeres-Tiefgründe aller Zonen und dessen geologischen Einfluss. Königlich Preussische Akademie der Wissenschaften zu Berlin, Abhandlungen, Jahre 1872, pp.131-399, pls.1-12.
- , 1873. Grössere Felsproben des Polycystinen-Mergels von Barbados mit weiteren Erläuterungen. Königlich Preussische Akademie der Wissenschaften zu Berlin, Monatsbericht, Jahre 1873, pp.213-263.

## PLATE 7

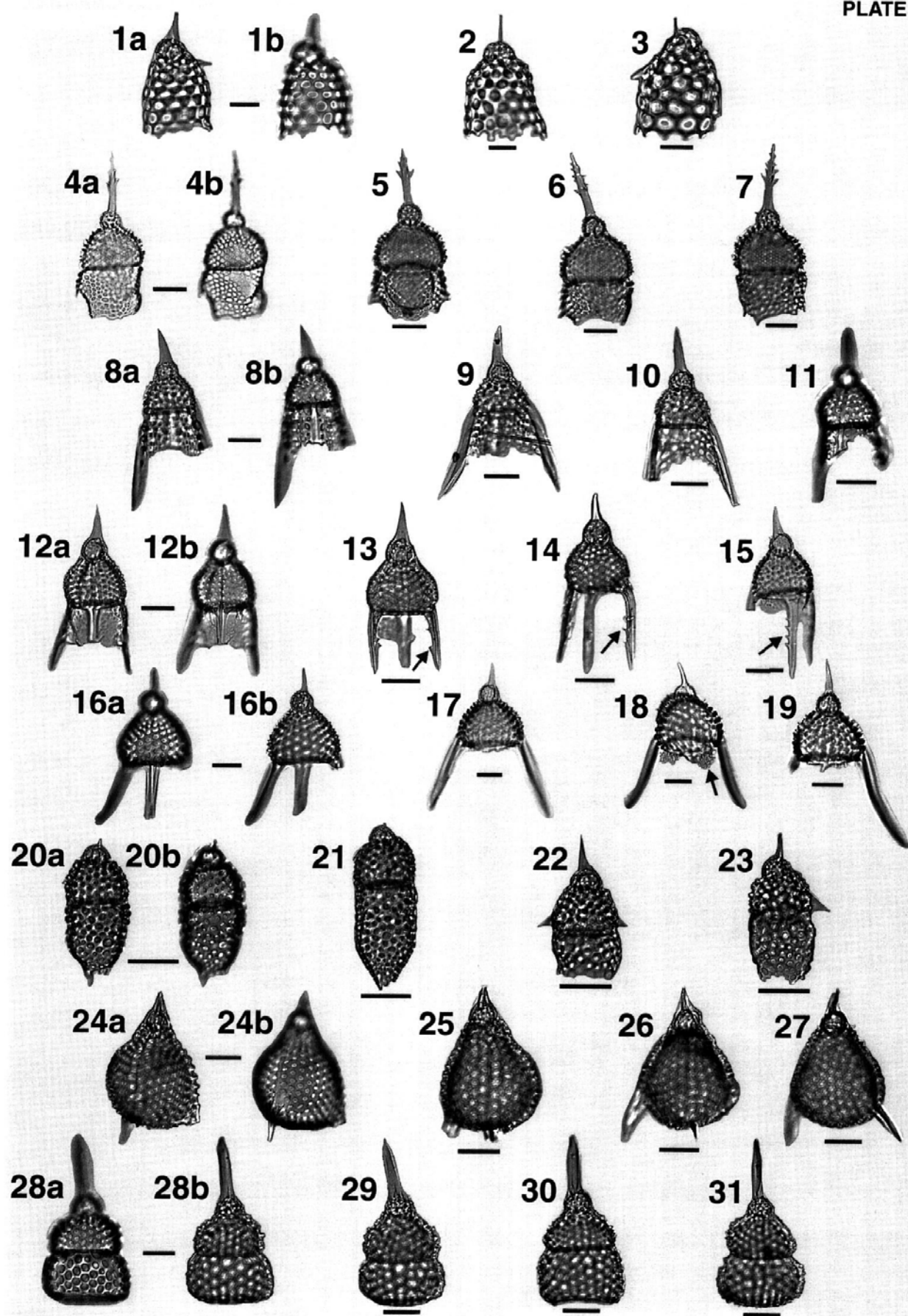
All illustrations are transmitted light photomicrographs. Illustrated specimens are from the following samples (see Table 1 for locality information): figs. 1a-2 - DH3; figs. 3, 22, 23 - CQ1; fig. 31 - BN1; figs. 4a-7 - BN2; fig. 19 - BN3; fig. 17 - BN7; figs. 11, 18, 27 - FG1; figs. 8a-9, 12a-16b, 28a-30 - FG2; figs. 10, 20a-21 - FG3; figs. 24a-26 - FG4.

Scale bars for figs. 4a-31 are 50µm; scale bars for figs. 1a-3 are 20µm.

- 1a-3 *Eurystomoskevos cauleti* O'Connor n. sp. - 1a, b) holotype, R524, 1a) specimen focused through centre of cephalis, 1b) specimen focused on surface of thorax, 2, 3) paratypes R525 & R526, specimens focused near centre of cephalis.
- 4a-7 *Lophocyrtis (Lophocyrtis) haywardi* O'Connor n. sp. - 4a, b) holotype, R532, 4a) specimen focused through centre of cephalis, 4b) specimen focused on surface of thorax and abdomen, 5-7) paratypes R533-R535, specimens focused near centre of cephalis.
- 8a-11 *Lychnocanium alma* O'Connor n. sp. - 8a, b) holotype, R541, 8a) specimen focused through centre of cephalis, 8b) specimen focused on surface of thorax, 9-11) paratypes R542-R544, 9, 10) specimens focused through centre of cephalis, 11) specimen focused on surface of thorax.
- 12a-15 *Lychnocanium waiareka* O'Connor n. sp. - 12a, b) holotype, R551, 12a) specimen focused through centre of cephalis, 12b) specimen focused on surface of thorax, 13-15) paratypes R552-R554, arrows indicate attachment points of abdomen to feet, 13, 15) specimens focused through centre of cephalis, 14) specimen focused above centre of cephalis.
- 16a-19 *Lychnocanium waitaki* O'Connor n. sp. - 16a, b) holotype, R559, 16a) specimen focused on surface of thorax, 16b) specimen focused through centre of cephalis, 17-19) paratypes R560-R562, specimens focused through centre of cephalis, 18) arrow indicates abdominal remnants.
- 20a-23 *Pterosyringium hamata* O'Connor n. sp. - 20a, b) holotype, R569, 20a) specimen focused through centre of cephalis, 20b) specimen focused on surface of thorax and abdomen, 21-23) paratypes R570-R572, specimens focused through centre of cephalis.
- 24a-27 *Sethocyrtis cavipodis* O'Connor n. sp. - 24a, b) holotype, R579, 24a) specimen focused through centre of cephalis, 24b) specimen focused on surface of thorax, 25-27) paratypes R580-R582, specimens focused through centre of cephalis.
- 28a-31 *Thyrsoyrtis (T. ?) pinguisoides* O'Connor n. sp. - 28a, b) holotype, R588, 28a) specimen focused on surface of thorax, 28b) specimen focused through centre of cephalis, 29-31) paratypes R589-R591, specimens focused through centre of cephalis.



## PLATE 7

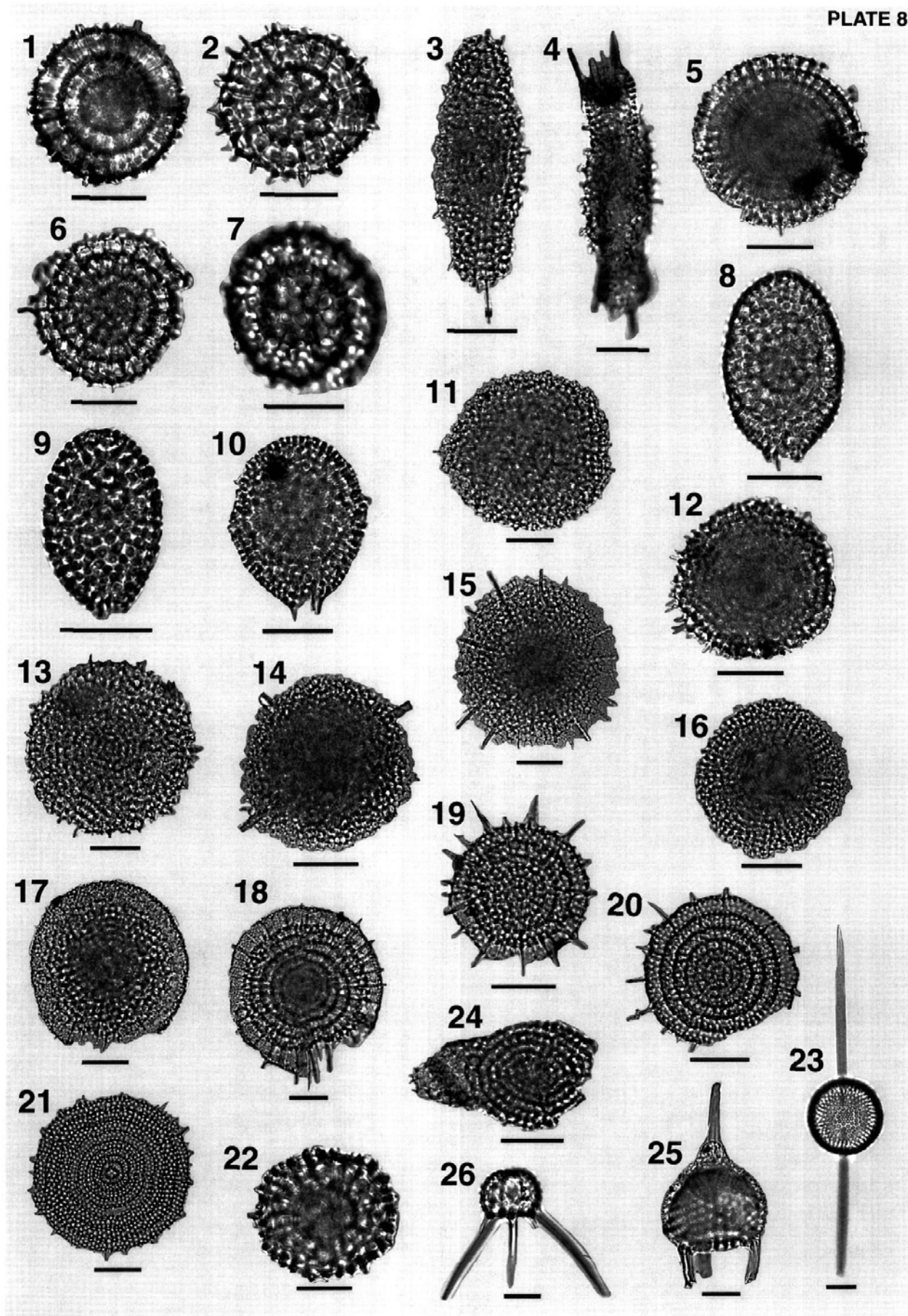


- , 1875. Fortsetzung der mikrogeologischen Studien als Gesamt-Übersicht der mikroskopischen Paläontologie gleichartig analysierter Gebirgsarten der Erde, mit specieller Rücksicht auf den Polycystinen-Mergel von Barbados. Königlich Preussische Akademie der Wissenschaften zu Berlin, Abhandlungen, Jahre 1875, pp.1-226, pls.1-30.
- FOREMAN, H. P., 1968. Upper Maestrichtian Radiolaria of California. Special Papers in Palaeontology, 3. The Palaeontological Association, London. 82 pp., 8 pls.
- , 1973. Radiolaria of Leg 10 with systematics and ranges for the families Amphipyndacidae, Artostrobiidae and Theoperidae. In: Worzel, J.L. et al. Initial Reports of the Deep Sea Drilling Project, Volume 10:407-474. Washington, DC: US Government Printing Office.
- FOREMAN, H. P. and RIEDEL, W. R., 1972. Catalogue of Polycystine Radiolaria, Series 1 (1834-1900), Volume 1 (Meyen, 1834 - Bury, 1862). Special Publication of the American Museum of Natural History, New York.
- , 1978. Polycystine Radiolaria, 1834-1930. 35 volumes (microfiche). National Technical and Information Service, Springfield, Virginia.
- FRIZZELL, D. L. and MIDDOUR, E. S., 1951. Paleocene Radiolaria from Southeastern Missouri. University of Missouri School of Mines and Metallurgy Bulletin, Technical Series, No.77.
- FUNAKAWA, S., 1994. Plagiacanthidae (Radiolaria) from the upper Miocene of Eastern Hokkaido, Japan. Transactions and Proceedings of the Palaeontological Society of Japan, new series, 174:458-483.
- GOLL, R. M., 1968. Classification and phylogeny of Cenozoic Trissocyclidae (Radiolaria) in the Pacific and Caribbean Basins, Part 1. Journal of Paleontology, 42:1409-1432.
- , 1969. Classification and phylogeny of Cenozoic Trissocyclidae (Radiolaria) in the Pacific and Caribbean Basins, Part 2. Journal of Paleontology, 43:322-339.
- , 1979. The Neogene evolution of *Zygocircus*, *Neosemantis* and *Callimitra*: their bearing on nassellarian classification. Micropaleontology 25: pp.365-396.
- GROVE, E., and STURT, G., 1886. On a fossil marine diatomaceous deposit from Oamaru, New Zealand. Part 1. Journal of the Quekett microscopical Club, series 2, 2(16):321-330.
- HAECKEL, E., 1862. Die Radiolarien (Rhizopoda Radiaria): Eine Monographie. Reimer, Berlin. xiv + 572pp., Atlas iv, 35 pls.
- , 1881. Entwurf eines Radiolarien-Systems auf Grund von Studien der Challenger-Radiolarien. Jenaische Zeitschrift für Naturwissenschaft, 15, new series, vol.8, pt.3:418-472.
- , 1887. Report on the Radiolaria collected by *H.M.S. Challenger* during the years 1873-76. Report on the scientific results of the voyage of the *H.M.S. Challenger*, Zoology 18. Two parts, clxxxviii + 1803pp., 140 pls., 1 map.
- HAYS, J. D., 1965. Radiolaria and Late Tertiary and Quaternary history of Antarctic seas. Biology of the Antarctic Seas, II. American Geophysical Union Antarctic Research Series, 5:125-184.
- , 1970. Stratigraphy and evolutionary trends of Radiolaria in North Pacific deep-sea sediments. Geological Society of America Memoir, 126:185-218.

## PLATE 8

All illustrations are transmitted light photomicrographs. Illustrated specimens are from the following samples (see Table 1 for locality information): figs. 1, 2, 5, 10, 12, 19, 26 - BN1; figs. 3, 7, 11, 13-18, 21, 22, 24 - BN2; fig. 20 - FG1; figs. 4, 6, 8, 9, 23, 25 - FG2. All scale bars are 50µm.

- |   |  |
|---|--|
| 1,2 <i>Actinommidae</i> gen. et sp. indet., R592 & R593 | 15 <i>Spongodiscus</i> sp., R606                   |
| 3 <i>Amphicraspedum prolixum</i> group, R594            | 16 <i>Spongodiscus nitidus</i> , R607              |
| 4 <i>Amphymenium splendarmatum</i> , R595               | 17 <i>Spongopyle spiralis</i> , R608               |
| 5 <i>Flustrella charlestonensis</i> , R596              | 18 <i>Spongopyle</i> sp., R609                     |
| 6 <i>Lithelius minor</i> , R597                         | 19 <i>Stylodictya</i> cf. <i>variabilis</i> , R610 |
| 7 <i>Lithelius nautiloides</i> , R598                   | 20 <i>Stylodictya</i> sp., R611                    |
| 8 <i>Prunopyle fragilis</i> , R599                      | 21 <i>Stylodictya targaeformis</i> , R612          |
| 9 <i>Prunopyle</i> cf. <i>titan</i> , R600              | 22 <i>Stylosphaera hexaxyphophora</i> , R613       |
| 10 <i>Prunopyle</i> sp., R601                           | 23 <i>Stylosphaera minor</i> , R614                |
| 11 <i>Spongodiscus maculatus</i> , R602                 | 24 <i>Lithelius</i> ? sp., R615                    |
| 12,13 <i>Spongodiscus pulcher</i> , R603 & R604         | 25 <i>Lychnocanium amphitrite</i> , R616           |
| 14 <i>Spongodiscus rhabdostylus</i> , R605              | 26 <i>Tristyluspyris tricerus</i> , R617.          |



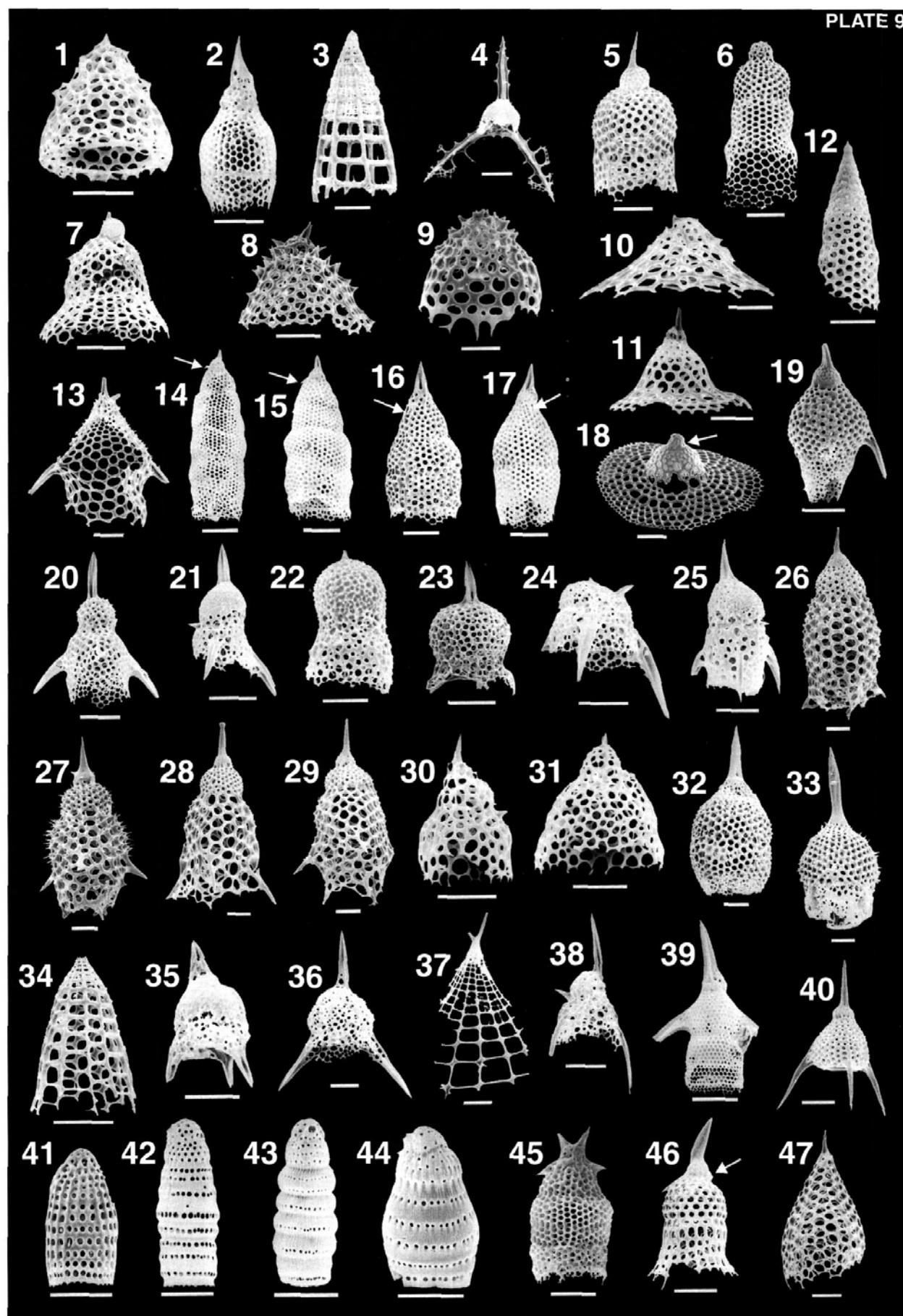
- HINDE, G. J., 1890. Notes on Radiolaria from the Lower Paleozoic rocks (Llandeilo-Caradoc) of the South of Scotland. The Annals and Magazine of Natural History, series 6, volume 6(1):40-59, pls. 3, 4.
- HINDE, G. J. and HOLMES, W. M., 1892. On the sponge-remains in the Lower Tertiary strata near Oamaru, Otago, New Zealand. Journal of the Linnean Society, Zoology, 24:177-262.
- HOLDSWORTH, B. K., 1975. Cenozoic Radiolaria biostratigraphy: Leg 30: tropical and equatorial Pacific. In: Andrews, J.E. et al. Initial Reports of the Deep Sea Drilling Project, Volume 30:499-537. Washington, DC: US Government Printing Office.
- HOLLIS, C. J., WAGHORN, D. B., STRONG, C. P. and CROUCH, E. M., 1997. Integrated Paleogene biostratigraphy of DSDP site 277 (Leg29): foraminifera, calcareous nannofossils, Radiolaria, and palynomorphs. Institute of Geological and Nuclear Sciences science report 97/07. 87pp.
- JOHNSON, D. A., 1974. Radiolaria from the eastern Indian Ocean, DSDP Leg 22. In: von der Borch, C.C. et al. Initial Reports of the

# PLATE 9

All illustrations are scanning electron micrographs. Illustrated specimens are from the following samples (see Table 1 for locality information): figs. 3, 9, 12, 14, 17, 28, 29, 34, 37, 39 - FH1; figs. 13, 20, 22, 36 - FH2; figs. 1, 10, 24 - FH3; figs. 25, 30, 31 - JP1; fig. 2 - JP2; figs. 8, 16, 21, 23, 44 - CQ1; figs. 11, 15, 42 - DH1; figs. 19, 32, 33, 40, 45 - FG1; fig. 38 - FG5; figs. 46, 47 - BN1; figs. 6, 7, 18, 26, 27, 35 - BN2; fig. 41 - BN3; fig. 4 - BN4; figs. 5, 43 - BN6. All scale bars are 50µm.

- |   |  |
|---|--|
| 1 <i>Ceratocyrtis</i> ? sp. B., R618  | 23 <i>Lithomelissa</i> cf. <i>haeckeli</i> , R640                                  |
| 2 <i>Anthocyrtidium stenum</i> , R619   | 24 <i>Lithomelissa</i> cf. <i>hertwigi</i> , R641                                  |
| 3 <i>Bathropyramis magnifica</i> , R620   | 25 <i>Lithomelissa</i> cf. <i>mitra</i> , R642                                     |
| 4 <i>Callimitra atavia</i> , R621   | 26-29 <i>Lophocyrtis</i> ( <i>Paralampterium</i> ?) <i>longiventer</i> , R643-R646 |
| 5 <i>Lophocyrtis</i> ( <i>Lophocyrtis</i> ?) <i>aspera</i> , R622               | 30 <i>Lophophaena</i> sp. A., R647   |
| 6 <i>Lophocyrtis</i> ( <i>Apoplanius</i> ) <i>semipolita</i> , R623             | 31 <i>Lophophaena</i> sp. B., R648   |
| 7 <i>Calocyclus</i> ? sp., R624   | 32 <i>Lophocyrtis</i> ( <i>Lophocyrtis</i> ) <i>jacchia hapsis</i> , R649          |
| 8 <i>Ceratocyrtis robustus</i> ?, R625  | 33 <i>Lychnocanium amphitrite</i> , R650   |
| 9 <i>Ceratocyrtis mashae</i> ?, R626  | 34 <i>Peripyramis</i> sp., R651  |
| 10 <i>Ceratocyrtis</i> sp. A., R627   | 35 Plagoniidae gen. et sp. indet. A., R652   |
| 11 <i>Clathrocyclas</i> sp., R628   | 36 Plagoniidae gen. et sp. indet. B., R653   |
| 12 <i>Cornutella californica</i> , R629   | 37 <i>Plectopyramis</i> sp., R654  |
| 13 <i>Dictyophimus</i> ? aff. <i>constrictus</i> , R630                         | 38 <i>Pseudodictyophimus gracilipes</i> , R655                                     |
| 14 <i>Eucyrtidium mariae</i> , R631, arrow indicates downward-directed Vs       | 39 <i>Pteropilium</i> sp., R656  |
| 15 <i>Eucyrtidium montiparum</i> , R632, arrow indicates downwardly-directed Vs | 40 <i>Sethocyrtis babylonis</i> group, R657  |
| 16 <i>Eucyrtidium spinosum</i> , R633, arrow indicates downwardly-directed Vs   | 41 <i>Siphocampe</i> cf. <i>acephala</i> , R658                                    |
| 17 <i>Eucyrtidium</i> sp., R634, arrow indicates downwardly-directed Vs         | 42 <i>Siphocampe nodosaria</i> , R659  |
| 18 <i>Ewingella</i> ? sp., R635, arrow indicates vertical tube                  | 43 <i>Siphocampe</i> aff. <i>nodosaria</i> , R660                                  |
| 19 <i>Lamptonium</i> ? aff. <i>pennatum</i> , R636                              | 44 <i>Dictyoprora urceolus</i> , R661  |
| 20 <i>Lithomelissa ehrenbergi</i> , R637  | 45 Theoperidae gen. et sp. indet., R662  |
| 21 <i>Lithomelissa</i> aff. <i>ehrenbergi</i> , R638                            | 46 <i>Verutotholus</i> cf. <i>doigi</i> , R663, arrow indicates vertical tube      |
| 22 <i>Lithomelissa</i> cf. <i>gelasinus</i> , R639                              | 47 <i>Zealithapium mitra</i> , R664.   |



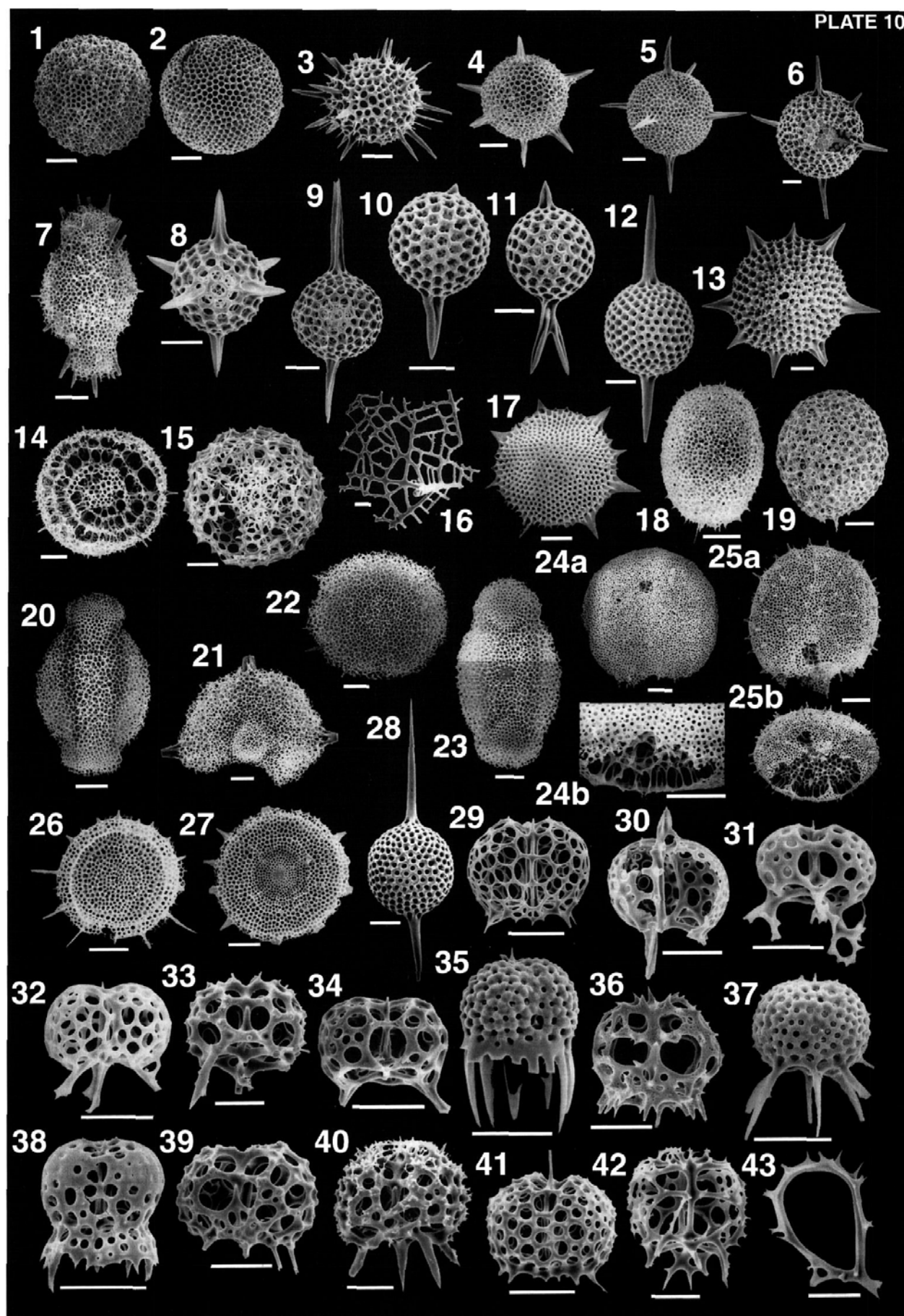


- Deep Sea Drilling Project, Volume 22:521-575. Washington, DC: US Government Printing Office.
- JÖRGENSEN, E., 1900. Protophyten und Protozoen im Plankton aus der norwegischen Westküste. Bergens Museum Aarbog, for 1899, 2, 6:1-112.
- KOZLOVA, G. E., 1967. Tipy stroeniya radiolarij iz sem. Porodiscidae (Types of skeletal structure in the family Porodiscidae). Zoological Journal, 46(8):1163-1172.
- KOZLOVA, G. E. and GORBOVETZ, A. N., 1966. On the radiolarians of the Upper Cretaceous and Upper Eocene deposits in the West-Siberian Lowland. Transactions of the Geological Scientific Research Institute for Petroleum, 248:1-119, pls.1-17.
- LAUTOUR, H. A. de, 1889. On the fossil marine diatomaceous deposit near Oamaru. Transactions of the New Zealand Institute, 21:293-311.
- LAZARUS, D., SCHERER, R. P. and PROTHERO, D. R., 1985. Evolution of the radiolarian species-complex *Pterocanium*: a preliminary survey. Journal of Paleontology, 59:183-220.
- LING, H., 1975. Radiolaria: Leg 31 of the Deep Sea Drilling Project. In: Karig, D.E. et al. Initial Reports of the Deep Sea Drilling Project, Volume 31:703-761. Washington, DC: US Government Printing Office.
- , 1992. Radiolarians from the Sea of Japan: Leg 128. In: Pisciotta, K.A. et al. Proceedings of the Ocean Drilling Program, Scientific Results, Volume 127/128 Part1:225-236. College Station, Texas: Ocean Drilling Program.
- LOEBLICH, A. R. and TAPPAN, H., 1961. Remarks on the systematics of the Sarkodina (Protozoa), renamed homonyms and new and validated genera. Proceedings of the Biological Society of Washington, 74:213-234.

# PLATE 10

All illustrations are scanning electron micrographs. Illustrated specimens are from the following samples (see Table 1 for locality information): fig. 17 - BN1; figs. 1, 13, 21, 22, 24a-25b - BN2; fig. 35 - BN3; figs. 29, 33, 39, 40 - BN4; fig. 30 - BN6; figs. 2, 4, 19, 43 - BN7; figs. 3, 14, 16, 31, 32, 42 - FH1; figs. 6, 12, 15 - FH2; figs. 5, 10, 11, 26, 27, 37 - JP1; fig. 8 - JP2; figs. 9, 28, 34, 36, 38, 41 - CQ1; fig. 23 - FG1; figs. 7, 20 - FG2; fig. 18 - FG5. All scale bars are 50µm.

- |   |   |
|---|---|
| 1-6 <i>Actinommidae</i> gen. et sp. indet., R665-670                          | 25a,b <i>Spongopyle</i> sp., R689, 25b) oblique view showing pylome |
| 7 <i>Amphicraspedum murrayanum</i> , R671                                     | 26 <i>Stylodictya</i> sp., R690                                     |
| 8 <i>Amphisphaera</i> aff. <i>spinulosa</i> , R672                            | 27 <i>Stylodictya targaeformis</i> , R691                           |
| 9 <i>Amphisphaera</i> sp. A., R673  | 28 <i>Stylosphaera minor</i> , R692                                 |
| 10,11 <i>Amphisphaera</i> sp. B., R674 & R675                                 | 29 <i>Dendrospyrus</i> aff. <i>anthocyrtoides</i> , R693            |
| 12 <i>Axoprunum pierinae</i> , R676   | 30 <i>Dendrospyrus</i> aff. <i>binapertonis</i> , R694              |
| 13 <i>Heliodiscus inca</i> , R677   | 31 <i>Dendrospyrus</i> sp. A., R695                                 |
| 14 <i>Lithelius minor</i> , R678  | 32 <i>Dendrospyrus</i> sp. B., R696                                 |
| 15 <i>Lithelius nautiloides</i> , R679  | 33 <i>Dendrospyrus</i> sp. C., R697                                 |
| 16 <i>Orosphaeridae</i> gen. et sp. indet., R680                              | 34 <i>Dendrospyrus</i> sp. D., R698                                 |
| 17 <i>Periphaena heliastericus</i> , R681                                     | 35 <i>Dorcadospyris argisca</i> , R699                              |
| 18 <i>Prunopyle polyacantha</i> , R682  | 36 <i>Dorcadospyris costatescens</i> , R700                         |
| 19 <i>Prunopyle</i> aff. <i>polyacantha</i> ?, R683                           | 37 <i>Dendrospyrus inferispina</i> , R701                           |
| 20 <i>Spongodiscus cruciferus</i> , R684                                      | 38 <i>Dorcadospyris</i> sp., R702                                   |
| 21 <i>Spongodiscus</i> aff. <i>rhabdostylus</i> , R685                        | 39 <i>Liriospyris clathrata</i> , R703                              |
| 22 <i>Spongodiscus</i> sp., R686  | 40 <i>Liriospyris</i> ? sp., R704                                   |
| 23 <i>Spongodiscus</i> cf. <i>cruciferus</i> , R687                           | 41 <i>Dendrospyrus tumidula</i> , R705                              |
| 24a,b <i>Spongopyle spiralis</i> , R688, 24b) close-up oblique view of pylome | 42 <i>Tholospyris</i> ? sp., R706                                   |
|   | 43 <i>Zygocircus buetschlii</i> , R707.                             |



- LOMBARI, G. and LAZARUS, D. B., 1988. Neogene cycladophorid radiolarians from North Atlantic, Antarctic, and North Pacific deep-sea sediments. *Micropaleontology*, 34:97-135.
- McKAY, A., 1877. Oamaru and Waitaki Districts. Reports of Geological Explorations during 1876-77, Colonial Museum and Geological Survey of New Zealand, 14:56-92.
- MARTIN, G. C., 1904. Radiolaria. Maryland Geological Survey (Miocene). Baltimore: Johns Hopkins Press, pp.447-459, pl. 130.
- MOORE, T. C., Jr., 1972. Mid-Tertiary evolution of the radiolarian genus *Calocyclus*. *Micropaleontology*, 18:144-152.
- NAKASEKO, K., 1963. Neogene Cyrtoida (Radiolaria) from the Isezaki Formation in Ibaraki Prefecture, Japan. Scientific Reports, College of General Studies, Osaka University, 12(2):165-198, pls.1-4.
- NIGRINI, C., 1967. Radiolaria in pelagic sediments from the Indian and Pacific Oceans. Bulletin of the Scripps Institution of Oceanography, Volume 11. 125pp.
- , 1970. Radiolarian assemblages in the North Pacific and their application to a study of Quaternary sediments in Core V20-130. Geological Society of America, Memoir 126:139-183.
- , 1977. Tropical Cenozoic Artostrobilidae (Radiolaria). *Micropaleontology*, 23:241-269.
- , 1985. Radiolarian biostratigraphy in the Central Equatorial Pacific, Deep Sea Drilling Project Leg 85. In: Mayer, L. et al. Initial Reports of the Deep Sea Drilling Project, Volume 85:511-551. Washington, DC: US Government Printing Office.
- NIGRINI, C. and LOMBARI, G., 1984. A guide to Miocene Radiolaria. Cushman Foundation for Foraminiferal Research Special Publication, 22. 467pp.
- NISHIMURA, A., 1992. Paleocene radiolarian biostratigraphy in the northwest Atlantic at Site 384, Leg 43, of the Deep Sea Drilling Project. *Micropaleontology*, 38:317-362.
- NISHIMURA, A. and YAMAUCHI, M., 1984. Radiolarians from the Nankai Trough in the Northwest Pacific. News of Osaka Micropaleontologists, Special Volume, 6. 148pp.
- NISHIMURA, H., 1990. Taxonomic study on Cenozoic Nassellaria (Radiolaria). Science Reports of the Institute of Geoscience, University of Tsukuba, Section B, Volume 11:69-172.
- O'CONNOR, B. M., 1993. Radiolaria from the Mahurangi Limestone, Northland, New Zealand. Unpublished M.Sc. thesis, Department of Geology, University of Auckland. 135pp.
- , 1994. Seven new radiolarian species from the Oligocene of New Zealand. *Micropaleontology*, 40:337-350.
- , 1996. Confocal Laser Scanning Microscopy: a new technique for investigating and illustrating fossil Radiolaria. *Micropaleontology*, 42:395-402.
- , 1997a. New Radiolaria from the Oligocene and Early Miocene of New Zealand. *Micropaleontology*, 43(1):63-100.
- , 1997b. Lower Miocene Radiolaria from Te Kopua Point, Kaipara Harbour, New Zealand. *Micropaleontology*, 43(2):101-128.
- PARK, F. G. S., 1918. The Geology of the Oamaru District, North Otago (Eastern Otago Division). New Zealand Geological Survey Bulletin, new series, 20. 124pp.
- PESAGNO, E. A., 1969. The Neosciadocapsidae, a new family of upper Cretaceous Radiolaria. *Bulletins of American Paleontology*, 56:373-439.
- , 1976. Radiolarian zonation and stratigraphy of the Upper Cretaceous portion of the Great Valley Sequence, California Coast Ranges. *Micropaleontology*, Special Publication 2. 95pp.
- PETRUSHEVSKAYA, M. G., 1962. The importance of skeleton growth in Radiolaria for their systematics. *Zoological Journal*, 41(3):331-341.
- , 1965. Osobennosti i konstruktii skeleta radiolyarii Botryoidae (otr. Nassellaria) (Peculiarities of the construction of the skeleton of radiolarians Botryoidae (order Nassellaria). *Trudy Zoologicheskogo Instituta AN SSSR* (In: Faunistics and Ecology of Animals. Transactions of the Institute of Zoology, Academy of Sciences, USSR (Special Print)), 35:79-118.
- , 1968. Homologies in the skeletons of nassellarian radiolarians 1: Principal arches in the family Cyrtoidae. *Zoological Journal*, 47(9) (special reprint):1296-1310.
- , 1969. Spumellarian and Nassellarian radiolarians in bottom sediments as indicators of hydrological conditions. In: Basic Problems of Micropaleontology and of the Accumulation of Organogenic Sediments in Oceans and Seas (reprint). Academy of Sciences Oceanographical Commission. pp.127-150.
- , 1971a. On the natural system of Polycystine Radiolaria (Class Sarcodina). In: Farinacci, A., (ed.), Proceedings of the II Planktonic Conference, Roma 1970. Edizioni Tecnoscienza, Roma, pp. 981-991.
- , 1971b. Radiolyarii Nassellaria v planktone Mirovogo Okeana (Nassellarian radiolarians in the plankton of the World Ocean). *Issledovaniya Fauny Morei* (Explorations of the Fauna of the Seas), 9(17):5-294.
- , 1975a. Cenozoic radiolarians of the Antarctic. In: Kennett, J.P. et al. Initial Reports of the Deep Sea Drilling Project, Volume 29:541-675. Washington, DC: US Government Printing Office.
- , 1975b. Morphological criteria in the systematics of the radiolarians of the order Nassellaria. In: Systematics and Stratigraphic Importance of Radiolarians. Transactions of the All Union Order of Lenin Awarded Geological Scientific Research Institute (VSEGEI), new series, Vol.226, Ministry of Geology, USSR. pp.25-32.
- , 1981. Radiolyarii otryada Nassellaria Mirovogo Okeana. (Radiolaria, order Nassellaria, in the World Ocean). *Izdavaemye Zoologicheskimi Institutami Akademii Nauk SSSR*, no.128. 406pp.
- PETRUSHEVSKAYA, M. G. and KOZLOVA, G. E., 1972. Radiolaria: Leg 14, Deep Sea Drilling Project. In: Hayes, D.E. et al. Initial reports of the Deep Sea Drilling Project, Volume 14:495-648. Washington, DC: US Government Printing Office.
- , 1979. Description of the radiolarian genera and species. Chapter 5. In: Strelkov, A.A. and Petrushevskaya, M.G., (eds). The history of the microplankton of the Norwegian Sea (on Deep Sea Drilling materials). Nauka, Leningrad. pp.86-157. (in Russian).
- POPOFSKY, A., 1908. Die Radiolarien der Antarktis. Deutsche Südpolar-Expedition 1901-1903, vol.10 (Zool. vol.2), part 3:183-305, pls.20-36. Georg Reimer, Berlin, Germany.
- PRINCIPI, P., 1909. Contributo allo studio dei Radiolari Miocenici Italiani. *Bollettino della Società Geologica Italiana*, 28:1-22, pl. 1.
- REYNOLDS, R. A., 1977. Radiolarians from the western North Pacific, Leg 57, Deep Sea Drilling Project. In: von Huene, R. et al. Initial Re-



- ports of the Deep Sea Drilling Project, Volume 57:735-769. Washington, DC: US Government Printing Office.
- RIEDEL, W. R., 1952. Tertiary Radiolaria in Western Pacific sediments. Göteborg Kungliga Vetenskaps- och Vitterhets-Samhälles Handlingar, Sjätte Följden, Series B, Band 6, number 3: 1-21.
- , 1958. Radiolaria in Antarctic sediments. B.A.N.Z. Antarctic Research Expedition Reports, Series B, Volume 6, Part 10:217-255.
- , 1959. Oligocene and Lower Miocene Radiolaria in tropical Pacific sediments. *Micropaleontology*, 5:285-302.
- , 1967a. Some new families of Radiolaria. Proceedings of the Geological Society of London, 1640:148-149.
- , 1967b. Subclass Radiolaria. In: Harland, W.B. (ed), The Fossil Record. Geological Society of London, London. pp.291-298.
- , 1971. Systematic classification of Polycystine Radiolaria. In: Funnell, B.M., and Riedel, W.R. (eds). The Micropaleontology of Oceans. Cambridge University Press, London. pp.649-661.
- RIEDEL, W. R. and CAMPBELL, A. S., 1952. A new Eocene radiolarian genus. *Journal of Paleontology*, 2:667-669.
- RIEDEL, W. R. and SANFILIPPO, A., 1970. Radiolaria, Leg 4, Deep Sea Drilling Project. In: Bader, R.G. et al. Initial reports of the Deep Sea Drilling Project, Volume 4:503-575. Washington, DC: US Government Printing Office.
- , 1971. Cenozoic Radiolaria from the western tropical Pacific, Leg 7. In: Winterer, E.L. et al. Initial Reports of the Deep Sea Drilling Project, Volume 7:1529-1672. Washington, DC: US Government Printing Office, Washington.
- , 1977. Cainozoic Radiolaria. In: Ramsay, A.T.S. (ed). Oceanic Micropaleontology (Volume 2):847-912. London: Academic Press.
- , 1981. Evolution and diversity of form in Radiolaria. In: Simpson, T.L. and Volcani, B.E. (eds). Silicon and siliceous structures in biological systems. New York: Springer-Verlag, pp. 323-346.
- , 1986. Morphological characters for a natural classification of Cenozoic Radiolaria, reflecting phylogenies. *Marine Micropaleontology*, 11:151-170.
- RÜST, D., 1885. Beiträge zur Kenntniss der fossilen Radiolarien aus Gesteinen des Jura. *Palaeontographica*, 31(3):273-321, pls.26-44.
- , 1898. Neue Beiträge zur Kenntniss der fossilen Radiolarien aus Gesteinen des Jura und der Kreide. *Palaeontographica*, 45:1-67, pls.1-19.
- SAKAI, T., 1980. Radiolarians from sites 434, 435 and 436, northwest Pacific, Leg 56, Deep Sea Drilling Project. In: Langseth, M. et al. Initial Reports of the Deep Sea Drilling Project, Volume 56, 57, Part 2:695-733. Washington, DC: US Government Printing Office.
- SANFILIPPO, A., 1990. Origin of the Subgenera *Cyclampterium*, *Paralampterium* and *Sciadiopeplus* from *Lophocyrtis* (*Lophocyrtis*) (Radiolaria, Theoperidae). *Micropaleontology*, 15:287-312.
- SANFILIPPO, A. and CAULET, J.-P., 1998. Taxonomy and evolution of Paleogene Antarctic and tropical lophocyrtid radiolarians. *Micropaleontology*, 44(1): 1-43.
- SANFILIPPO, A. and NIGRINI, C., 1995. Radiolarian stratigraphy across the Oligocene/Miocene transition. *Marine Micropaleontology*, 24:239-285.
- SANFILIPPO, A. and RIEDEL, W. R., 1973. Cenozoic Radiolaria (Exclusive of theoperids, artostrobiids and amphipyndacids) from the Gulf of Mexico, Deep Sea Drilling Project Leg 10. In: Worzel, J.L. et al. Initial Reports of the Deep Sea Drilling Project, Volume 10:475-611. Washington, DC: US Government Printing Office.
- , 1979. Radiolaria from the northeastern Atlantic Ocean, DSDP Leg 48. In: Montadert, L. et al. Initial Reports of the Deep Sea Drilling Project, Volume 48:493-511. Washington, DC: US Government Printing Office.
- , 1980. A revised generic and suprageneric classification of the Artiscins (Radiolaria). *Journal of Paleontology*, 54:1008-1011.
- , 1982. Revision of the radiolarian genera *Theocotyle*, *Theocotylissa* and *Thyrsoyrtis*. *Micropaleontology*, 28:170-188.
- , 1992. The origin and evolution of Pterocorythidae (Radiolaria): a Cenozoic phylogenetic study. *Micropaleontology*, 38:1-36.
- SANFILIPPO, A., WESTBERG-SMITH, M. J. and RIEDEL, W. R., 1985. Cenozoic Radiolaria. In: Bolli, H.M., Saunders, J.B. and Perch-Nielsen, K. (eds). Plankton stratigraphy. Cambridge University Press. pp.631-712.
- SQUINABOL, S., 1903. Le radiolarie dei noduli selciosi nella scaglia degli Euganei. *Contribuzione 1. Riv. Ital. Paleontol.*, 9(4):105-150, pls. 8-10.
- STRONG, C. P., HOLLIS, C. J. and WILSON, G. J., 1995. Foraminiferal, radiolarian and dinoflagellate biostratigraphy of Late Cretaceous to Middle Eocene pelagic sediments (Muzzle Group), Mead Stream, Marlborough, New Zealand. *New Zealand Journal of Geology and Geophysics*, 38:171-212.
- TAKEMURA, A., 1986. Classification of Jurassic nassellarians (Radiolaria). *Palaeontographica Abt. A*, 195:29-74.
- , 1992. Radiolarian Paleogene biostratigraphy in the southern Indian Ocean, Leg 120. In: Wise, S.W., Jr. et al. Proceedings of the Ocean Drilling Program, Scientific Results, Volume 120:735-756. College Station, Texas: Ocean Drilling Program.
- VINASSA de REGNY, P. E., 1900. Radiolari Miocenici Italiani. *Memorie Reale Accademia Scienza Istituto Bologna*, ser 5, 8:227-257 (565-595), pls. 1-3.
- WANG, Y. and YANG, Q., 1992. Neogene and Quaternary radiolarians from Leg 125. In: Freyer, P. et al. Proceedings of the Ocean Drilling Program, Scientific Results, Volume 125:95-112. College Station, Texas: Ocean Drilling Program.
- WEAVER, F. M., 1976. Antarctic Radiolaria from the southeast Pacific Basin, Deep Sea Drilling Project, Leg 35. In: Hollister, C.D. et al. Initial Reports of the Deep Sea Drilling Project, Volume 35:569-603. Washington, DC: US Government Printing Office.
- , 1983. Cenozoic radiolarians from the southeast Atlantic, Falkland Plateau region, Deep Sea Drilling Project Leg 71. In: Ludwig, W.J. et al. Initial Reports of the Deep Sea Drilling Project, Volume 71:667-686. Washington, DC: US Government Printing Office.
- WEAVER, F. M. and DINKELMAN, M. G., 1978. Cenozoic radiolarians from the Blake Plateau and the Blake-Bahama Basin, DSDP Leg 44. In: Benson, W.E. et al. Initial Reports of the Deep Sea Drilling Project, Volume 44:865-885. Washington, DC: US Government Printing Office.
- WETZEL, O., 1935. Die Mikropaläontologie des Heiligenhafener Kieseltones (Ober-Eozän). *Jahresbericht des Niedersächsischen geologischen Vereins*, 27:41-75, pls.8-10.

Manuscript received December 11, 1996  
 Manuscript accepted December 12, 1997